2005-09-01

The Identification of Cooperating Mutations in TAL1-Mediated Leukemia in the Mouse: A Dissertation

Jennifer Ann Calvo
University of Massachusetts Medical School

A Dissertation Presented

By

Jennifer Ann Calvo

Submitted to the Faculty of the

University of Massachusetts Graduate School of Biomedical Sciences, Worcester

In partial fulfillment of the requirements for the degree of

DOCTOR OF PHILOSOPHY

2005

THE IDENTIFICATION OF COOPERATING MUTATIONS IN TAL1-MEDIATED LEUKEMIA IN THE MOUSE

A Dissertation Presented

By

Jennifer Ann Calvo

Approved as to style and content by:

Lucio Castilla, Chair of Committee

Stephen Jones, Member of Committee

Rachel Gerstein, Member of Committee

Timothy Kowalik, Member of Committee

Barbara Osborne, Member of Committee

Michelle Kelliher, Dissertation Mentor

Anthony Carruthers, Dean of the Graduate
School of Biomedical Sciences

Interdisciplinary Graduate Program
Cancer Biology
September, 2005

Acknowledgements

I would like to thank my mentor, Michelle Kelliher, for her guidance and support throughout my graduate career. I also appreciate the support, advice and criticism of my committee members, Lucio Castilla, Stephen Jones, Rachel Gerstein, Timothy Kowalik, and Barbara Osborne. I am also grateful to the members of the Kelliher lab for their support, encouragement and helping to provide a wonderful working environment. I would like to thank Leslie Cunningham for contributing the MoMLV RIM experiment (Figure 16), Veena Krishnamoorthy for contributing the DAPT-sensitivity assay (Figure 17B and 18A). Additionally, I would like to thank Jennifer O'Neil for performing the Notch mutational analysis (Table 3). I would like to thank the UMass Transgenic Animal Modeling Core for their generation of mice for this work.

We appreciate the generosity of Dr. Jos Domen from Duke University who provided us with the *H2K-Bcl-2* transgenic mice, Dr. Anthony Capobianco of The Wistar Institute for providing us with the *Eμ/tTA/Notch*^{IC} transgenic mice, and Dr. Dean Felsher from Stanford University for the *Eμ/tTA/Myc* transgenic mice. I would like to thank Dr. Naomi Rosenberg from Tufts University for providing the MoMLV and p16 cDNA probe. Additionally, I also want to thank Dr. Manoj Bhasin, from Dana Farber Cancer Institute for assistance in the microarray analysis.

I also want to thank my parents and husband for their overwhelming support, encouragement and love. I am extremely grateful and could not have done this without you.

Abstract

A sequential series of mutational events is necessary for the development of leukemia. The misexpression of TAL1, a basic helix-loop-helix (bHLH) transcription factor, is the most common mutation in T cell acute lymphoblastic leukemia (T-ALL). *Tal1* transgenic mice develop leukemia with a long latency and incomplete penetrance indicating additional mutations are necessary to develop disease. To investigate additional mutational events that potentially contribute to TAL1-expressing T-ALL patients, we sought to identify cooperating mutations in *tal1* transgenic mice. Clinical studies implicated the loss of the *INK4a/ARF* locus, which encodes two tumor suppressors, $p16^{INK4a}$ and $p14^{ARF}$, in the majority of T-ALL patients. We demonstrated disease acceleration in *tal1/ink4a/arf+/-*, *tal1/*$p16^{ink4a}$*+/-* and *tal1/*$p19^{arf}$*+/-* mice, thereby providing genetic evidence that Tal1 cooperates with loss of either $p16^{Ink4a}$ or $p19^{Arf}$ in leukemogenesis. The cooperation of Tal1 with the loss of $p16^{Ink4a}$ or $p19^{Arf}$, is consistent with our observation that Tal1 alters cell cycle regulation in leukemia by promoting S phase induction and apoptosis *in vivo*.

An additional mutational event common in *tal1* tumors is activation of the Notch1 signaling pathway. We provide evidence that the majority of *tal1* tumors express increased levels of Notch1, and exhibit activating *notch1* mutations. Additionally, *tal1* tumors display sensitivity to the pharmacologic inhibition of γ-secretase activity *in vitro*, indicating that γ-secretase inhibitors may prove an efficacious treatment for TAL1-expressing T-ALL patients. Furthermore, we developed a doxycycline-regulated $Notch^{IC}$ T-ALL cell line, which will allow the identification of important $Notch1^{IC}$ target genes in leukemogenesis.

Table of Contents

List of Tables

List of Figures

List of Abbreviations

ac/sc	*Achaete-Scute*
bHLH	Basic helix loop helix
BrdU	5-Bromo-2'-deoxyuridine
bZIP	Basic leucine zipper
CDK	cyclin dependent kinase
CDKI	cyclin dependent kinase inhibitor
CFE	colony forming efficiency
CK2	casein kinase 2
CSL	CBF-1, Su(H), Lag-1
DAPT	N-[N-(3,5-Difluorophenacetyl-L-alanyl)]-S-phenylglycine *t*-Butyl Ester
Dox	Doxycycline
E(spl)	*Enhancer of Split*
FTOC	fetal thymic organ cultures
GSI	gamma secretase inhibitor
HD	heterodimerization domain
HLF	hepatic leukemia factor
HSC	hematopoetic stem cells
Id	Inhibitor of differentiation/DNA binding
Ig	Immunoglobulin
LOH	loss of heterozygosity
LNR	lin-12 notch repeat module
MAML	Mastermind Like
MEFs	mouse embryonic fibroblasts
MMTV	mouse mammary tumor virus
MoMLV	Moloney Murine Leukemia Virus
NEC	Notch extracellular subunit
Nf2r2	nuclear receptor subfamily 2, group F, member 2
Nrarp	Notch regulated ankryin repeat protein
NTM	Notch transmembrane subunit
PBX1	pre-B cell leukemic homeobox 1
PUC	preubiquitination complex
RIM	retroviral insertional Mutagenesis
SKP2	S phase kinase-associated protein 2
Su(H)	*Suppressor of Hairless*
TACE	TNF-a converting enzyme
Tal1	T-cell acute lymphocytic leukemia 1
T-ALL	T cell acute lymphoblastic leukemia
TCR	T cell receptor

CHAPTER 1

INTRODUCTION

Leukemia/lymphoma is cancer of the blood-forming tissues or the lymphatic system, afflicting approximately 95,000 people annually (American Cancer Society, 2004). It is a heterogeneous disease caused by a multiple genetic abnormalities: chromosomal translocations, deletions, or mutations. Nonrandom chromosomal translocations and inversions are observed in over 65% of acute leukemias (Look, 1997). One mechanism translocations induce leukemia is through proto-oncogene activation. This occurs when a proto-oncogene is juxtaposed to either the T cell receptor (TCR) locus or the immunoglobulin (Ig) locus, resulting in deregulated expression of the oncogene. Another way chromosomal translocation induces leukemia is through the formation of chimeric fusion genes; two genes disrupted by the translocation fuse to encode a chimeric protein with unique properties. The modular structure of transcription factors facilitates the formation of functional chimeric transcription factors such as E2A-PBX1, AML-ETO, and E2A-HLF.

Leukemogenesis is a multi-step process in which multiple mutations occur to deregulate pathways essential for proliferation, differentiation, survival, or self-renewal. Often times the fusion oncoproteins are considered the initiating mutation, being necessary but not sufficient to induce leukemia. The acquirement of additional cooperating mutations allows the progression to acute leukemia. Consistent with this, chromosomal translocations occur *in utero* (McHale et al., 2003; Mori et al., 2002), but childhood acute lymphoblastic leukemia (ALL) does not develop until years later, indicating additional mutations are essential for leukemogenesis. The cooperating mutations often function to enhance proliferation, survival or self-renewal capabilities.

One common event in leukemogenesis is the inactivation of the basic helix-loop-helix (bHLH) protein, E2A. Two nonrandom translocations, t(1;19)(q23;p13) and t(17;19)(q23;p13.3), and more recently the inversion, inv(19)(p13;q13), has been shown to disrupt the E2A locus and result in 25% of B cell acute lymphoblastic leukemia (B-ALL) (Brambillasca et al., 1999; Hunger et al., 1992; Inaba et al., 1992; Mellentin et al., 1989). In addition, E2A is functionally inhibited by the misexpression of TAL1 or other bHLH proteins in the thymus in the majority of T cell acute lymphoblastic leukemia (T-ALL) (Bash et al., 1995).

HLH proteins

Helix-loop-helix proteins (HLH) are a family of evolutionarily-conserved transcription factors important for various developmental processes such as hematopoesis, myogenesis, neurogenesis, and pancreatic development (Bain et al., 1994; German et al., 1991; Olson, 1990). The conserved HLH structure consists of two amphipathic alpha helices separated by a flexible loop structure that functions as a protein dimerization domain (Murre et al., 1989). Basic residues adjacent to the HLH domain confer DNA-binding ability (Ellenberger et al., 1994). HLH proteins have been recently categorized into 6 classes based on expression profiles and the ability to dimerize and bind DNA (Massari and Murre, 2000). Class I HLH proteins, or E proteins, are widely expressed and bind DNA as homodimers or as heterodimers with class II HLH proteins. They induce transcription through two separable transcription activation domains, AD1 and LH (Aronheim et al., 1993; Quong et al., 1993). Conversely, class II HLH proteins are expressed in a tissue-specific manner and bind DNA only as a

heterodimer with E proteins. Class V HLH proteins, or Id proteins, are negative regulators of either class I or II HLH proteins. They contain a HLH domain but lack a functional DNA-binding domain. Therefore, they function as dominant-negative factors, forming heterodimers with both class I and class II HLH proteins, sequestering them into nonfunctional complexes (Benezra et al., 1990; Jen et al., 1992; Kreider et al., 1992; Riechmann et al., 1994). This focus of this thesis is to determine how the inhibition of E proteins, either through structural disruption by the t(17;19) translocation, or functional disruption by the misexpression of TAL1, induces leukemia.

E2A

E2A, a member of the class I HLH proteins, was originally identified through its ability to bind to E-boxes (CANNTG) within the immunoglobulin enhancer regions (Henthorn et al., 1990; Murre et al., 1989). The E2A gene encodes two proteins, E12 and E47, which are alternative spliced gene products and differ only in the exon encoding the bHLH domain (Sun and Baltimore, 1991). E proteins, which consist of E2A, HEB, and E2-2, are widely expressed proteins. E proteins form heterodimers with class II bHLH proteins such as, Tal1, NeuroD/Beta2, MyoD, and Myogenin, and are essential for various developmental processes, such as regulation of hematopoesis, myogenesis, and neurogenesis (Bain et al., 1994; Lee et al., 1995; Lemercier et al., 1997). For example, E proteins form heterodimers with the pancreatic-specific class II HLH transcription factor, Beta2, to regulate gene expression of α and β cells within the pancreas (Nelson et al., 1990). Furthermore, *beta2* null mice exhibit an extreme reduction of insulin-producing β cells and become severely diabetic (Naya et al., 1997). Similarly, in skeletal

muscle cells, E47 forms heterodimers with myogenic regulatory factors (MRF) to regulate myogenesis (Olson, 1990). Furthermore, the regulation of many class II bHLH proteins such as, Mash1, Math1, Neurogenin, and NeuoD by E proteins is essential for proper neurogenesis (Ben-Arie et al., 1997; Guillemot et al., 1993; Ma et al., 1996). The importance of E proteins to multiple developmental processes is underscored by the postnatal lethality observed in mice deficient for E2A, HEB, or E2-2 (Bain et al., 1994; Barndt et al., 1999; Zhuang et al., 1996).

Lymphoid Development

The stages of thymocyte maturation are determined by expression of the co-receptors, CD4 and CD8 [reviewed in (Zuniga-Pflucker and Lenardo, 1996)]. Immature thymocytes lack both CD4 and CD8, and are classified as double negative (DN) cells, which can be further subdivided by expression of CD44 and CD25 into 4 stages: DN1, DN2, DN3, and DN4. Following productive TCRβ rearrangement, signaling through the pre-TCR complex allows the survival, proliferation, and maturation into CD4+ CD8+ double positive (DP) thymocytes. During the DP stage of maturation, thymocytes rearrange the TCRα chain to form a αβ TCR, and following positive and negative selection, differentiate into either mature CD4+ single positive (SP) or CD8+ SP cells.

Similarly, B lymphocyte development depends on rearrangement and expression of immunoglobulin genes, and also requires expression of factors, E2A, EBF, IL7R, and Pax-5 [reviewed in (Hardy and Hayakawa, 2001)]. The expression of a productively rearranged heavy-chain immunoglobulin on the cell surface indicates the transition of pro-B cell to pre-B cell. Pre-B cell receptor (pre-BCR) signaling results in proliferation,

IgH alleleic exclusion, and IgL chain gene rearrangement. Following expression of the B cell receptor (BCR) on the cell surface, the immature B lymphocytes undergo selection or optimal antigen binding, and surviving mature B cells migrate to the periphery.

E2A and Hematopoesis

E proteins are essential for proper development of both B and T lymphocytes (Bain et al., 1997; Bain et al., 1994; Zhuang et al., 1994). In contrast to other tissues where E proteins function as heterodimers with class II HLH proteins, in lymphoid cells, E proteins bind DNA as homodimers. In B lymphocytes, a unique from of E2A exists: an E47 homodimer functions to induce expression of genes important in differentiation, such as EBF, Pax-5, Rag1 and IL7Rα (Kee and Murre, 1998; Murre et al., 1991; Shen and Kadesch, 1995). The unique existence of functioning E47 homodimers in B cells has been suggested to be due to the phosphorylation status of E2a or the presence of an intermolecular disulfide bond (Markus and Benezra, 1999; Sloan et al., 1996).

The importance of E2a in B cell development was first illustrated through the targeted disruption of the *e2a* allele. *E2a* null mice exhibit a complete block in B lineage differentiation prior to Ig heavy chain (D_H-J_H) rearrangement (Bain et al., 1994; Zhuang et al., 1994). In addition, *e2a-/-* mice lack the expression of lymphoid regulatory transcripts Pax-5, λ5, CD19, mb-1 and Rag-1 (Bain et al., 1994; Zhuang et al., 1994). Furthermore, transgenic mice overexpressing the negative regulator of E proteins, Id1, exhibit a B cell differentiation arrest, further confirming the essential role of E2a in B cell development (Sun, 1994). E2a has been demonstrated to be essential for various stages of B cell development. For example, E2a is implicated in the regulation of the

rearrangement of both Ig heavy and light chains, perhaps through induction of Rag1/2 (Kee and Murre, 1998; O'Riordan and Grosschedl, 1999). Furthermore, E2a expression is essential to promote Ig class switch recombination upon B cell activation (Quong et al., 1999). Expression of E2a must be tightly regulated; ectopic expression of E2a is capable of inappropriately promoting Ig gene rearrangement and inducing transcription of Rag1, λ5, IL7-Rα, EBF, TdT, and Pax5 in several cell lines (Choi et al., 1996; Kee and Murre, 1998; Schlissel et al., 1991). Although E47 binds DNA as homodimers in B cells, other members of the E protein family, E2-2 and Heb, also contribute to B cell development. Investigation of fetal liver cells from *e2-2*- and *heb*-deficient mice, or *e2a/e2-2, e2a/heb, e2-2/heb* transheterozygote mice reveals drastic decreases in pro-B cells (Zhuang et al., 1996).

Similarly, in T lymphocytes, E47/HEB heterodimers bind DNA and induce genes important for differentiation at various stages of thymocyte development. For example, E47/Heb heterodimers bind to E boxes in the regulatory regions and induce transcription of CD4 and preTα in thymocytes (Sawada and Littman, 1993; Takeuchi et al., 2001). Accordingly, *e47* and *heb*-deficient thymocytes show reduced levels of CD4 and preTα expression (Tremblay et al., 2003; Zhuang et al., 1996). The importance of E proteins in thymocyte development was further elucidated by the reduced thymocyte cellularity and the thymocyte differentiation arrest in *e2a- heb-* or *e47-* deficient mice (Bain et al., 1997; Bain et al., 1999; Barndt et al., 1999). *E2a* deficient mice display dramatically reduced numbers of total thymocytes, and decreases in both DN and DP cells, and a subsequent increase in CD8+ SP, and CD4+ SP cells (Bain et al., 1997). *E47* deficient mice display an equivalent thymocyte differentiation arrest, resulting from a decreased survival of DP

cells and enhanced positive selection to both class I and class II-restricted T cell receptors (Bain et al., 1999). Additionally, *e2a* deficient thymocytes demonstrate an arrest at the most immature DN1 stage (CD44+CD25-) (Bain et al., 1997). This complex thymocyte arrest illustrated E2a functions during multiple stages of thymocyte development, including DN development and β-selection. Moreover, E2a is implicated during γδ thymocyte development; *e2a* deficient mice demonstrate a drastic reduction of γ/δ T lymphocytes, illustrating E2a is a critical regulator of γ and δ V(D)J rearrangement (Bain et al., 1999).

In addition to regulating lymphocyte differentiation, E2a may also function to maintain lymphocyte viability. For example, inhibition of E2a by expression of Id3 in primary B lymphocyte progenitors induces apoptosis, suggesting E2a is required to maintain the viability of lymphocyte progenitors (Kee et al., 2001). Furthermore, *e47-/-* DN thymocytes displayed increased levels of apoptosis *in vivo* and following a 24h culture *in vitro* (Kee et al., 2002). However, Bcl-2 is unable to rescue these lymphopoietic defects observed in *e47-/-* mice, again indicating E47 does not solely maintain survival of lymphocytes, but also has additional roles during lymphopoesis (Kee et al., 2002).

E2a may function in the fate decision of a common lymphoid progenitor towards B cell development at the expense of natural killer cells (NK) and dendritic cells (DC). A downregulation of E2a and subsequent upregulation of Id2 occurs during DC differentiation (Hacker et al., 2003), and expression of Id3 in fetal liver organ cultures (FTOC) resulted in an inhibition of T cell development, and an enhancement of in NK cells development (Heemskerk et al., 1997). However, *e2a -/-* bone marrow derived

cells are pluripotent and can differentiate into dendritic, NK, myeloid, and T lineages, but not B lymphocytes *in vitro* and following reconstitution of lethally-irradiated recipients (Ikawa et al., 2004). This suggests that E2a is absolutely essential for formation of B lymphocytes, but may not be essential for development of other hematopoetic lineages. Functional redundancy amongst E proteins may explain this occurrence; Heb and E2-2 may compensate for the absence of E2a and allow development of dendritic, NK, myeloid and T cell lineages.

E2a and leukemia

The majority of *e2a*-deficient mice that survive the common postnatal lethality develop T cell lymphomas with a mean latency of 150 days (Bain et al., 1997). *E47-/-* mice do not suffer from postnatal lethality, but nonetheless develop thymomas with a mean latency of 123 days (Bain et al., 1997). Therefore, E2a has been speculated to function as a lymphoid-specific tumor suppressor. Consistent with this, transgenic overexpression of proteins that inhibit E2A function, such as Id proteins and Tal1, also induces leukemia in mice (Kelliher et al., 1996; Kim et al., 1999; Morrow et al., 1999). Another protein overexpressed in leukemic patients, NOTCH1, has also been shown to inhibit E2A activity although this mechanism has not been fully elucidated (Nie et al., 2003; Ordentlich et al., 1998; Talora et al., 2003).

Disruption of the *e2a* gene is also observed in three chromosomal translocations displayed in human leukemic patients. The t(17;19)(q22;p13) and t(1;19)(q23;p13) translocations generate the chimeric transcription factors, E2A-HLF and E2A-PBX1, respectively (Inaba et al., 1992; Mellentin et al., 1989). These translocations fuse the

transactivation domains of E2A to the DNA-binding domain and protein dimerization domain of either hepatic leukemia factor (HLF) or pre-B cell leukemic homeobox1 (PBX1), yielding novel transcription factors. The leukemogenic function of these chimeric transcription factors has been demonstrated through *in vitro* transformation assays, bone marrow transplantation assays, and transgenic mouse models (Honda et al., 1999; Kamps and Baltimore, 1993; Monica et al., 1994; Smith et al., 2002; Smith et al., 1999; Sykes and Kamps, 2004; Yoshihara et al., 1995). In addition, the cryptic inv(19)(p13;q13) also disrupts the E2A locus, resulting in the fusion protein E2A-FB1 (Brambillasca et al., 1999). Therefore, preferential disruption of *E2A*, either functional or genetic inactivation, suggests that *E2A* inactivation contributes to leukemogenesis.

E2A-HLF

E2A-HLF is a chimeric transcription factor arising from a chromosomal translocation, t(17;19)(q22;p13), observed in 1% of acute pro-B cell ALL (Inaba et al., 1992; Raimondi et al., 1991). The fusion creates a chimeric transcription factor placing the bZIP domain of HLF under control of the *E2A* promoter. There are two documented types of translocations, depending on the breakpoint within the *E2A* locus; both result in the fusion of the two transactivation domains of E2A to the DNA-binding and protein dimerization domains of HLF (Hunger et al., 1994). Both translocations conserve the reading frame of HLF, often times through an unique insertion of intronic DNA, and nontemplated nucleotides (Hunger et al., 1994; Inaba et al., 1992). This strict conservation of the reading frame of HLF suggests that the bZIP domain of HLF provides some leukemogenic function to the fusion protein.

HLF is a member of proline and acidic amino acid rich (PAR) subfamily of basic leucine-zipper (bZIP) transcription factors, which include thyrotroph embryonic factor (TEF) and albumin promoter D-box binding protein (DBP) (Fonjallaz et al., 1996). These PAR bZIP transcription factors are circadian clock output regulators expressed in a cyclic manner in the suprachiasmatic nucleus (Fonjallaz et al., 1996). Interestingly, recent microarray experiments indicate HLF expression is induced in hematopoetic stem cells(HSC) (Georgantas et al., 2004; Ivanova et al., 2002; Shojaei et al., 2005). Furthermore, HLF confers repopulating capacity to human hematopoetic stem cells by inducing BCL-2 expression to inhibit apoptosis (Shojaei et al., 2005). Although, HLF is normally highly expressed in liver, lung and central nervous system, the chromosomal translocation to the E2A locus, results in the misexpression of the bZIP domain of HLF in the lymphoid lineages (Hitzler et al., 1999; Hunger et al., 1992; Inaba et al., 1992).

E2A-HLF expression has been reported to be anti-apoptotic in multiple *in vitro* systems. E2A-HLF inhibited apoptosis in IL-3 dependent cells following cytokine withdrawal, and expression of a dominant-negative E2A-HLF induces apoptosis in leukemic cells expressing E2A-HLF (Inaba et al., 1996). In addition, E2a-Hlf abrogates p53-mediated apoptosis in the myeloid leukemic cells (Altura et al., 1998). Furthermore, HLF expression induced BCL-2 expression in HSC, thereby inhibiting apoptosis (Shojaei et al., 2005). The mechanism by which E2A-HLF inhibits apoptosis is predicted by the similarity between the bZIP domain of HLF and the bZIP domain of a *C.elegans* protein, CES-2 (Horvitz, 1999). CES-2 functions in a cell death specification pathway, ultimately inducing the death of two neurosecretory motor neurons (NSM) during nematode embyogenesis (Ellis and Horvitz, 1991; Metzstein et al., 1996). CES-2 functions as a

negative regulator of CES-1 (Ellis and Horvitz, 1991), inhibiting apoptosis by interfering with the function of EGL-1 (homolog of BH3-only protein) (Conradt and Horvitz, 1998; Ellis and Horvitz, 1991). Interestingly, in a human t(17;19) leukemic cell line, E2A-HLF expression induced the expression of SLUG, a CES-1 homolog (Horvitz, 1999; Inukai et al., 1999). Therefore, it has been proposed that E2A-HLF expression may contribute to leukemogenesis by interfering with this evolutionarily conserved cell death pathway (Figure 1).

Consistent with the association of the t(17;19) translocation and B-ALL, expression of E2A-HLF induces transformation in various experimental settings. Expression of E2A-HLF in NIH3T3 cells induces anchorage-independent growth, which depends on both the transactivation domains of E2A and the bZIP domain of HLF (Yoshihara et al., 1995). Furthermore, expression of E2A-HLF cooperates with BCL-2 expression in the transformation of primary bone marrow cells (Smith et al., 2002). Additionally, two transgenic mouse models expressing E2a-Hlf using lymphoid-specific promoters exhibit differentiation arrest of lymphoid cells and develop T cell leukemia (Honda et al., 1999; Smith et al., 1999).

E2A disruption occurs in another nonrandom translocation, t(1;19), which results in a similar chimeric transcription factor, E2A-PBX1. Expression of E2A-PBX1 is observed in 20% of pre-B ALL (LeBrun and Cleary, 1994; Lu et al., 1994; Williams et al., 1984), activates expression of HOX/PBX1 target genes in lymphoid cells (Kamps et al., 1996; Lu and Kamps, 1997), and transforms multiple cell types *in vitro* (Kamps et al., 1991; Kamps and Wright, 1994). Additionally, *e2a-pbx1* transgenic mice develop T cell

leukemia (Kamps and Baltimore, 1993) and a bone marrow reconstitution model develop myeloid leukemias (Monica et al., 1994).

Tal1

The *TAL1* gene (also known as *SCL* and *TCL5*) encodes a 42 kD class II bHLH transcription factor. In addition, the allele also encodes a truncated 22kDa isoform, which lacks the transactivation domain (Cheng et al., 1993), and results from the translational initiation at an internal methionine. Tal1 is normally expressed during murine development at embryonic day 7.5 (E7.5) in both embryonic and extraembyronic tissues, and in adult mice in myeloid and erythroid lineages, as well as, megakaryocytes and mast cells (Begley et al., 1989; Green and Begley, 1992; Kallianpur et al., 1994; Mouthon et al., 1993; Visvader et al., 1991). In addition, high Tal1 expression is observed in all murine and human erythroid cell lines (Aplan et al., 1992; Visvader et al., 1991). In addition to hematopoetic tissues, Tal1 is also observed in the central nervous system, and endothelial lineages (Kallianpur et al., 1994).

Tal1 functions during erythroid and megakaryocyte differentiation. Specifically, ectopic expression of TAL1 enhanced erythroid differentiation in leukemic cell lines (Hoang et al., 1996), and increased erythroid and megakaryocytic differentiation in human hematopoietic CD34(+)cells (Elwood et al., 1998). In addition, Tal1 expression increased upon differentiation of murine erythroleukemia (MEL) cells (Green et al., 1991). Moreover, antisense Tal1 prevented erythroid differentiation in MEL cells (Aplan et al., 1992). However, another Tal1 antisense experiment showed an induction of erythroid differentiation in human erythroleukemic cells (Green et al., 1991). During

erythroid differentiation, Tal1 induces transactivation of genes involved in erythroid or megakaryocytic differentiation as part of a multi-protein complex containing E2A, LMO2, Ldb1 and GATA1 (Valge-Archer et al., 1994; Wadman et al., 1997). Recruitment of transcriptional coactivators p300 (Huang et al., 1999), and P/CAF (Huang et al., 2000), or corepressor mSin3A (Huang and Brandt, 2000) regulate transcription.

Targeted gene disruption demonstrated Tal1 is essential for embryonic hematopoesis. *Tal1* deficient mice are embryonic lethal at E(8.5-10), and completely lack blood and yolk sac hematopoesis (Porcher et al., 1996; Robb et al., 1995). Furthermore, *tal1-/-* ES cells are unable to differentiate into erythroid or myeloid lineages *in vitro* or *in vivo*, and are unable to produce B or T cells in a *rag-2*-deficient blastocyst complementation assay (Porcher et al., 1996). Together this suggests that Tal1 is essential for development of all hematopoietic lineages. However, conditional disruption of *Tal1* in adult mice indicated continuous Tal1 expression is essential for proper differentiation of erythroid and megakaryocytic precursors, but is dispensable for myeloid, lymphoid lineages, and the function of hematopoetic stem cells (HSCs) (Hall et al., 2003; Mikkola et al., 2003).

Transgenic rescue of hematopoetic defects in *Tal1* null embryos by expression of Tal1 under control of the *gata1* promoter revealed an additional function for Tal1 in angiogenesis (Visvader et al., 1998). Although embryonic hematopoesis is rescued completely, the *tal1-/-/gata1-tal1* transgenic mice still display embryonic lethality at E(9.5), due to severe angiogenic defects in the yolk sac, including a complete absence of vitelline vessels (Visvader et al., 1998). This role for Tal1 in angiogenesis is consistent

with the expression of Tal1 in endothelial cells in the blood island E(8.5), the kidney, and the lung E(13.5-15.5) (Bash et al., 1995).

Tal1 functions both in the development of hematopoetic and endothelial angiogenesis suggesting it may function in hemangioblasts, a precursor of both hematopoetic and endothelial lineages. Consistent with this, Tal1 expression rescues both hematopoetic and endothelial defects in zebrafish *cloche* mutant embryos(Liao et al., 1998), and Tal1 expression partially rescued the hemangioblast defect of *flk1-/-* embryoid bodies *in vitro* (Ema et al., 2003). Although endothelial cells develop normally in *Tal1* null mice (Visvader et al., 1998), this data demonstrates that Tal1 has essential functions in both hematopoesis and angiogenesis.

Tal1 and Leukemia

Tal1 is the most commonly misexpressed oncogene in human T-ALL patients; it is observed in over 60% of T-ALL patients (Begley et al., 1989). TAL1 was originally identified through its involvement in the t(1;14)(p33;q11) translocation, which juxtaposed TAL1 to the TCRδ chain (Aplan et al., 1990; Begley et al., 1989; Brown et al., 1990). Since then, it has also been shown to be disrupted in a t(1;7)(p32;q35) translocation, which juxtaposed TAL1 to the TCRβ locus (Fitzgerald et al., 1991). The presence of nontemplated nucleotides and V(D)J signal sequences indicate that illegitimate V(D)J recombination may generate these translocations, consistent with the transcriptional activity of the *tal1* locus at the initiation of RAG activity (Aplan et al., 1990; Herblot et al., 2000). Additional T-ALL patients display a 90kb intergenic deletion, which places *TAL1* under control of the *SIL* promoter (Aplan et al., 1991; Bash et al., 1995).

Furthermore, many T-ALL patients display an increase of TAL1 levels without evidence of translocation or deletion (Bash et al., 1993). Increased TAL1 expression has been suggested to be due to mutations in either *cis*-acting regulatory sequences or *trans*-acting regulatory factors (Bash et al., 1995; Ferrando et al., 2004). Additionally, LYL1 and TAL2, two proteins sharing significant similarity to the bHLH region of TAL1, are also found disrupted in translocations in T-ALL patients (Mellentin et al., 1989; Xia et al., 1991).

Transgenic mice mimicking Tal1 misexpression in the thymus, which express *tal1* under control of the thymus-specific proximal-*lck* promoter, develop leukemia (Condorelli et al., 1996; Kelliher et al., 1996). These mice develop T cell malignancies with an incomplete penetrance and a long latency of disease, indicating additional mutations are required for leukemogenesis. However, other groups developed *CD2-Srα-tal1*, *Ly-6E.1-tal1,* and *pSIL/tal1* transgenic mice, which do not develop leukemia on a wild type background (Aplan et al., 1997; Goardon et al., 2002; Robb et al., 1995). The discrepancy between the phenotypes observed in the *tal1* transgenic models is likely due to expression of the transgene during the appropriate stage(s) of thymocyte development, but may also be explained by transgene copy number, or transgene expression levels.

Lck-tal1 transgenic mice demonstrated a thymocyte differentiation arrest, and 27% of mice develop T-ALL with a median survival of 350 days (Kelliher et al., 1996). This long latency of disease and low penetrance indicated additional mutations are required for leukemogenesis. Transgenic animals expressing a DNA-binding domain mutant, *lck-tal1(R188G;R189G)* mice, also exhibit a thymocyte differentiation arrest, and develop T cell malignancies, demonstrating a functional DNA-binding domain is not

essential for leukemia, and suggests that Tal1 may contribute to leukemia by inhibiting E2A activity. Consistently, the *tal1/heb*+/- and *tal1/e2a*+/- mice exhibit severely perturbed thymocyte development, decreased expression of E47/Heb target genes, and disease acceleration (O'Neil et al., 2004).

Id proteins

There are 4 members of the inhibitor of differentiation/DNA binding (Id) proteins (Id1-Id4), which are classified as class V bHLH proteins (Massari and Murre, 2000; Riechmann et al., 1994). Id proteins are widely expressed and form heterodimers with class I and class II bHLH proteins *in vitro* and *in vivo* (Benezra et al., 1990; Jen et al., 1992; Kreider et al., 1992; Riechmann et al., 1994). Since Id proteins lack a basic DNA-binding domain, they form functionally inert heterodimers (Benezra et al., 1990). Id proteins are highly expressed in proliferative cells, and inhibit differentiation in various tissues, by inhibiting bHLH proteins (Atherton et al., 1996; Desprez et al., 1995; Melnikova and Christy, 1996; Shoji et al., 1994). *Id* transgenic mice verified the role of Id proteins as inhibitors of E proteins. *Lck-id1* and *lck-id2* mice demonstrate reduced thymic cellularity, and substantial T-cell developmental defects, more similar to what is seen in *e2a* null mice or *tal1* transgenic mice (Chervinsky et al., 1999; Kim et al., 1999; Morrow et al., 1999; O'Neil et al., 2004). However, the thymocyte differentiation arrest in *Id1* transgenic mice is more severe compared to *E2a* null mice, consistent with Id proteins inhibiting not only E2a, but also Heb and E2-2. Similarly, transgenic mice expressing Id1 in B lymphocytes display a complete lack of B cells, an equivalent phenotype to that observed in *e2a* null mice (Sun, 1994). Consistent with Id proteins

inhibiting the tumor suppressor activity of E2A; *lck-id1* and *lck-id2* transgenic mice develop T cell lymphoma (Kim et al., 1999; Morrow et al., 1999).

Cell Cycle and Leukemia

Uncontrolled proliferation is a hallmark of cancer, and the frequent mutation of cell cycle regulatory machinery in human cancers underscores the importance of tight control of cell cycle machinery. The eukaryotic cell cycle is regulated by cyclin-dependent kinases (CDKs), which bind to their activator partners, cyclins D, E, and A. Following quiescence (G_0), mitogenic stimulus induces expression of D-type cyclins (cyclin D1, D2 and D3). Since cyclin D is only synthesized following mitogenic stimulation, and is negatively regulated by SKP/CUL-mediated ubiquitination(Yu et al., 1998), constant mitogenic stimulation is required to proceed through the G_1/S restriction point. Cyclin D binds either CDK4 or CDK6, which then phosphorylates the retinoblastoma protein (pRB). In an unphosphorylated form, pRB binds and negatively regulates the transcription factor, E2F. However, upon phosphorylation, pRB releases E2F, allowing E2F to induce expression of many S-phase genes: dihydrofolate reductase (DHFR), thymidine kinase (TK), cdc2, E2F1, cyclin A, and importantly cyclin E (DeGregori et al., 1995; Duronio and O'Farrell, 1995; Schulze et al., 1995). Cyclin E binds CDK2 and catalyzes the G_1/S transition through the continued phosphorylation of pRB, and other substrates essential for replication origin firing, centrosome duplication, and histone biosynthesis (Ma et al., 2000; Okuda et al., 2000; Zhao et al., 1998). Once cells enter S-phase, phosphorylation of cyclin E by CDK2 results in its ubiquitin-dependent proteolysis (Won and Reed, 1996).

Multiple proteins inhibit cyclin D/CDK4,6 complexes, and therefore negatively regulate G_1 progression. One family of cyclin-dependent kinase inhibitors (CDKI) includes $p21^{CIP1}$, $p27^{KIP1}$, and $p57^{KIP2}$, which all contain an amino-terminal CDK inhibitory domain (Chen et al., 1995; Luo et al., 1995). These CDKIs induce G1 arrest when ectopically expressed (el-Deiry et al., 1994; Harper et al., 1993; Lee et al., 1995; Polyak et al., 1994), and bind to and inhibit cyclin A/CDK2, cyclin B/CDC2, cyclin E/CDK2 and cyclin D/CDK4 complexes *in vitro* (Lee et al., 1995; Xiong et al., 1993). Another family of CDKIs is the **in**hibitors of CD**K4** and CDK6, which includes $p16^{INK4a}$, $p15^{INK5b}$, $p18^{INK4c}$ and $p19^{INK4d}$. These inhibitors specifically bind and inhibit cyclin D1/CDK4 and CDK6, but do not inhibit the other CDKs (Guan et al., 1994; Hannon and Beach, 1994; Hirai et al., 1995; Serrano et al., 1993). In addition, ectopic expression of the INK4a family members induce G1 arrest in multiple cells (Greenwald and Rubin, 1992; Hirai et al., 1995).

Cell cycle and cancer

Mutations targeting the cell cycle regulatory proteins are common in human cancers. For example, chromosomal translocations affecting cyclin D1 are observed in parathyroid adenomas containing inv(11)(p15;q13) (Motokura et al., 1991), and in B lineage mantle cell lymphomas with t(11;14)(q13;q32) (Williams et al., 1993). Amplification of cyclin D1 (11q13) is commonly observed in adult carcinomas (Somers et al., 1990; Yoshida et al., 1988), and amplification of the catalytic partner of cyclin D1, CDK4, is amplified in sarcomas and gliomas (Khatib et al., 1993; Reifenberger et al., 1994; Schmidt et al., 1994; Su et al., 1997). In addition, mutation of the *INK4a* allele is

commonly observed in melanoma, gliomas, ALL, and sarcomas, and mutation of *RB* is associated with retinoblastomas and osteosarcomas (Borg et al., 1996; Francke and Kung, 1976; Friend et al., 1986; Godbout et al., 1983; Hatta et al., 1995; He et al., 1994; Kovar et al., 1997). However, other cell cycle regulatory molecules, for example, cyclin A, cyclin E, and $p21^{CIP1}$ are rarely found mutated in human cancers, suggesting that regulation of the G_1/S restriction point is critical to prevent tumorigenesis.

E2A and cell cycle

There is substantial evidence implicating E2a in cell cycle control. Ectopic expression of E47 in NIH3T3 cells induces growth inhibition, as indicated by a reduction in colony forming efficiency (CFE) (Peverali et al., 1994). In addition, the other E proteins, Heb and E2-2, also confer similar growth inhibition in colony forming assays (Pagliuca et al., 2000). Moreover, when endogenous levels of E47 were restored in Jurkat cells by inhibiting Tal1/E47 heterodimers, the cells underwent growth arrest and subsequent apoptosis (Park et al., 1999). This growth inhibition is consistent with the hypothesis that E proteins transcriptionally regulate CDKIs. In fact, E boxes are present in the proximal promoter sequences of $p21^{CIP}$, $p15^{INK5B}$, and $p16^{INK4}$ (Pagliuca et al., 2000; Prabhu et al., 1997). In addition, E47 induces transcription of these CDKIs in reporter assays (Pagliuca et al., 2000), which can be inhibited by Id or Tal1 expression (Hansson et al., 2003). Moreover, expression of Id1, Id2, and Id3 stimulates cell growth in various cell types (Atherton et al., 1996; Deed et al., 1997; Iavarone et al., 1994; Lasorella et al., 1996; Prabhu et al., 1997). Antisense oligonucleotides against Id proteins prevent G_1 progression, suggesting E2A induces cell cycle arrest *in vitro* (Barone et al.,

1994; Hara et al., 1994). Moreover, *E47* null mice show a 3-fold increase in BrdU positive DN3 cells, suggesting that E47 also contributes to a cell cycle arrest *in vivo* (Engel and Murre, 2004).

However, additional evidence indicates E2A expression may not inhibit the cell cycle but may promote cell cycle progression (Engel et al., 2001; Pagliuca et al., 2000; Song et al., 2004; Zhao et al., 2001). Closer analysis following ectopic E47 expression demonstrates that the reduced CFE may be explained by increased levels of cell death instead of growth arrest (Engel and Murre, 1999; Pagliuca et al., 2000; Zhao et al., 2001). In addition, a conditional E47 system demonstrated E47 expression promotes proliferation in B and non-B cells (Zhao et al., 2001), whereas E47 suppression caused a downregulation of cyclin D3, cdc2, p27 and p21 expression (Chu and Kohtz, 2001; Zhao et al., 2001). Consistent with this, E47 transactivated the cyclin D3 promoter in reporter assays (Song et al., 2004), and fetal liver cells from E2A null mice display reduced levels of cyclin D2 and cyclin D3 (Zhao et al., 2001).

INK4A

A deletion of chromosome 9p21 is commonly observed in leukemic patients (Chilcote et al., 1985; Diaz et al., 1988; Hecht and Hecht, 1986; Pollak and Hagemeijer, 1987) and the tumor suppressor, $p16^{INK4a}$, was mapped to this chromosomal region. $p16^{INK4a}$ was first identified through its interaction with CDK4, and later established to be an inhibitor of cyclin D/CDK4,6 complexes *in vivo* (Serrano et al., 1993; Xiong et al., 1993). Binding of $p16^{INK4a}$ to CDK4 or CKD6 inhibits the interaction between CDK4 and cyclin D, and thereby prevents the catalytic activity of the cyclin D/CDK4-6

complexes (Serrano et al., 1993). Expression of $p16^{INK4a}$ inhibits the phosphorylation of RB *in vitro* and *in vivo* (Koh et al., 1995). Importantly, ectopic expression of $p16^{INK4a}$ induces a G_1 arrest, which is dependent on the presence of functional RB (Koh et al., 1995; Lukas et al., 1995; Medema et al., 1995). Significantly, single amino-acid mutations in $p16^{INK4a}$ observed in human cancer patients prevent its ability to bind cyclinD/CDK4, phosphorylate RB, and induce G1 arrest (Koh et al., 1995; Lukas et al., 1995).

Interestingly, within the *p16^INK4a* allele, another tumor suppressor was discovered to be encoded by an **a**lternative **r**eading **f**rame (Quelle et al., 1995). The $p16^{INK4a}$ transcript is encoded from exon 1α, 2 and 3, whereas $p14^{ARF}$ ($p19^{Arf}$ in mice) is encoded by exon 1β, 2 and 3. Although both genes utilize exons 2 and 3, they are controlled by distinct promoters and are transcribed in alternate reading frames. Therefore, $p16^{INK4a}$ and $p14^{ARF}$ are divergent in both sequence and function. Ectopic $p19^{ARF}$ expression in NIH3T3 cells, which lack the $p16^{INK4a}$ allele, induced a G_0/G_1 arrest indicating that $p19^{ARF}$ functions independently of $p16^{INK4a}$ (Quelle et al., 1995). In addition, $p19^{ARF}$ does not interact with cyclins A, D, E, CDK2, CDK4, CDK6, or CDC2 demonstrating that $p19^{ARF}$ does not function as a CDKI to induce cell cycle arrest (Quelle et al., 1995). $p19^{ARF}$ interacts *in vivo* with Mdm2, preventing the Mdm2-induced ubiquitination and degradation of p53 (Pomerantz et al., 1998). Expression of $p19^{ARF}$ is upregulated upon hyperproliferative signals from Ras, Myc, E1A, and E2F and through the inhibition of Mdm2, results in either p53-dependent apoptosis or cell cycle arrest (Bates et al., 1998; de Stanchina et al., 1998; Palmero et al., 1998; Zindy et al., 1998). For this reason,

$p19^{ARF}$ has been proposed to function as a sensor of oncogenic stresses, resulting in the apoptosis or cell cycle arrest of cells displaying aberrant proliferation.

Mice deficient for both $p16^{Ink4a}$ and $p19^{Arf}$ were generated by the targeted disruption of the shared exons 2 and 3 of the *ink4a* allele. *Ink4a/arf-/-* mouse embryonic fibroblasts (MEFs) overcome senescence at a faster rate compared to wild type MEFs, and are susceptible to transformation with activated ras ($Ha\text{-}ras^{val12}$) (Serrano et al., 1996). Consistent with the *ink4a/arf* allele encoding two tumor suppressors, 69% of *ink4a/arf-/-* mice develop spontaneous fibrosarcomas and lymphomas with a mean latency of 203 days (Serrano et al., 1996). *Ink4a* exon 1β was then disrupted to create $p19^{arf}$ knock-out mice, of which 80% develop various malignant tumors, including sarcomas and T-cell lymphoma within the first year (Kamijo et al., 1999; Kamijo et al., 1997). Additionally, $p19^{arf}$-/- MEFs also demonstrate increased proliferation and susceptibility to H-ras-mediated transformation (Kamijo et al., 1997). Next, $p16^{ink4a}$-/- mice were generated through the targeted disruption of exon 1α. $p16^{ank4a}$-/- MEFs do not exhibit increased immortalization, or susceptibility to H-ras-mediated transformation as observed in *ink4a/arf-/-* and $p19^{arf}$-/- MEFs (Serrano et al., 1996; Sharpless et al., 2001). However, the absence of $p16^{Ink4a}$ still results in tumor formation; 25% of $p16^{ink4a}$-/- mice develop soft-tissue sarcomas, splenic lymphomas and melanomas with a mean latency of disease of 300 days (Sharpless et al., 2001).

Ink4a and Leukemia

A deletion of chromosome 9p21, which encodes the tumor suppressors, $p16^{INK4a}$, $p19^{ARF}$, and $p15^{INK5b}$ is commonly observed in leukemic patients (Chilcote et al., 1985;

Murphy et al., 1989). It has been assumed that the loss of $p16^{INK4a}$ primarily contributes to leukemogenesis. In fact, a summary of numerous published studies demonstrated that 326/564 (58%) of T-ALL patients display deletions of $p16^{INK4a}$ (Drexler, 1998). Disruption of the *INK4a* locus occurs through deletion via illegitimate V(D)J recombination (Cayuela et al., 1997), inactivating point mutations (Ohnishi et al., 1995; Quelle et al., 1997), or methylation of CpG islands in the promoter region (Guo et al., 2000). In addition, tumor associated mutations in exon 2 inhibit the activity of $p16^{INK4a}$ to induce growth arrest, whereas the same mutations do not affect the functional activity of $p14^{ARF}$ (Quelle et al., 1997).

Additional studies suggest deletion of $p14^{ARF}$ may also contribute to leukemogenesis. For example, the majority of published studies mentioned above detect loss of $p16^{INK4a}$ by a loss of exon 2, which also indicates deletion of $p14^{ARF}$. Therefore, the majority of T-ALL patients also exhibit deletions of $p14^{ARF}$ (Haidar et al., 1995; Kamb et al., 1994; Okuda et al., 1995). In addition, some leukemic patients display deletions of $p14^{ARF}$, whereas $p16^{INK4a}$ remains intact (Gardie et al., 1998). Therefore, clinical studies implicate the deletion of $p16^{INK4a}$ and/or $p14^{ARF}$ in leukemia, but fail to distinguish the relative roles of each (Figure 2). Consistent with this possibility, *ink4a/arf-*, $p16^{ink4a}$-, and $p19^{arf}$- deficient mice all develop lymphoid malignancies (Kamijo et al., 1997; Serrano et al., 1996; Sharpless et al., 2001).

Importantly, a recent clinical study finds 78% of TAL1-expressing leukemic patients contain deletions of exon 2 of the *INK4a* allele, suggesting that loss of both $p16^{INK4a}$ and $p14^{ARF}$ may contribute to leukemogenesis (Ferrando et al., 2002). This suggests that loss of the *INK4a* allele may cooperate with TAL1 expression in

leukemogenesis. The work presented in this thesis demonstrates that loss of the *ink4a* allele cooperates with Tal1 expression to induce leukemia in the mouse. Moreover, in contrast to the general perception that loss of $p16^{Ink4a}$ is the important genetic event in leukemogenesis, we provide genetic evidence that Tal1 expression cooperates with not only the loss of $p16^{Ink4a}$ but also $p19^{Arf}$.

The Notch family

The four members of the mammalian Notch family (Notch1-4), are evolutionarily-conserved single-pass transmembrane receptors essential for cell fate decisions (Artavanis-Tsakonas et al., 1999). Notch1 is a 300kDa polypeptide that undergoes proteolytic cleavage by a furin-like protease in the Golgi apparatus to yield two associated subunits, a transmembrane subunit (NTM) and an extracellular subunit (NEC) (Logeat et al., 1998). The NTM subunit contains a RAM domain and an ankryin repeat (ANK) domain, which are both important for protein-protein interactions (Kurooka et al., 1998). The NTM also contains the negative regulatory PEST domain and a transactivation domain (Rechsteiner, 1988). The NEC domain consists of 36 epidermal growth factor (EGF)-like repeats responsible for ligand binding, as well as three lin-12 repeats (LNR) (Rebay et al., 1991).

Activation of the Notch receptor occurs by binding to ligands of either the Jagged- or Delta-like families (Bettenhausen et al., 1995; Lindsell et al., 1995). Following ligand-binding, Notch undergoes two successive cleavage events. The first cleavage occurs just external to the transmembrane (TM) region by a TNF-α converting enzyme (TACE), a member of the ADAM metalloproteases (Brou et al., 2000). The

second cleavage occurs within the TM region at valine 1744 by a γ-secretase complex that includes Presenilin1, Aph1, Nicastrin, and Pen-2 (De Strooper, 2003; De Strooper et al., 1999). These cleavages allow the intracellular region of Notch1 ($Notch^{IC}$) to translocate to the nucleus, where it induces transcription as part of a multifactorial complex, including CSL/RBP-Jκ, Mastermind, and p300/CBP (Oswald et al., 2001; Wu et al., 2002). CSL/RBP-Jκ (also known as CBF1, Su(H), Lag-1), normally represses transcription through the interaction with corepressors N-CoR/SMRT, KyoT2, and CIR (Hsieh et al., 1999; Kao et al., 1998; Taniguchi et al., 1998). However, through the interaction of CSL/RBP-Jκ with $Notch^{IC}$, the corepressors are displaced, and $Notch^{IC}$ recruits the coactivators p300, PCAF, and GCN5 (Kurooka and Honjo, 2000; Oswald et al., 2001). Notch signaling is negatively regulated through ubiquitin/proteasome degradation pathway; Sel-10 (Wu et al., 2001), or the HECT-domain protein Itch (Qiu et al., 2000) function as E3 ubiquitin ligases of Notch *in vitro*. Additionally, Numb negatively regulates Notch activity by facilitating interaction with the E3 ligase Itch, (McGill and McGlade, 2003). The Fringe family (Lunatic, Manic, and Radical) are glycosyltransferases and modify Notch1 function by modulating their response to ligand (Moloney et al., 2000; Yang et al., 2005). The numerous proteins regulating the Notch pathway indicate the importance of tightly controlled Notch signaling.

Notch function

The Notch protein family regulates the differentiation of progenitor cells and controls cell fate specification during development (Artavanis-Tsakonas et al., 1999; Greenwald, 1998). The *Notch* gene was originally identified in *Drosophila melanogaster*

as a loss of function mutation, resulting in a notch phenotype within the wing margin (Morgan, 1917). Notch uses lateral inhibition to control cell fate specification during development of numerous tissues (Simpson, 1990). For example, in developing nervous system of *Drosophila*, a few cells within a population of equipotent cells are selected for Notch activation. Following Notch activation, *Suppressor of Hairless [Su(H)]* transcriptionally activates *Enhancer of split [E(Spl)],* which through the inhibition of *acaete-scute* complex, downregulates the expression of Delta and other proneural genes (Bailey and Posakony, 1995; Kunisch et al., 1994). Therefore, cells receiving a Notch signal develop into an epidermal fate, whereas neighboring cells develop into neural precursors. Consistent with the role of Notch in regulating differentiation of progenitors, uncontrolled Notch signaling often inhibits differentiation along a specific fate pathway. For example, ectopic expression of Notch1 has been shown to inhibit the differentiation of myeloid (Bigas et al., 1998), granulocytic (Milner et al., 1996), lymphoid (Wilson et al., 2001), and intestinal cells (Fre et al., 2005; van Es et al., 2005).

Targeted disruption of the *notch1* allele in mice results in embryonic lethality at E(11.5) due to abnormal somitogenesis (Conlon et al., 1995; Swiatek et al., 1994). *Notch1*-deficient embryos developed normally until E(9.5) (14 somite stage), and then displayed growth arrest, neural-specific cell death, and pericardial edema (Conlon et al., 1995; Swiatek et al., 1994). This phenotype is consistent with Notch functioning as a component of the segmentation clock during development (Bessho and Kageyama, 2003; Rida et al., 2004). In addition, Notch has been reported to be essential in various stages of neural tissue development (Yoon and Gaiano, 2005), and pancreatic cell differentiation (Apelqvist et al., 1999). The importance of the Notch signaling pathway during multiple

stages of development is underscored by the embryonic or postnatal lethality phenotype observed in mice deficient in CSL/RBP-Jκ (Oka et al., 1995), Presenilin1 (Shen et al., 1997), Notch2 (Hamada et al., 1999), or processing-deficient Notch1 knock-in mice (Huppert et al., 2000).

Notch family members are implicated in development and maintenance of hematopoetic stem cells (HSC). Notch1 and Notch2 are expressed in hematopoietic progenitor cells (Bigas et al., 1998; Milner et al., 1994), and *notch1*-deficient paraaortic splanchnopleura (P-Sp) organ cultures demonstrate impaired hematopoetic cell development (Kumano et al., 2003). Additionally, expression of activated Notch1 in murine primitive bone marrow cells resulted in the development of cytokine-dependent hematopoietic stem cell line with the capacity to differentiate into cells with either myeloid and lymphoid characteristics *in vivo* and *in vitro* (Varnum-Finney et al., 2000). Moreover, expression of Notch1 inhibits myeloid, erythroid, and granulocytic differentiation *in vitro*, and allows expansion of undifferentiated cells (Bigas et al., 1998; Kumano et al., 2001; Milner et al., 1996). Similarly, treatment with Notch1 ligands, Jagged1, Jagged2, and Delta1 inhibit differentiation of hematopoetic stem cells (Carlesso et al., 1999; Han et al., 2000; Varnum-Finney et al., 1998).

Further analysis of the *notch*-deficient mice indicated a role for Notch signaling in regulating embryonic vascular morphogenesis (Krebs et al., 2000). Both *Notch1-/-* and *Notch1/Notch4* double knock-out (DKO) mice display severe defects in angiogenic vascular remodeling in the yolk sac, placenta and embryo (Krebs et al., 2000). In addition, *jagged1* and *delta1*-deficient mice die from vascular defects and hemorrhaging at E(10.5) (Hrabe de Angelis et al., 1997; Xue et al., 1999). In addition, the importance

of Notch signaling in adult vascular homeostasis is indicated by the presence of missense mutations in Notch3 in patients with CADASIL, a degenerative vascular disease (Joutel et al., 1996).

Notch and Hematopoesis

Notch1 is known to play an essential role in T cell fate specification. Notch receptors and their ligands are expressed widely in bone marrow and thymic stromal cells during T cell differentiation (Anderson et al., 2001; Radtke et al., 2004; Singh et al., 2000). Several lines of evidence suggest that in lymphoid progenitor cells, the default pathway is B cell development, but upon increased Notch activation, progenitors differentiate into T lymphocytes. Conditional disruption of *notch1* in the thymus using the Mx1-Cre system resulted in thymocyte differentiation arrest and the ectopic presence of B cells in the thymus (Radtke et al., 1999; Wilson et al., 2001). Moreover, pharmacologic inhibition of Notch signaling with γ-secretase inhibition in fetal thymic organ cultures (FTOC) also blocked thymocyte differentiation and resulted in the development of B lymphocytes (Doerfler et al., 2001; Hadland et al., 2001). Furthermore, ectopic expression of the Notch modulator, Lunatic Fringe, in the thymus resulted in a similar decrease in T cells and increase of B cells (Koch et al., 2001). Conversely, ectopic expression of $Notch1^{IC}$ in the bone marrow results in early block in B cell maturation and the inappropriate development of T cells in the bone marrow compartment (Pui et al., 1999).

Notch1 is implicated in various fate decisions during thymocyte development; such as, the αβ versus γδ lineage decision (Ma et al., 1999), and the CD4 versus CD8

lineage decision (Deftos et al., 2000; Robey et al., 1996). Although conditional disruption of Notch1 induces a thymocyte differentiation arrest and a accumulation of thymic B cells, the development of myeloid, NK, and dendritic cells was normal, suggesting that Notch1 is dispensable for normal development of myeloid and other lineages (Radtke et al., 1999).

Notch and E2A

Vertebrate Notch1 is capable of inhibiting MyoD function, a myogenic class II bHLH protein (Kopan et al., 1994; Shawber et al., 1996). Similarly, Notch1 signaling also has been reported to inhibit the class I bHLH protein, E2A. The intracellular domains of Notch1, Notch2, and the Notch target gene, Deltex, completely repress the transcriptional activity of E2A in transfection studies (Ordentlich et al., 1998). Mutational analysis demonstrated that transcriptional inhibition of E2A is independent of Notch binding to CSL/RBP-Jκ, suggesting that inhibition is independent of CSL/RBP-Jκ, -mediated transcription (Ordentlich et al., 1998). The authors speculate Notch/Deltex inhibits Ras signaling, thereby preventing Ras-mediated activation of E47 (Ordentlich et al., 1998). Closer analysis demonstrated that Notch may inhibit E2A activity through its ability to promote the ubiquitination and degradation of E2A in a CSL/RBP-Jκ-dependent manner (Nie et al., 2003). Specifically, in the presence of Notch1 signaling, E2A is phosphorylated by MAP kinases, ubiquitinated by SCF^{Skp2} and degraded by the proteosome (Nie et al., 2003). A preubiquitination complex (PUC) consisting of E47, CHIP, Hsc70, and Skp2 forms to facilitate the interaction of E2A with the E3 ligase,

SCF^{Skp2} (Huang et al., 2004). Consistent with this pathway, Notch1 has recently been shown to directly induce SKP2 expression (Sarmento et al., 2005).

Another report demonstrates Notch signaling may inhibit the ability of E2A to bind DNA (Talora et al., 2003). *Notch3^{IC}* transgenic mice have drastically reduced levels of E box-binding complexes, which correlates with a 9-fold increase in Id1 levels, suggesting Notch inhibits E2A by inducing transcription of Id1 (Talora et al., 2003). Following TCR-mediated ligation, the ERK/MAPK induces Id3 expression levels and inhibits E2A activity (Bain et al., 2001). Similarly, $Notch3^{IC}$ downregulated E2A activity by the induction of Id1, which is dependent on pre-TCR signaling through the ERK/MAPK pathway (Talora et al., 2003).

Notch and leukemia

The human *NOTCH1* gene was originally identified from the t(7;9)(q34;q34.3) translocation, which juxtaposes the *NOTCH1* gene to the TCRβ locus (Ellisen et al., 1991). This translocation is associated with less than 1% of T cell leukemic patients, and results in a truncated allele that signals independently of ligand binding. This constitutively-active protein induces transformation *in vitro*, and induces T-cell leukemia in mouse bone marrow reconstitution experiments (Capobianco et al., 1997; Pear et al., 1996). In addition, transgenic mice misexpressing the activated allele of Notch1 in the thymus develop aggressive, immature T cell tumors (Beverly and Capobianco, 2003; Deftos and Bevan, 2000; Robey et al., 1996). Mutational analysis demonstrate that the ANK repeats and the transactivation domains are required for *in vitro* transformation, whereas the RAM and PEST domains are dispensable (Aster et al., 2000). In addition,

activation of the Notch1 pathway cooperates with other oncogenes to induce T-cell malignancies. Activating mutations in Notch1 are observed in retroviral insertional mutagenesis (RIM) of *e2a-pbx1* transgenic mice and *MMTV^{D}/myc* transgenic mice (Feldman et al., 2000; Girard et al., 1996). Other members of the Notch family are also implicated in leukemogenesis. For example, truncation of *NOTCH2* is capable of transformation *in vitro* (Capobianco et al., 1997), and *notch3^{IC}* transgenic mice develop T-cell leukemia (Bellavia et al., 2000). Lastly, truncations of Notch4 are observed in a mouse mammary tumor virus (MMTV) insertional mutagenesis screen (Robbins et al., 1992).

Recent evidence suggests that NOTCH1 activation may contribute to a greater frequency of T-ALL patients than the <1% displaying the t(7;9)(q34;q34.3) translocation. Screening various cell lines found NOTCH1 and the NOTCH target gene, HES1, overexpressed in the majority of T cell leukemia patients (Bellavia et al., 2002; Chiaramonte et al., 2003; Jundt et al., 2002). In addition, mutations within the heterodimerization domain (HD) and/or the PEST domain of Notch1 are seen in 56% of T-ALL patients (Weng et al., 2004). Mutations of the HD domain have been suggested to weaken the association between the NTM and NEC subunits, increasing the probability of ligand-independent activation. PEST mutations often result in frameshift mutations and a premature STOP, thereby deleting the negative regulatory PEST domain and increasing the stability of NTM domain. Significantly, 39% of TAL1-expressing leukemic patients display NOTCH1 mutations, suggesting *NOTCH1* mutations may cooperate with TAL1 during leukemogenesis (Weng et al., 2004).

The work presented in this thesis demonstrates that using RIM we identified Notch1 as a common insertion site, suggesting Notch1 activation may cooperate with Tal1 expression during leukemogenesis. Interestingly, the vast majority of spontaneous *tal1* tumors express cleaved Notch1 protein and Notch target genes, Deltex and Hes1, indicating that the tumors remain dependent on Notch signaling. Moreover, we find frequent mutations in the PEST and/or HD region of *notch1* as well as sensitivity to treatment with γ-secretase inhibitors. In an attempt to determine how Notch1 activation contributes to leukemia, I generated a conditional Notch1 cell line. This cell line demonstrates continuous Notch1 expression is essential for leukemic cells, as cells undergo G1 arrest and apoptosis in the absence of Notch1 signaling.

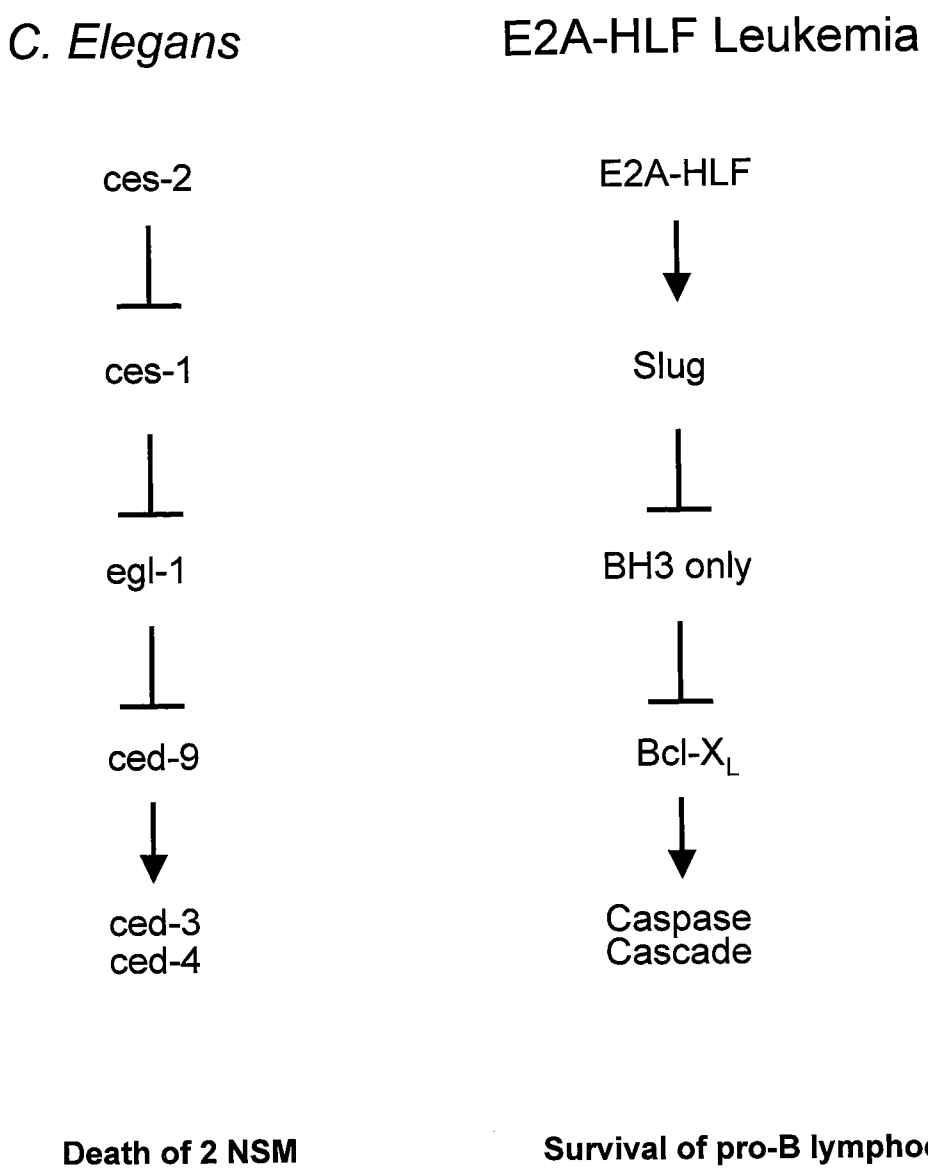

Figure 1: Model of conserved survival pathway in *C. Elegans* and putative leukemogenic function of E2A-HLF. CES-2 induces the death of 2 neurosecretory motor neurons during *C. elegans* development by inhibiting the anti-apoptotic protein CES-1. CES1 inhibits apoptosis by binding and inhibiting the pro-apoptotic protein, EGL-1, which therefore inhibits the caspase cascade. It has been proposed that E2A-HLF replaces a B cell specific CES-2 homolog and induces the transcription of SLUG. SLUG inhibits apoptosis by sequestering pro-apoptoic BH3 proteins, thereby allowing BCL-X_L to inhibit the caspase cascade.

A.

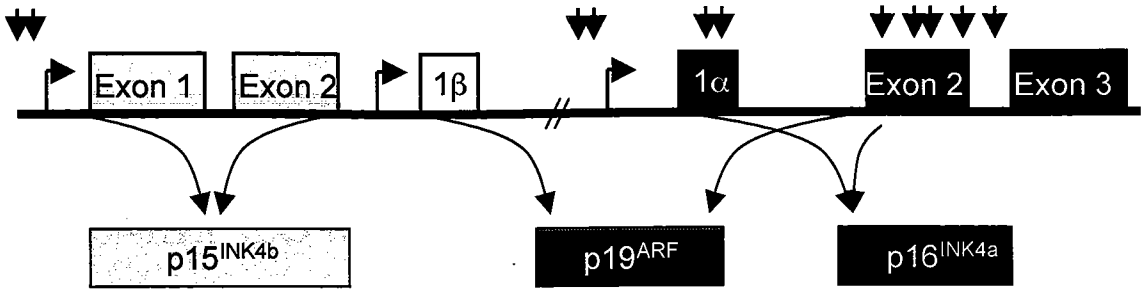

B.

Common Deletions

Alleles deleted

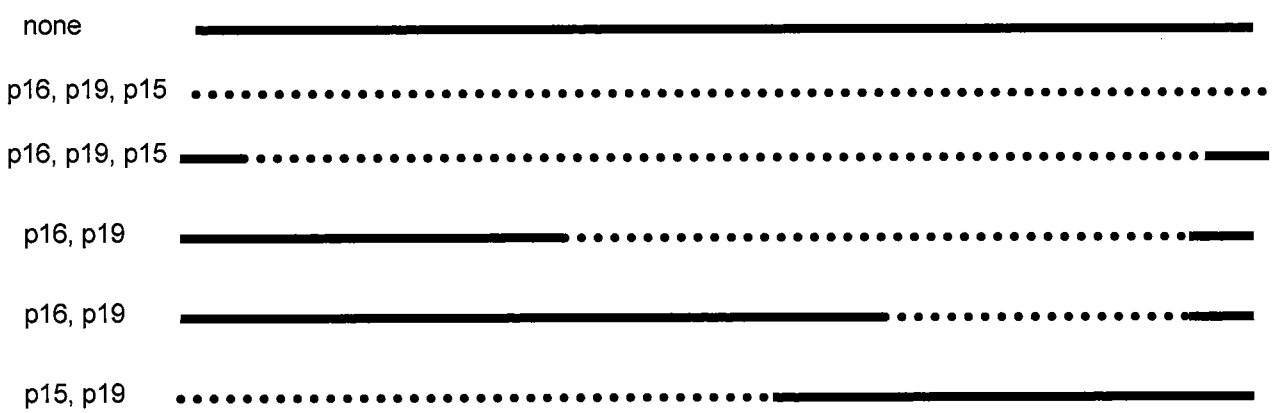

Adapted from Haber, Cell 91:551 and Cayuela et. al. Blood 87:2180.

Figure 2. Schematic representation of the INK4a locus and genetic mutations associated with cancer. A. The $p15^{INK4b}$, $p16^{INK4a}$, and $p14^{ARF}$ genes are shown schematically. Black arrowheads represent point mutations associated with human cancers, and red arrowheads represent methylation of CpG promoter regions. B) Deletions associated with T-ALL represented below the schematic representation of the INK4a allele. The deletions are organized by the alleles deleted.

CHAPTER II

E2A-HLF EXPRESSION REQUIRES ADDITIONAL COOPERATING MUTATIONS TO INDUCE LEUKEMIA IN THE MOUSE

Introduction

E2A-HLF is a chimeric transcription factor resulting from the t(17;19)(q21-22;p13) translocation, which is associated with 1% of B-ALL (Raimondi et al., 1991). Although the occurrence of the t(17;19)(q21-22;p13) translocation is rare, the prognosis is exceedingly poor; all the documented patients displaying E2A-HLF died as a result of their leukemia (Devaraj et al., 1994; Hunger et al., 1994; Ohyashiki et al., 1991).

There are two distinct types of translocations that result in the E2A-HLF fusion protein, depending on the breakpoint within E2A [reviewed in (Hunger, 1996)]. In type I translocations, the breakpoint occurs within intron 12 of E2A and fuses the first 12 exons of *E2A* to exon 4 of *HLF* (Hunger et al., 1994; Hunger et al., 1992; Inaba et al., 1992). A direct fusion would not conserve the reading frame of *HLF* exon 4. However, an uncommon event occurs in which intronic DNA and nontemplated nucleotides are inserted, which conserves the reading frame of HLF (Hunger et al., 1994). In type II translocations, the breakpoint occurs within intron 13 of E2A and results in a direct fusion of the first 13 exons of *E2A* to the fourth exon of *HLF* (Hunger et al., 1994). Therefore, both types of translocation conserve the reading frame of HLF and result in a fusion protein containing two strong transactivation domains from the bHLH protein, E2A, fused to the basic leucine zipper (bZIP) of HLF (Hunger et al., 1994).

The oncogenicity of the E2A-HLF fusion protein have been demonstrated through the transformation of both NIH3T3 cells in soft-agar assays (Yoshihara et al., 1995), and bone marrow precursors in cooperation with BCL-2 expression (Smith et al., 2002). Mutational analysis demonstrated that transformation depends on both the transactivation

domains of E2A and the DNA-binding and protein dimerization domains of HLF, suggesting that both E2A and HLF contributes to the leukemogenicity of the fusion protein (Yoshihara et al., 1995).

The role of HLF in an evolutionarily conserved survival pathway has been proposed due to the significant homology between the bZIP domain of HLF to the bZIP domain of the *C. elegans* apoptotic protein, CES-2. CES-2 induces death in two neurosecretory motor neurons (NSM) during embryogenesis (Ellis and Horvitz, 1991). Genetic studies indicated that CES-2 is a negative regulator of the anti-apoptotic protein, CES-1 (Ellis and Horvitz, 1991). Importantly, representative differential analysis (RDA) demonstrated that E2A-HLF induces the expression of SLUG, a homolog of the *C. elegans* apoptotic protein CES-1 (Inukai et al., 1999). Consistent with E2A-HLF interfering with a survival pathway, expression of E2A-HLF inhibits apoptosis in various cytokine-dependent cell lines following cytokine withdrawal (Inaba et al., 1996; Inukai et al., 1998). In addition, E2A-HLF abrogates p53-induced apoptosis (Altura et al., 1998), whereas functional inhibition of E2A-HLF in t(17;19) cell lines induces apoptosis (Inaba et al., 1996). Therefore, E2A-HLF may induce leukemia by inappropriately inducing the anti-apoptotic protein, SLUG, and thereby interferes with an evolutionarily conserved survival pathway, resulting in the enhanced survival of pro-B lymphocytes (Figure 1).

Two groups generated transgenic mouse models overexpressing E2a-Hlf under control of lymphoid-specific promoters (Honda et al., 1999; Smith et al., 1999). In contrast to the B-ALL observed in t(17;19) patients, both *e2a-hlf* transgenic models developed T-cell malignancies and rarely B-cell malignancies. The development of T-ALL in these transgenic mice precluded their use in determining how E2a-Hlf contributes

to transformation of B cell progenitors and leukemogenesis. One transgenic model demonstrated reduced thymocyte numbers due to increased thymocyte apoptosis, and a B cell maturation arrest (Honda et al., 1999). The other transgenic model displayed a progressive T cell differentiation arrest, thymic involution, and the development of an unusual $CD3^{-}4^{lo}8^{-}$ thymocyte population (Smith et al., 1999). Expression levels of E2a-Hlf in the lymphoid lineages varied considerably between the two models which may partially explain the phenotypic differences. In addition, the differences in phenotype may also be explained by transgene insertional effects, or transgene copy number.

To more accurately mimic the t(17;19) human translocation associated with B-ALL, and to determine how E2A-HLF induces B cell transformation, we generated *e2a-hlf* knock-in mice. Similar to leukemic patients, these mice expressed the E2a-Hlf fusion protein under control of the endogenous *e2a* promoter. As a result, one *e2a* allele is the inactivated by the mutant allele, further mimicking the human translocation. I obtained germline transmission of the mutant *e2a-hlf* allele, and the *e2a* allele was disrupted through this mutation. Homozygous *e2a-hlf* knock-in mice display a T cell differentiation arrest and a complete lack of B lymphocytes, similar to *e2a* null mice (Bain et al., 1994; Zhuang et al., 1994). However, *E2a-hlf* knock-in mice fail to develop leukemia, even following chemical mutagenesis, indicating that E2a-Hlf expression requires additional cooperating mutations to induce leukemia in the mouse.

Results

Generation of E2a-Hlf Knock-In Mice

To recapitulate the t(17;19)(q21-22;p13) translocation observed in B-ALL patients, we generated an *e2a-hlf* knock-in mouse using homologous recombination. We modeled the type I translocation, which fuses the first 13 exons of *E2A* to exon 4 of *HLF*, and includes the insertion of 53 nucleotides to conserve the reading frame of HLF (Hunger et al., 1994; Hunger et al., 1992; Inaba et al., 1992). The fusion region containing a mouse genomic fragment encoding *e2a* exons 10-13, the 53 bp DNA linker, and human *HLF* exon 4 was generated by overlap PCR. A rabbit β-globin polyadenylation cassette was inserted downstream of the translational stop codon of *HLF* exon 4 to ensure proper stability of the fusion gene transcript. The targeting construct also contained a neomycin (NEO) drug resistance marker and a herpes-simplex virus thymidine kinase (TK) gene to facilitate positive and negative selection, respectively (Figure 3). The *e2a-hlf* knock-in targeting construct was electroporated into AB2.2 embryonic stem (ES) cells, and underwent positive (G418) and negative (FIAU) selection. Four hundred ES cell clones were screened for homologous recombination using Southern blot analysis; ES cell clones were digested with *EcoRI* and a 3' flanking probe was used to identify the four clones that correctly displayed both the wild type 18.8kb and the mutant 6.9kb bands (Figure 4). Further analysis with a 5' flanking probe demonstrated that 3 of the 4 ES cell clones correctly underwent homologous recombination (Figure 4).

Western blot analysis indicated ES cells express sufficient levels of E2a to allow us to confirm proper expression of the *e2a-hlf* transcript in the targeted ES cells prior to

blastocyst injection (data not shown). RNA was extracted from wild-type and targeted AB2.2 cells, and *e2a-hlf* expression was assayed using RT-PCR. The targeted ES cells expressed *e2a-hlf*, whereas the wild type ES cells did not, indicating that the *e2a-hlf* ES cells correctly expressed the fusion gene (Figure 5). Two targeted ES cell clones were injected into blastocysts, and following transfer into foster mothers generated two high-degree chimeras (50 and 80%). Mating the 80% chimera to C57BL/6 females gave rise to agouti F1 progeny, and Southern blot analysis demonstrated germline transmission of the *e2a-hlf* mutant allele (data not shown).

Phenotype of *E2a-Hlf/+* mice

E2a-hlf heterozygous mice were viable, fertile, and appeared phenotypically normal. To analyze *e2a-hlf* expression, RNA was extracted from lymphoid tissues of wild type and *e2a-hlf/+* mice. RT-PCR analysis using a primer to exon 12 of *e2a* and exon 4 of *hlf* demonstrated presence of the *e2a-hlf* transcript in the bone marrow, spleen and the thymus of *e2a-hlf/+* mice but not in hematopoetic tissues of wild type littermates (Figure 6). Subsequent sequence analysis of the PCR product revealed correct splicing from *e2a* exon 12, to exon 13, to the 53bp linker, and finally to *HLF* exon 4.

Genotyping one hundred pups from heterozygous matings, 35 were wild type, 55 were *e2a-hlf/+* and 10 were *e2a-hlf/e2a-hlf*, which varied from the expected Mendelian ratios (25 wild type, 50 *e2a-hlf/+*, and 25 *e2a/hlf/e2a/hlf*). *E2a/hlf* homozygous mice are indistinguishable from littermates at birth, but within the first week displayed severe growth defects, and all died within three weeks. Necropsy revealed that internal organs appeared grossly normal, but muscle mass appeared reduced. The growth defects and

postnatal lethality is comparable to that observed in *e2a* null mice, consistent with the functional disruption of E2a by replacing the bHLH domain exons of E2a with HLF in the *e2a-hlf* homozygous mice (Bain et al., 1994; Zhuang et al., 1994).

To determine if E2a-Hlf expression induced a differention arrest in lymphoid tissues, we performed flow cytometry analysis on spleen, thymus, and bone marrow from wild type, *e2a-hlf/+*, and *e2a-hlf/e2a-hlf* mice. Lymphocytes isolated from *e2a-hlf/+* mice display no reproducible alterations in B or T cell profiles compared to wild type lymphocytes (Figure 7). However, *e2a-hlf* homozygous mice demonstrate a differentiation arrest in both B and T lymphocytes. *E2a-hlf* homozygous mice contain drastically reduced numbers of B220+ cells, similar to what is published for *e2a* null mice (Bain et al., 1994; Zhuang et al., 1994) (Figure 7). However, the T cell differentiation arrest observed in *e2a-hlf* homozygous mice differs from that observed in *e2a* null mice. *E2a* null mice demonstrate decreases in DP populations and subsequent increases in DN and SP populations (Bain et al., 1997). However, *e2a-hlf* homozygous mice display an increase in DN and a decrease in DP cells, but do not display an increase in SP cells (Figure 7). This demonstrates *e2a-hlf* homozygous mice display a similar B cell arrest but a divergent T cell arrest when compared to *e2a* null mice. This difference in the T-cell differentiation arrest indicates that the *e2a-hlf* fusion gene not only functionally disrupts the *e2a* allele, but provides additional biologic effects on T cell differentiation.

E2a-Hlf expression requires cooperating mutations to induce leukemia in the mouse

Since E2A-HLF expression is associated with human B-ALL and *e2a-hlf* transgenic mice develop T cell malignancies, we wanted to determine if mice expressing E2a-Hlf under control of the endogenous *e2a* promoter develop leukemia. To test this possibility, a small cohort of *e2a-hlf/+* mice (n=12) were aged and analyzed regularly for signs of disease. No disease was observed in the cohort of *e2a-hlf* heterozygous mice during the two years of the study, indicating that E2a-Hlf expression under control of the *e2a* promoter is not sufficient to induce leukemia in the mouse.

It is possible that E2a-Hlf contributes to leukemogenesis, but requires additional mutations. It has been previously shown that E2a-Hlf cooperates with Bcl-2 to transform bone marrow progenitors *in vitro* (Smith et al., 2002). To test the possibility that E2a-Hlf cooperates with Bcl-2 to induce leukemia, we mated the *e2a-hlf* knock-in mice to *H2K-bcl-2* transgenic mice (Domen et al., 1998). During the course of study, no mice in the small cohort of *e2a/hlf/bcl-2* mice developed disease (n=15), suggesting that E2a-Hlf does not cooperate with Bcl-2 to induce leukemia *in vivo*.

To provide additional mutations to the *e2a-hlf* knock-in mice, we performed N-ethyl-N-nitrosourea (ENU) mutagenesis. *E2a-hlf/+* mice (n=18) and wild type littermate controls (n=9) were injected with 50mg/kg body weight with ENU, and monitored regularly for 40 weeks for signs of disease. One ENU-treated *e2a-hlf/+* mouse (2705) developed a CD4-negative, CD8-negative, and CD3-positive thymoma. In addition, ten ENU-treated *e2a-hlf* and wild type mice were sacrificed after exhibiting weight loss, lethargy, and vaginal bleeding. Upon necropsy, these mice exhibited large uterine masses (15mm), and histological analysis indicated endometrial hyperproliferation and carcinoma. This phenotype has been previously published following ENU mutagenesis

in other mouse models (Mitsumori et al., 2000; Takahashi et al., 1996; Watanabe et al., 2002). Overall, there was no difference in the survival in ENU-treated *e2a-hlf* knock-in mice compared to ENU-treated wild type mice (Figure 8).

Discussion

We generated a knock-in mouse model to mimic the t(17;19)(q21-22;p13) translocation observed in B-ALL patients. The *e2a-hlf* heterozygous mice expressed *e2a-hlf* fusion transcript in the lymphoid lineages, and appeared phenotypically normal. *E2a-hlf/e2a-hlf* mice displayed growth defects, postnatal lethality, and differention arrest in both B and T cells. This phenotype is similar to phenotype of *e2a*-deficient mice, and consistent with the replacement of the HLH domains of E2A with bZIP domain of HLF (Bain et al., 1994; Zhuang et al., 1994). However, the thymocyte differentiation arrest observed in *e2a-hlf* homozygous mice varied compared to *e2a* null mice, suggesting that the *e2a-hlf* mutant allele is not a true null allele, but that the bZIP domain of HLF provides some biological function. Although the genetic backgrounds differ between the *e2a* null mice and the *e2a-hlf* homozygous mice, it is unlikely this accounts for the phenotypic differences, since the *e2a-hlf* homozygous mice were analyzed on two genetic backgrounds, Balb/c and 129/Sv.

There are multiple possibilities why expression of E2a-Hlf failed to induce leukemia in this mouse model. The simplest explanation is that E2a-Hlf is not sufficiently expressed in the *e2a-hlf* knock-in mice. Although *e2a-hlf* RNA was detected by RT-PCR, the absence of an informative antibody precluded our ability to detect E2a-Hlf protein expression levels. The Hlf antibody is no longer commercially available, and the majority of the E2A antibodies either react with the replaced bHLH domain, or reacts with a non-specific band migrating at 62kDa, which is the size of E2a-Hlf. However, the expression of *e2a-hlf* RNA and the minor phenotypic differences between the *e2a-*

hlf/e2a-hlf and *e2a* null mice suggests that the fusion protein is expressed. However, Northern blot analysis should be performed to establish the expression levels of the *e2a-hlf* transcript, and compare them to cell lines from *E2A-HLF* leukemic patients.

Another explanation why the *e2a-hlf* mice did not develop leukemia may be that the reciprocal fusion protein, Hlf-E2a, may contribute to leukemogenesis, but is not modeled in the *e2a-hlf* mice. A chromosomal translocation often results in two reciprocal fusion proteins, and both may function during leukemogenesis. For example, in t(17;19) translocation, two fusion proteins, PML-RARα, and RARα-PML, are expressed and contribute to leukemogenesis (Alcalay et al., 1992). In another example, the reciprocal fusion protein of BCR-ABL, ABL-BCR, is observed in 60% of leukemic patients displaying the t(9;22) translocation (Melo et al., 1993). Although HLF-E2A has not been published to be expressed in t(17;19) leukemic patients, presumably because HLF is not expressed in lymphoid cells, the recent evidence suggesting HLF is expressed in HSC indicates HLF-E2A may contribute to leukemogenesis.

E2A-HLF has been shown to prevent apoptosis in various cell culture systems (Inaba et al., 1996; Inukai et al., 1998). However, its expression may actually induce apoptosis in some instances. For example, thymus from *e2a-hlf* transgenic mice displayed increased levels of apoptosis following TUNEL staining (Honda et al., 1999). Perhaps expression of E2a-Hlf is not compatible in lymphoid progenitors. Consistent with this, both *e2a-hlf* transgenic models express low levels of E2a-Hlf, despite using transgenic constructs that previously yielded high expression levels in other transgenic models (Adams et al., 1985; Yukawa et al., 1989). However, Annexin V staining of

spleen, thymus and bone marrow from 4 week *e2a-hlf* /+ mice failed to reveal any evidence of increased apoptosis (data not shown).

This experiment indicates that expression of E2a-Hlf under control of the *e2a* promoter is not sufficient to induce leukemia in the mouse, suggesting multiple additional mutations are necessary to cooperate with E2a-Hlf expression to induce leukemia in the mouse.

Materials and Methods

Generation of *e2a-hlf* knock-in targeting construct

A 1.8kb genomic fragment of 5' homology was generated by combining a 800bp PCR fragment containing *e2a* exon 10 with a 1kb *e2a* fragment containing exons 11-13 (gift from Yuan Zhuang). Using the 5' homology and the *E2A-HLF* cDNA (gift from Stephen Hunger) as templates, overlap PCR was performed to insert the published 53bp of linker DNA immediately downstream of *e2a* exon 13, and fuse it in frame to human *HLF* exon 4 (GenBank accession no. M95586). A β-globin polyadenylation cassette (pCAGGS) was inserted immediately following *HLF* exon 4. To enable positive selection, PGK-neomycin cassette was inserted downstream of the β-globin polyadenylation signal. For the 3' homology, a 3.2-kb *EcoRV-HindIII e2a* genomic fragment containing the bHLH exons of *e2a* (gift from Gretchen Bain) was inserted following the PGK-Neo cassette. Finally, a HSV-thymidine kinase cassette was inserted to facilitate negative selection.

Generation of *e2a-hlf* knock-in ES cells and chimeras

The *e2a-hlf* knock-in construct was linearized at a unique *NotI* site, purified, and electroporated into AB2.2 ES cells. Following positive and negative selection with G418 and FIAU, respectively, clones were picked and screened by Southern blot analysis. ES cell clones were digested overnight with *EcoRI*, electrophoresed on a 1% agarose gel, transferred to a nitrocellulose membrane and probed with 3' flanking probe. Putative positives were additionally screened with a 5' flanking probe. Correctly targeted ES cells clones were microinjected into C57BL/6 blastocysts and implanted into pseudopregnant foster mice using standard protocols. Chimeric offspring are identified by presence of

agouti coat color and the highest degree chimera (80%) was mated to C57BL/6 females to assay for germline transmission of the *e2a-hlf* mutant allele.

Mice

E2a-hlf homozygous mice were maintained on 129Sv/Ev, and Balb/c backgrounds. To genotype the *e2a-hlf* mice, PCR was performed to identify the presence of the *e2a-hlf* fusion allele with JAS7 (5'-CTC-CTT-CCT-CAA-GTC-AGC-CAC-3') and JAS15 (5'-GGT-GAC-ATT-TAG-GGA-CTC-CAG-3') and to identify the wild type *e2a* allele with JAS8 (5'-CAA-GAT-GGA-GGA-CCG-CTT-GG-3') and JAS22 (5'-CTA-AGT-CAC-TCT-TCA-GCC-CTG-AG-3'). To determine if E2a-Hlf cooperated with Bcl-2 to induce leukemia, *e2a-hlf* mice were mated to *H2K-bcl-2* mice (a gift from Jos Doman). Mice were monitored regularly for signs of disease

Reverse-Transcriptase PCR

RNA was isolated from ES cells, bone marrow, thymus and spleen using Trizol Reagent (Invitrogen, Carlsbad, CA). cDNA was synthesized using the Superscript First-Strand Synthesis System (Invitrogen) and amplified with JAS13 (5'-TCA-CAG-AGA-CCT-CCC-GAC-TC-3') and JAS14 (5'GCA-AAA-ATG-CCA-TCC-TAC-AGG-3') to detect presence of the fusion construct in the ES cells. To ensure correct splicing from exon 12 into the fusion construct, a 428 bp fragment corresponding to *e2a* exon 12, exon 13, linker and *HLF* exon 4 was amplified with JAS8 (5'-CAA-GAT-GGA-GGA-CCG-CTT-G-3') and JAS16 (5'-GGT-TCT-CTT-TCA-GCC-TCC-G-3). The resulting PCR product was cloned into pCR4-TOPO (Invitrogen), and sequenced to confirm correct splicing.

Flow cytometry

Bone marrow, spleen, and thymus were isolated from wild type, *e2a-hlf/+* and *e2a-hlf/e2a-hlf* mice and minced into single-cell suspensions. $2x10^6$ cells were stained with PE-conjugated anti-mouse Ly-2 (CD8), FITC-conjugated L3T4 (CD4), and PE-conjugated CD45R/B220 (BD Pharmingen, San Diego, CA). Cells were fixed with 1% paraformaldehyde and analyzed by flow cytometry.

ENU mutagenesis

E2a-hlf heterozygous and wildtype littermate controls between the ages of 1 and 5 months were given one IP injection of ENU (50mg/kg body weight) (Sigma Chemical, St. Louis). Mice were monitored regularly for signs of disease. Upon necropsy, tissues were fixed in neutral-buffered formalin. 4 mm sections were cut and stained with hematoxylin and eosin by the Diabetes and Endocrinology Research Center Morphology Core Laboratory, University of Massachusetts Medical School. Histological evaluation was performed by Dr. Garlik, University of Massachusetts Cancer Biology Department.

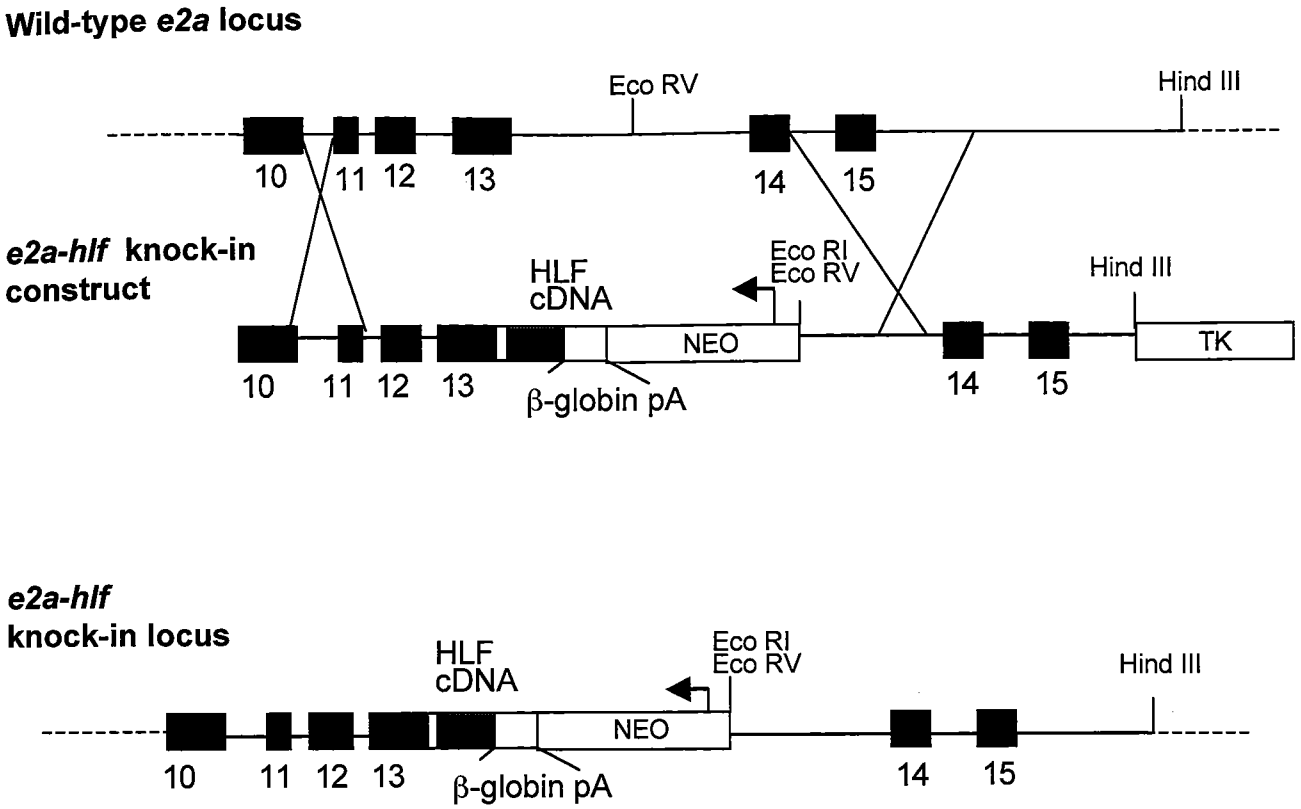

Figure 3: Schematic of *e2a-hlf* knock-in targeting construct. This construct models type I E2A-HLF translocation by fusing the *e2a* exons 10-13 to the 53bp linker to *HLF* exon 4. β-globin poly A is added to ensure stability. Approximately 3.2kb of 3' homologous sequence including exon 14 and 15, and the pgk-NEO and HSV-TK cassettes were added to complete the construct.

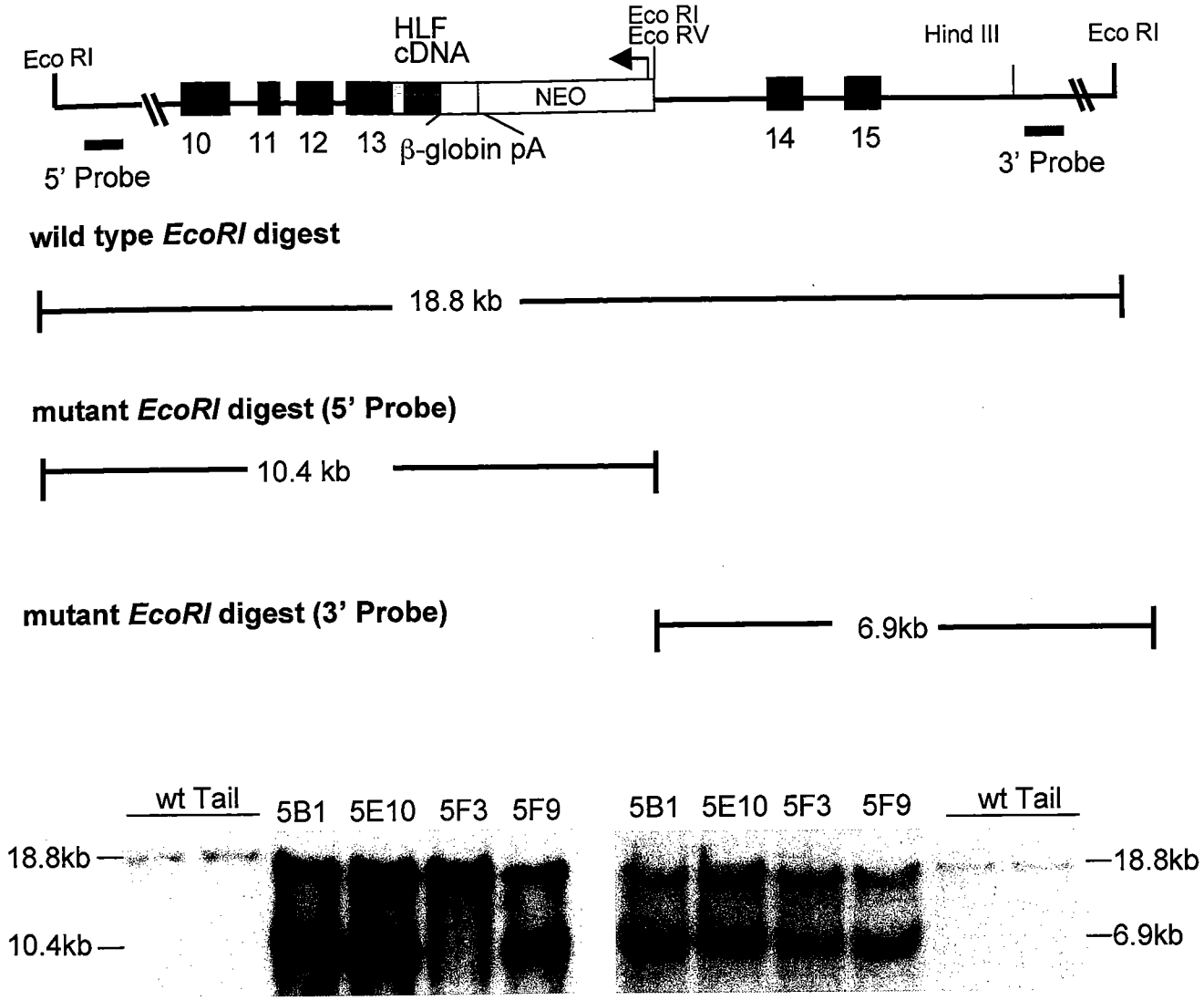

Figure 4. Screening of targeted *e2a-hlf* ES cells. Targeted ES cells were digested overnight with EcoRI and Southern blot analysis was performed. Probing with a 3' flanking probe yields a 18.8kb band corresponding to the wild type allele, and due to an EcoRI site found in the NEO cassette, the mutant band drops down to 6.9kb. Similarly, probing with a 5' flanking probe yields a 18.8 kb band for the wild type allele and a 10.4kb band for the mutant allele.

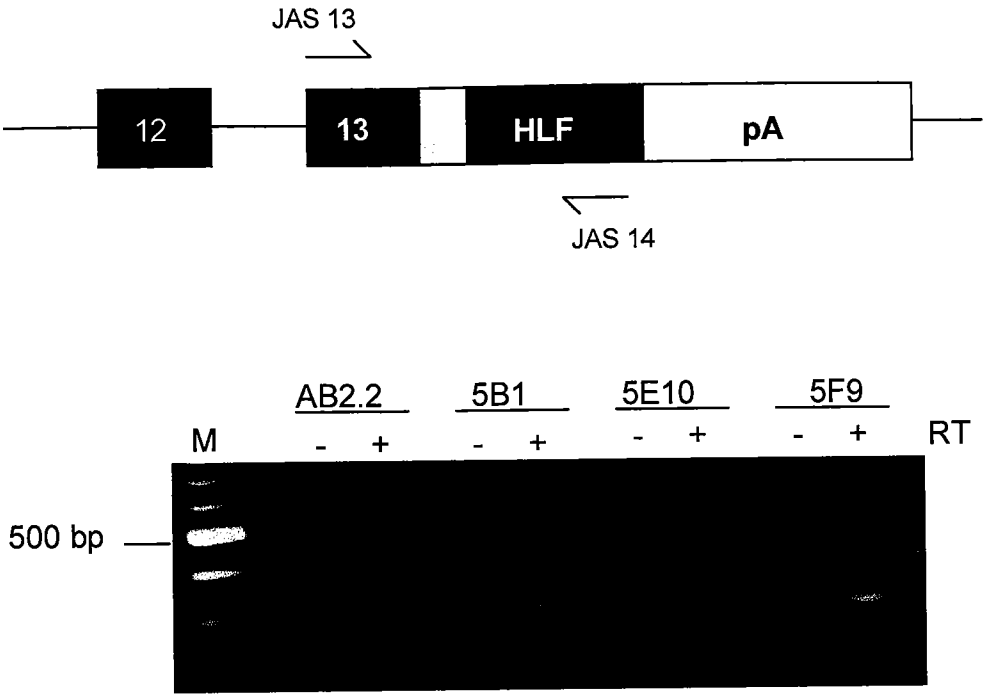

Figure 5. *e2a-hlf* is expressed in targeted ES cells. RT-PCR was performed on wild type AB2.2 and targeted ES cells. The 370bp fragment obtained using a primer to exon 13 of *e2a* and exon 4 of *HLF* corresponded to *e2a-hlf* expression.

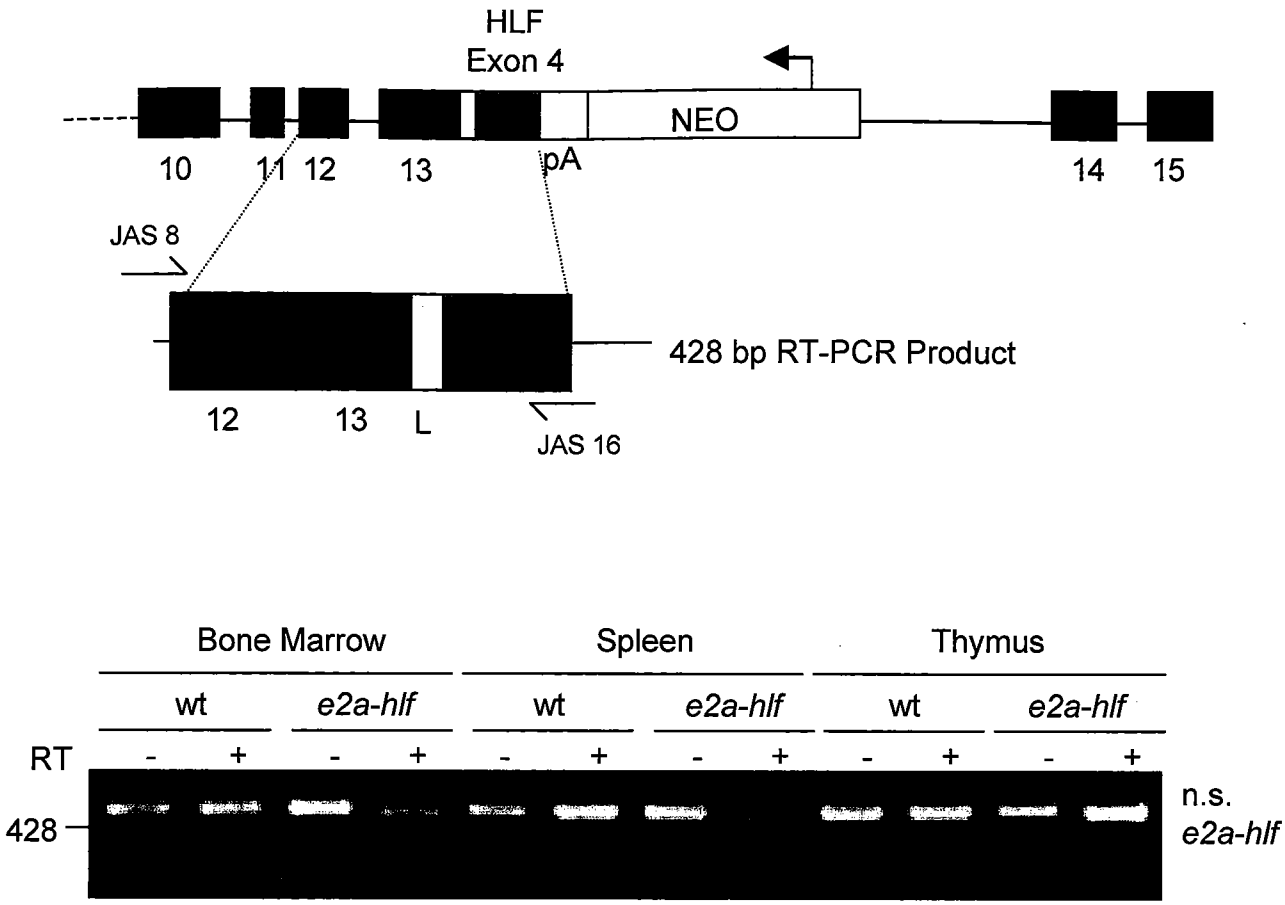

Figure 6. ***e2a-hlf*** **knock-in mice express** ***e2a-hlf*** **in lymphoid tissues.** RT-PCR was performed on bone marrow, spleen and thymus from wild type and *e2a-hlf* mice. The 428bp fragment obtained from using primers to exon 12 of *e2a* and exon 4 of *HLF* corresponds to expression of *e2a-hlf*. Sequence analysis confirmed correct splicing from exon12 to exon 13 of E2a.

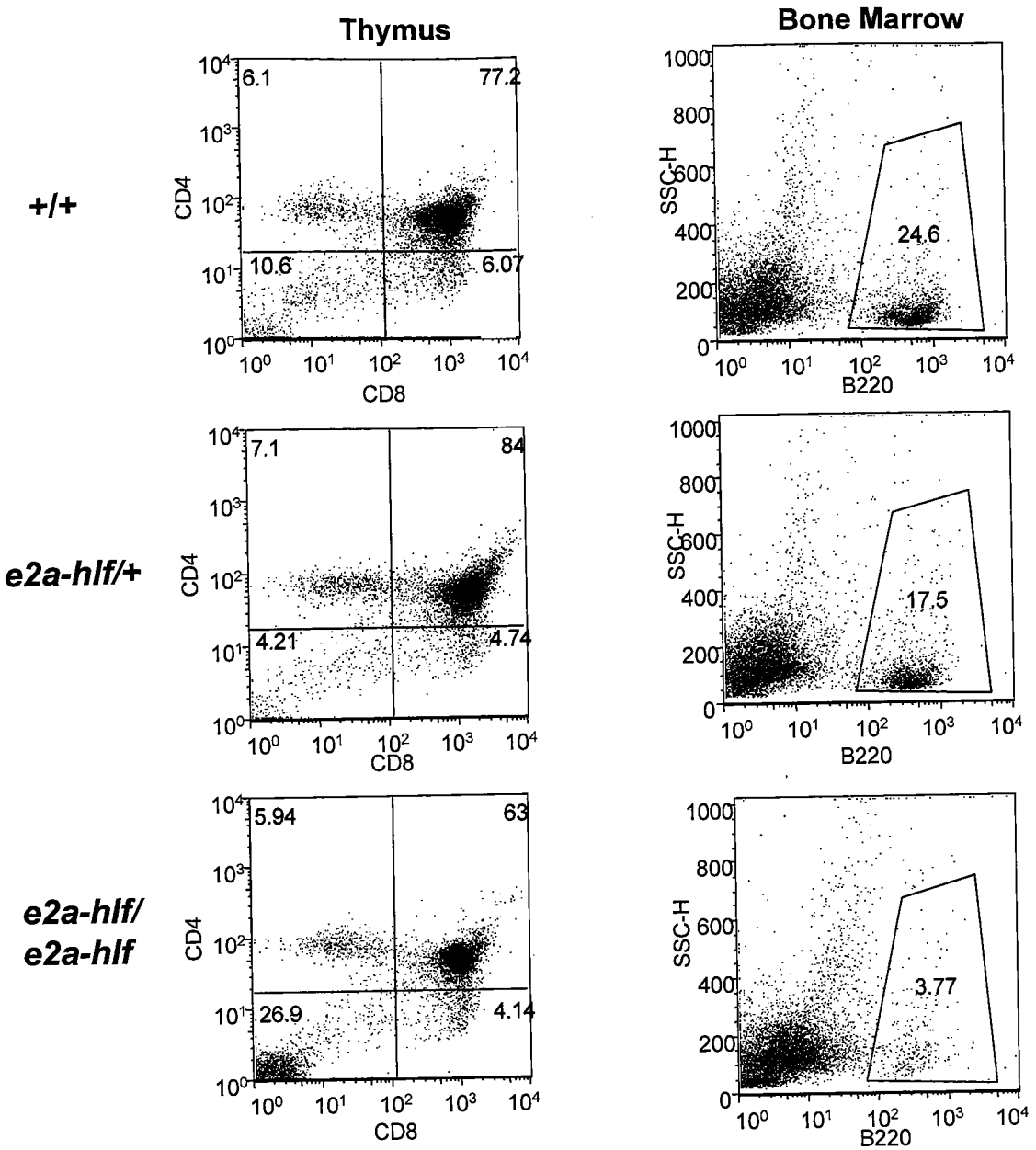

Absolute numbers

	DN	B220+
+/+	$8.8X10^6$	$7.09X10^6$
e2a-hlf/+	$5.6X10^6$	$5.86X10^6$
e2ahlf/e2a-hlf	$5.32X10^6$	$1.99X10^5$

Figure 7. Differentiation arrest in B and T lymphocytes in *e2a-hlf/e2a-hlf* mice. Bone marrow cells and thymocytes were isolated from wild type and 2-3 week old e2a-hlf heterozygous and homozygous mice and stained with anti-CD4, anti-CD8, and anti-B220 and analyzed by flow cytometry. The table lists the absolute numbers of B220+ bone marrow cells and DN thymocytes.

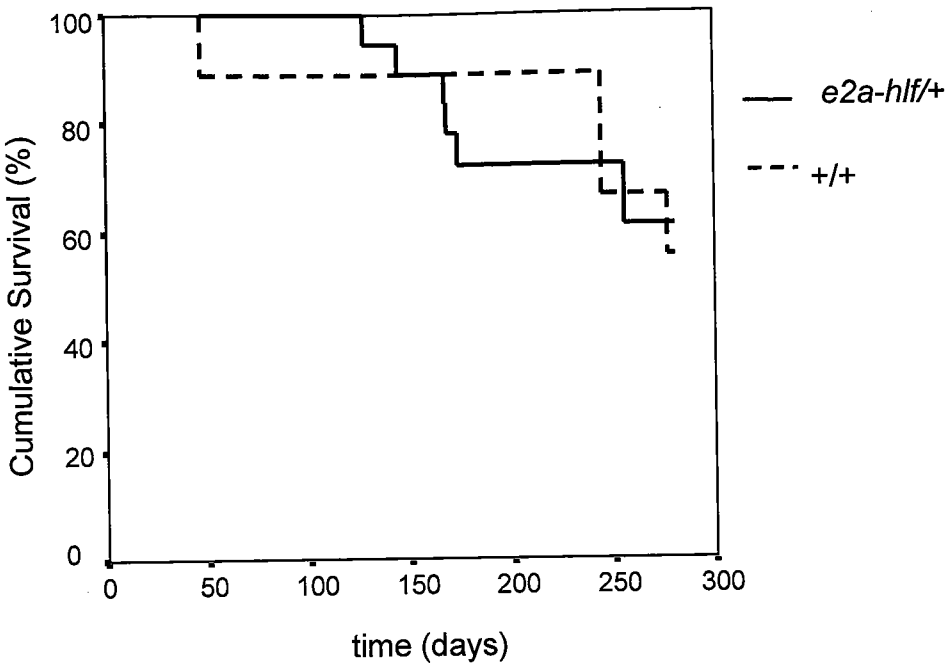

Figure 8. No acceleration of disease upon ENU-mutagenesis of *e2a-hlf* mice. Kaplan-Meier survival plot of ENU-treated *e2a-hlf* and wild type mice. A cohort of ENU-treated *e2a-hlf* cohort consisted of n=18, and ENU-treated wild type cohort consisted of n=9 animals. Mice were monitored regularly for signs of disease, and upon sacrifice, postmortem examination performed.

CHAPTER III

ALTERATION OF THE INK4A/ARF LOCUS CONTRIUBTES TO TAL1-INDUCED LEUKEMOGENESIS IN MICE

Introduction

T cell leukemia is caused by activation of several oncogenes including TAL1, LMO2, MYC, HOX11 and more recently by mutations in NOTCH1 (Ferrando et al., 2004; Look, 1997; Weng et al., 2004). We and others have shown that misexpression of Tal1 in the thymus alters thymocyte development by interfering with the expression of E47/HEB target genes including Rag1/2, Pre-Tα, CD4, CD5, CD3, and the TCRα/β chains (Herblot et al., 2000; O'Neil et al., 2001; O'Neil et al., 2004). Although Tal1 induces leukemia in mice, it does so after a long latency revealing that additional genetic events are required (Condorelli et al., 1996; Kelliher et al., 1996). Analysis of the *INK4A/ARF* locus in human T-ALL patients revealed the frequent homozygous deletion of exon 2, the common exon to both $p16^{INK4A}$ and $p14^{ARF}$ genes (Cayuela et al., 1995; Cayuela et al., 1996; Drexler, 1998; Ferrando et al., 2002; Gardie et al., 1998; Hebert et al., 1994). Additional T-ALL patients exhibit alterations in the *INK4A/ARF* locus that only affect either $p16^{INK4A}$ or $p14^{ARF}$. For example, in some cases, T-ALL patients exhibit promoter methylation of $p16^{INK4A}$, while others display specific loss of $p14^{ARF}$, as detected by loss of exon 1β (Batova et al., 1997; Drexler, 1998; Gardie et al., 1998). Ninety-two percent (13/14) of TAL1-expressing patients demonstrate deletions of exon 2, indicating the loss of $p16^{INK4A}$ and $p14^{ARF}$ may contribute to leukemogenesis (Ferrando et al., 2002). However, the relative contribution of the two tumor suppressors to leukemia remains unclear.

To model the *INK4A/ARF* deletion in mice, and to determine the overall contribution of loss of $p16^{Ink4a}$ and $p19^{Arf}$ to leukemia, we mated our *tal1* transgenic mice to *ink4a/arf-/-*, $p16^{ink4a}$*-/-*, and $p19^{arf}$*-/-* mice and generated cohorts of *tal1/ink4a/arf+/-*,

tal1/p16^{ink4a}+/- and *tal1/p19^{arf}+/-* mice. We observe disease acceleration in *tal1/ink4a/arf+/-*, *tal1/p16^{ink4a}+/-*, and *tal1/p19^{arf}+/-* mice, providing novel genetic evidence that Tal1 cooperates with loss of either p16^{Ink4a} or p19^{Arf} to cause leukemia in the mouse.

Preleukemic studies reveal that in addition to its effects on thymocyte differentiation, Tal1 expression stimulates entry into the cell cycle and thymocyte apoptosis *in vivo* (O'Neil et al., 2004). Interestingly, mice expressing a DNA binding mutant of Tal1 exhibit blocks in thymocyte development but do not show any changes in cell cycle (O'Neil et al., 2001). Hence, the ability to stimulate thymocyte proliferation appears dependent on the ability of Tal1 to bind DNA, but appears independent of the effects of Tal1 on thymocyte differentiation. Consistent with the S phase induction, an increase in thymocyte apoptosis was also observed in preleukemic *tal1* mice but not in *tal1/ink4a/arf-/-* mice, suggesting Tal1 induces apoptosis in a p19^{Arf}-p53-dependent manner. Taken together, these studies suggest that Tal1, like the c-Myc oncogene, contributes to leukemogenesis by inhibiting differentiation, stimulating cell cycle entry and activating the p19^{Arf}-p53 apoptotic pathway (Coppola and Cole, 1986; Dmitrovsky et al., 1986; Eischen et al., 1999; Evan et al., 1992).

Results

Loss of an *ink4a/arf* allele cooperates with Tal1 to induce T cell leukemia in mice.

Human TAL1-expressing T-ALL patients commonly contain deletion of the *INK4A/ARF* locus, which encodes for tumor suppressors $p16^{INK4a}$ and $p14^{ARF}$ ($p19^{Arf}$ in mice) (Ferrando et al., 2002). To test whether alteration of the *ink4a/arf* locus contributes to Tal1-induced leukemogenesis in the mouse, we mated our *tal1* transgenic mice to *ink4a/arf-/-* mice and established a cohort of *tal1/ink4a/arf+/-* mice. *Tal1* transgenic mice develop T cell lymphoblastic leukemia with a median survival period of 350 days (Kelliher et al., 1996). However, *tal1/ink4a/arf+/-* mice develop disease rapidly with a median survival period of 168 days (Figure 9). Additionally, there is a highly significant increase in disease penetrance in the *tal1/ink4a/arf+/-* mice compared to *tal1* mice ($p<0.0001$). Only 28% of *tal1* mice on a wild type background develop T cell lymphoblastic leukemia, whereas 100% of *tal1/ink4a/arf+/-* mice develop disease. The tumors that arise in *tal1/ink4a/arf+/-* mice are identical to those observed in *tal1* mice and express both CD4 and CD8 or CD8 alone (Table 1) (Kelliher et al., 1996; O'Neil et al., 2004). Interestingly 8/11 *tal1/ink4a/arf+/-* tumors express high CD25 levels, a feature also observed in thymocytes expressing activated Notch1 or T cell tumors arising in *Notch* 3^{IC} transgenic and *e2a*-deficient mice (Bain et al., 1997; Bellavia et al., 2000).

ink4a/arf alterations are detected in mouse *tal1/ink4a/arf+/-* tumors.

Since homozygous deletion of exon 2 of the *INK4A/ARF* locus is commonly observed in T cell leukemia patients (Cayuela et al., 1995; Cayuela et al., 1996; Hebert et al., 1994), we examined our mouse *tal1/ink4a/arf+/-* tumors for evidence of LOH using

PCR. Tumor DNA was isolated and genomic PCR performed to examine the integrity of $p16^{Ink4a}$-specific exon 1α, $p19^{Arf}$-specific exon 1β, and the shared exon 2 of the *ink4a/arf* locus. We detected low levels of exon 2 in 2/8 tumors examined, suggesting that the majority of cells in the tumor had undergone LOH (Figure 10A). To confirm these findings, Southern blot analysis was performed to confirm LOH in the *tal1/ink4a/arf*+/- tumors. Tumor DNA was digested with the restriction enzyme *Pst I*, transferred to a membrane and hybridized with a cDNA probe containing part of exon 1α and exon 2. Five of eighteen (27%) tumors exhibited evidence of LOH, as the wild type 9kb fragment containing exon 2 was not detected in these tumors, indicating these tumors lose expression of both $p16^{Ink4a}$ and $p19^{Arf}$ (Figure 10B and data not shown). The reduced levels of exon 2 observed in lanes 5 and 8 of the genomic PCR correspond to the LOH observed in lanes 2 and 5 of the Southern Blot, respectively (Figure 10A and B).

Southern blot analysis detects the presence of exon 1α (2.5kb band) and exon 2 in the remaining *tal1/ink4a/arf*+/- tumors examined, suggesting additional mutations or promoter methylation may affect expression of $p16^{Ink4a}$ or $p19^{Arf}$ in the remaining tumors (Figure 2B). To determine if methylation of the $p16^{ink4a}$ promoter occurs in *tal1/ink4a/arf*+/- tumors, we performed methylation-specific PCR. Genomic DNA isolated from the tumors was treated with sodium bisulfite and methylated CpG islands were amplified with primers specific for both unmethylated and methylated region of the $p16^{ink4a}$ promoter (Sharpless et al., 2001). We find evidence of $p16^{ink4a}$ methylation in 2 of 7 (28%) *tal1/ink4a/arf*+/- tumors examined, indicating that the methylation of the $p16^{ink4a}$ promoter and the subsequent loss of $p16^{Ink4a}$ expression contributes to Tal1-induced leukemia in the mouse (Figure 10C and data not shown).

Loss of either $p16^{Ink4a}$ or $p19^{Arf}$ cooperates with Tal1 to induce leukemogenesis in mice.

Human T-ALL patients frequently display homozygous loss of the *INK4A/ARF* locus, but some patients demonstrate the specific loss of $p14^{ARF}$ or $p16^{INK4A}$, indicating loss of either tumor suppressor may contribute to leukemogenesis (Cayuela et al., 1995; Cayuela et al., 1996; Drexler, 1998; Gardie et al., 1998; Hebert et al., 1994). Similarly, analysis of *tal1/ink4a/arf*+/- tumors suggested that loss of either $p19^{Arf}$ or $p16^{Ink4a}$ may contribute to disease development in the mouse. To genetically determine the relative contribution of loss of the $p16^{Ink4a}$ and $p19^{Arf}$ tumor suppressor genes to Tal1-induced leukemia in the mouse, we mated the *tal1* transgenic mice to $p16^{ink4a}$-/- or $p19^{arf}$-/- mice and generated cohorts of *tal1/*$p16^{ink4a}$+/- (n= 26) and *tal1/*$p19^{arf}$+/- mice (n=28). Consistent with the loss of $p16^{Ink4a}$ and $p19^{Arf}$ in the tumors derived from *tal1/ink4a/arf*+/- mice, both the *tal1/*$p16^{ink4a}$+/- and *tal1/*$p19^{arf}$+/- mice develop leukemia at an accelerated rate compared to *tal1* mice on a wild type background (Figure 11; $p<0.0001$ for *tal1/*$p19^{Arf}$+/- and $p<0.0092$ for *tal1/*$p16^{ink4a}$+/- mice). The difference in disease kinetics observed between *tal1/*$p19^{Arf}$+/- and *tal1/*$p16^{ink4a}$+/- mice was not statistically significant ($p=0.11$). Interestingly, differences in tumor target cell were observed. In contrast to *tal1* and *tal1/ink4a/arf*+/- mice, which display a varied immunophenotype, there was an increased number of *tal1/*$p19^{Arf}$+/- and *tal1/*$p16^{ink4a}$+/- tumors were CD8 single positive (SP), suggesting either a immature single positive (ISP) or a CD8 SP thymocyte is the target cell in these mice (Table 1) (Kelliher et al., 1996). To distinguish between these possibilities, additional FACS experiments must be

performed on premalignant and tumor cells, because ISP can be distinguished from CD8 SP by the expression of TCRβ^{lo} (Yu et al., 2004).

An increase in S phase cells in *tal1* preleukemic thymocytes

Ink4a/arf loss in the *tal1/ink4a/arf*+/- tumors suggests that ectopic expression of Tal1 may stimulate thymocyte proliferation *in vivo* and thereby trigger loss of the cell cycle inhibitor $p16^{Ink4a}$ or alternatively stimulate the oncogene sensor $p19^{Arf}$. To determine if Tal1 expression alters the cell cycle in thymocytes, we performed *in vivo*-BrdU incorporation studies on preleukemic *tal1* mice. To examine thymocyte cell cycle, wild type and *tal1* transgenic mice were injected intraperitoneally with BrdU, and following a four hour rest, thymocytes were stained with anti-BrdU antibodies. In wild type mice, 14.52% (± 1.4%) BrdU-positive thymocytes were detected. Interestingly, in the *tal1* transgenic mice, 24.47% (± 2.8%) of cells were detected in S phase of the cell cycle ($p<.008$) (Figure 12). This 70% increase in the percentage of thymocytes in S phase suggests that Tal1 expression may stimulate thymocytes to inappropriately enter the cell cycle.

S phase induction is dependent on a functional DNA-binding domain of Tal1.

Inhibition of E2A activity has been associated with increased proliferation (Iavarone et al., 1994; Lasorella et al., 1996; Pagliuca et al., 2000; Peverali et al., 1994). Tal1 and the DNA binding mutant of Tal1 (mut Tal1 R188G;R189G) inhibit E2A activity and induce leukemia in mice (O'Neil et al., 2001; O'Neil et al., 2004). Therefore, the S phase induction may be mediated by the ability of Tal1 (and mut Tal1 R188G;R189G) to

inhibit the transcriptional activity of E47/HEB. Alternatively, the ability to stimulate the cell cycle may reflect the ability of the Tal1/E47 or Tal1/HEB heterodimers to transactivate the expression of novel genes. In order to distinguish between these possibilities, we compared thymocyte proliferation in preleukemic *tal1* and *mut tal1 R188G;R189G* transgenic mice. In contrast to the 24.47% (±2.8%) S phase cells observed in *tal1* mice, *mut tal1 R188G;R189G* mice contain 15.2% (±2.1%) cells in S phase of the cell cycle, similar to the 15.5% (±1.5%) observed in wild type littermates (Figure 13). Thus, the ability of Tal1 to stimulate the cell cycle appears dependent on a functional DNA-binding domain and suggests that Tal1/E47 or Tal1/HEB heterodimers stimulate S phase by influencing gene expression. Thus, although the DNA binding mutant of mut Tal1 R188G;R189G functions like an Id and interacts with and inhibits E protein function, it appears unable to affect cell cycle control.

Tal1 stimulates thymocyte apoptosis *in vivo* that is $p19^{Arf}$ dependent.

Oncogenes, such as c-Myc and E1a, stimulate inappropriate entry into the cell cycle and activate a protective apoptotic pathway that involves activation of the $p19^{Arf}$-p53 proteins (Evan et al., 1992; Rao et al., 1992; Zindy et al., 1998). Consistent with this, BrdU analysis demonstrates that the S phase induction observed in preleukemic *tal1* thymocytes is accompanied by an increase in $subG_1$ cells (Figure 6). Although the percentage of apoptotic thymocytes was variable and ranged from a 5-10 fold increase in $subG_1$ cells, the percentage of $subG_1$ thymocytes consistently correlated with the increase in S phase cells observed. To test whether Tal1-associated apoptosis requires an intact *ink4a/arf* locus, we examined thymocyte proliferation/apoptosis in an *ink4a/arf-/-* genetic

background. In contrast to Tal1 expression in a wild type or *ink4a/arf* heterozygous background which results in 12% subG$_1$ cells, only 2.7% of thymocytes were detected in the subG$_1$ population when Tal1 was expressed on a *ink4a/arf-/-* background (Figure 14). Therefore, the induction of apoptosis associated with Tal1 activation appears dependent on p19^{Arf}. In contrast, the S phase cells induction is observed on both the *ink4a/arf+/-* and *ink4a/arf-/-* backgrounds, indicating the ability of Tal1 to stimulate S phase entry is independent of the p16^{Ink4a} locus (Figure 14).

Notch and Wnt activation in preleukemic *tal1* thymocytes

To identify how Tal1 activation may stimulate thymocyte proliferation, we used gene expression profiling to compare genes activated/repressed in Tal1 expressing thymocytes compared to littermate controls. Consistent with the perturbed thymocyte development observed in preleukemic *tal1* mice and with our previous microarray experiments performed on *tal1* DP thymocytes (O'Neil et al., 2004), we found the expression of multiple E47/HEB target genes repressed in *tal1* thymocytes including Rag1/2, pre-Tα, CD4,CD5, and CD6 (Table 2).

Interestingly, consistent with the S phase induction, analysis of Tal1-regulated genes revealed activation of the Notch and Wnt receptor pathways. Specifically, Wnt5b and its downstream target gene, c-Myc, appeared upregulated in *tal1* thymocytes compared to littermate controls (Table 2) (He et al., 1998). In fact, real-time PCR analysis reveals on average a 32-fold increase in Wnt5b expression in preleukemic *tal1* thymocytes (Figure 15). Additionally, evidence of Notch activation was also detected in preleukemic *tal1* thymocytes with increased expression of the Notch 1 target genes,

Deltex, CD25, and Hes1, in preleukemic *tal1* thymocytes (Table 2 and Figure 15). As activation of the Wnt and Notch pathways have been implicated in regulating cell proliferation, activation of these signaling pathways in preleukemic *tal1* thymocytes raises the possibility they may be responsible for the increased thymocyte proliferation observed in *tal1* mice.

Discussion

We and others have shown that Tal1 expression perturbs thymocyte development by interfering with the expression of E47/Heb target genes (Herblot et al., 2000; O'Neil et al., 2004). Although Tal1 has been implicated in the proliferation of hematopoietic precursors (Condorelli et al., 1997; Green et al., 1991; Valtieri et al., 1998), this study suggests that Tal1 stimulates cell cycle entry in preleukemic thymocytes. The S-phase induction observed in *tal1* thymocytes during the preleukemic phase of the disease is accompanied by an increase in apoptosis that appears $p19^{Arf}$-dependent. Thus, ectopic expression of Tal1 shares features with deregulated c-Myc, in that both bHLH proteins inhibit differentiation and are capable of stimulating the cell cycle and inducing apoptosis *in vivo* (Coppola and Cole, 1986; Eischen et al., 1999; Evan et al., 1992).

Independent of its effects on thymocyte differentiation, Tal1 stimulates the cell cycle and this appears to be an effect of the Tal1/E47 or Tal1/HEB heterodimers on transcription, as no increase in S phase cells is observed in mice expressing a DNA binding mutant of Tal1. Although it remains unclear how the increase in S phase cells is mediated by Tal1, analysis of gene expression profiles influenced by Tal1 suggests that the cell cycle effects may involve activation of the Wnt and/or the Notch receptor pathways. We find Wnt5b and Myc, Deltex, Hes1 and CD25α expression induced in preleukemic *tal1* thymocytes compared to littermate controls. Activation of either the Notch and Wnt pathways inhibit differentiation and therefore promote self-renewal in multiple stem cells lineages, such as: hematopoetic (Reya et al., 2003; Varnum-Finney et al., 2000), intestinal (Fre et al., 2005; Pinto et al., 2003; van Es et al., 2005), and muscle (Polesskaya et al., 2003). Additionally, multiple studies demonstrate cross-talk between

these two pathways, indicating cooperativity in regulating self-renewal and proliferation (Espinosa et al., 2003; Galceran et al., 2004). In addition, recent studies suggest that the Wnt and Notch1 pathways may synergize to inhibit differentiation and promote self renewal in hematopoietic stem cell populations (Duncan et al., 2005), raising the possibility that a similar pathway may be activated in Tal1-induced leukemia.

Mice expressing a DNA binding mutant of Tal1 develop disease, questioning the overall biologic significance of the effects of Tal1 on the cell cycle (O'Neil et al., 2001). We speculate that the inappropriate cell cycle entry and apoptosis associated with Tal1 expression *in vivo* may provide additional selective pressure to disrupt the *ink4a/arf* locus. This hypothesis predicts that *ink4a/arf* alterations would be observed at greater frequencies in tumors derived from *tal1* transgenic mice than in tumors derived from the DNA binding mutant mice.

Disruption of the *ink4a/arf* allele is an important genetic event in Tal1-induced leukemia with both alterations of both $p16^{Ink4a}$ and $p19^{Arf}$ observed in *tal1/ink4a/arf*+/- tumors. Unlike the published studies on *Eμ-myc/ink4a/arf*+/- mice which all undergo LOH (Eischen et al., 1999), 27% of the *tal1/ink4a/arf*+/- tumors exhibit LOH and an additional 28% of tumors exhibit methylation of the $p16^{ink4a}$ promoter. In contrast to the common perception that loss of $p16^{Ink4a}$ is the important genetic event in leukemia, we provide important evidence that loss of not only $p16^{Ink4a}$ but also $p19^{Arf}$ cooperates with Tal1 expression in leukemogenesis. Both *tal1*/$p16^{ink4a}$+/- and *tal1*/$p19^{arf}$+/- mice exhibit an increased penetrance and disease acceleration compared to *tal1* mice on a wild type background. Therefore, the work presented in this thesis may change the common

viewpoint that only the loss of $p16^{Ink4a}$ contributes to leukemogenesis, and entice the field to determine how loss of $p14^{Arf}$ contributes to leukemia.

This study demonstrates that loss of $p16^{Ink4a}$ or $p19^{Arf}$ cooperates with ectopic Tal1 expression to induce T cell leukemia in mice. Studies of leukemic patients suggest that *INK4A/ARF* loss is a poor prognostic indicator of ALL and consistent with these observations, *tal1/ink4a/arf*+/-, *tal1/*$p16^{ink4a}$+/- and *tal1/*$p19^{arf}$+/- mice rapidly develop disease (Harrison, 2001; Kees et al., 1997; Zhou et al., 1997). Importantly, 100% of *tal1/ink4a/arf*+/- mice develop T cell leukemia, making this model useful for testing the sensitivity of these mice to current therapies and for the development of new therapeutics.

Materials and Methods

Mice and tumor cell culture

Proximal *lck-tal1* and *mut tal1 R188G;R189G* mice have been described previously (Kelliher et al., 1996; O'Neil et al., 2001). *ink4a/arf* -, $p16^{ink4a}$- and $p19^{arf}$- deficient mice have been described previously (Kamijo et al., 1997; Serrano et al., 1996; Sharpless et al., 2001) and obtained from the Mouse Models of Human Cancers Consortium (MMHCC). Cohorts of *tal1/ink4a/arf*+/- (n=27), *tal1/*$p16^{ink4a}$+/- (n=20), *and tal1/*$p19^{arf}$+/- (n=26) mice were established and monitored daily for signs of disease. Kaplan-Meier analysis was performed on, *tal1/ink4a/arf*+/- mice, *tal1/*$p16^{ink4a}$+/- mice, and *tal1/*$p19^{arf}$+/- mice and compared to *tal1* mice on a wild type background. All mice are maintained on a FVB/N genetic background.

Flow Cytometry

Primary tumor cells were stained with PE-conjugated anti-mouse Ly-2 (CD8), FITC-conjugated L3T4 (CD4), and PE-conjugated CD25 antibodies (BD Pharmingen, San Diego, CA) and analyzed using flow cytometry. For *in vivo*-BrdU-incorporation assays, four- to six-week old *tal1*, *mut tal1 (R188G;R189G)*, *tal1/ink4a/arf*+/-, and *tal1/ink4a/arf-/-* mice were injected intraperitoneally with 1mg bromodoxyuridine (BrdU) and allowed to rest for 3 hours. The mice were injected again with 1mg of BrdU and allowed to rest for 1 h. Thymocytes were isolated and $2x10^6$ cells were stained with anti-mouse Ly-2 (CD8), FITC-conjugated L3T4 (CD4) antibodies. The thymocytes were then fixed, permeabilized and stained with APC-conjugated anti-BrdU antibody and 7-amino-actinomycin D (7-AAD) as described in APC BrdU Flow kit (BD Pharmingen). Values

are provided as mean ± standard deviation, and p-values are from Student's t-test analysis.

Real-time PCR

Wnt5b real-time primer sequences were obtained from Georg A. Holländer 5'-GGC-ATT-GGG-ATG-GGT-TGA-GG-3' and 5'-GGA-GTT-GGC-GTC-AGT-CAG-CAG-3'. Primers for c-Myc (5'-CTG-TTT-GAA-GGC-TGG-ATT-TCC-T-3' and 5'-GTC-GTG-GCT-GTC-TGC-GG-3'), Deltex (5'-TGC-CTG-GTG-GCC-ATG-TAC-T-3' and 5'-GAC-ACT-GCA-GGC-TGC-CAT-C-3'), and Notch1 (5'-AAG-AGC-TGC-GCA-AGC-ACC-3' and 5'-TAG-ACA-ATG-GAG-CCA-CGG-ATG-3') were designed using Primer Express (Applied Biosystems). Relative quantities of mRNA expression were analyzed using QRT-PCR in the presence of SYBR green (Applied Biosystems ABI Prism 7300 Sequence Detection System, Applied Biosystems). For the normalization of each sample the expression level of the gene was divided by that of β-actin. The relative expression level was determined by comparing the normalized value (/β-actin) to that in the reference sample (another normal tissue) included in the same reaction.

Microarray Analysis

Thymocytes were pooled from four age-matched (4 weeks) wild type and *tal1* mice, RNA extracted using Trizol reagent (Invitrogen, Carlsbad, CA), and purified using Qiagen RNeasy Mini Kit (Qiagen, Valencia, CA). RNA was hybridized to Affymetrix Mouse Genome 430A 2.0 arrays (Affymetrix, Santa Clara, CA). Data sets were analyzed using Rosetta Resolver by Manoj Bhasin (Dana Farber Cancer Institute).

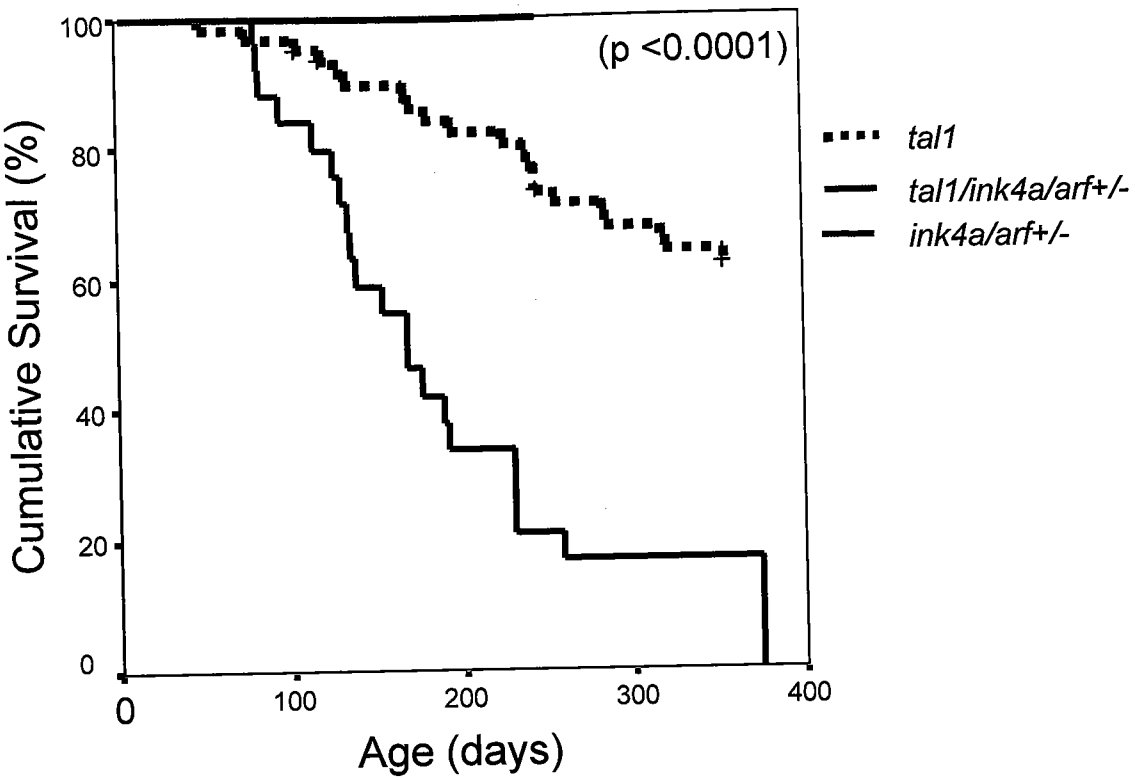

Figure 9. Disease acceleration in *tal1/ink4a/arf*+/- mice. Kaplan-Meier survival plot of *tal1* and *tal1/ink4a/arf*+/- mice is shown. The *tal1* cohort consisted of n=64 animals, and the cohort of *tal1/ink4a/arf*+/- mice consisted of n=27. Tarone-Ware statistical analysis demonstrates a highly statistically significant difference in survival between the *tal1* transgenic mice and the *tal1* transgenic mice on the *ink4a/arf* heterozygous background ($p < 0.0001$).

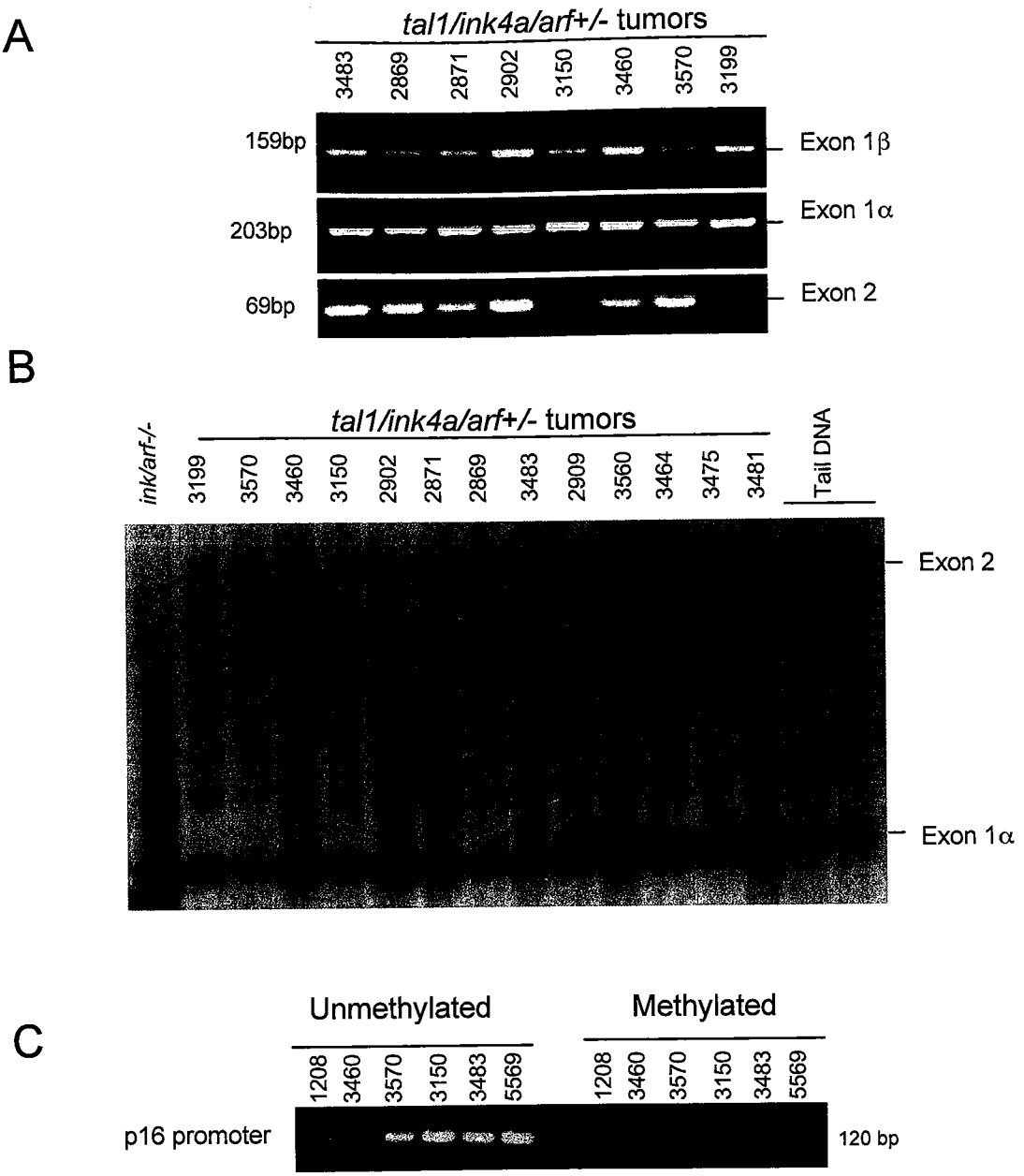

Figure 10. Alterations in the *ink4a/arf* locus in *tal1/ink4a/arf*+/- tumors. A) To examine the integrity of the *ink4a/arf* locus, genomic DNA was isolated from *tal1/ink4a/arf*+/- tumors and screened for the presence of exon 1α, exon 1β, and exon 2 using PCR. **B)** To further analyze the status of exon 2, genomic DNA from *tal1/ink4a/arf*+/- tumors was digested with *Pst I*, transferred to a membrane, and probed with cDNA probe corresponding to exon 1α and exon 2. **C)** To analyze the methylation status of the $p16^{ink4a}$ promoter, bisulfite-treated *tal1/ink4a/arf*+/- tumor DNA was amplified using primers specific for the $p16^{ink4a}$ methylated promoter and $p16^{ink4a}$ unmethylated promoter as described in (Sharpless, Bardeesy et al. 2001).

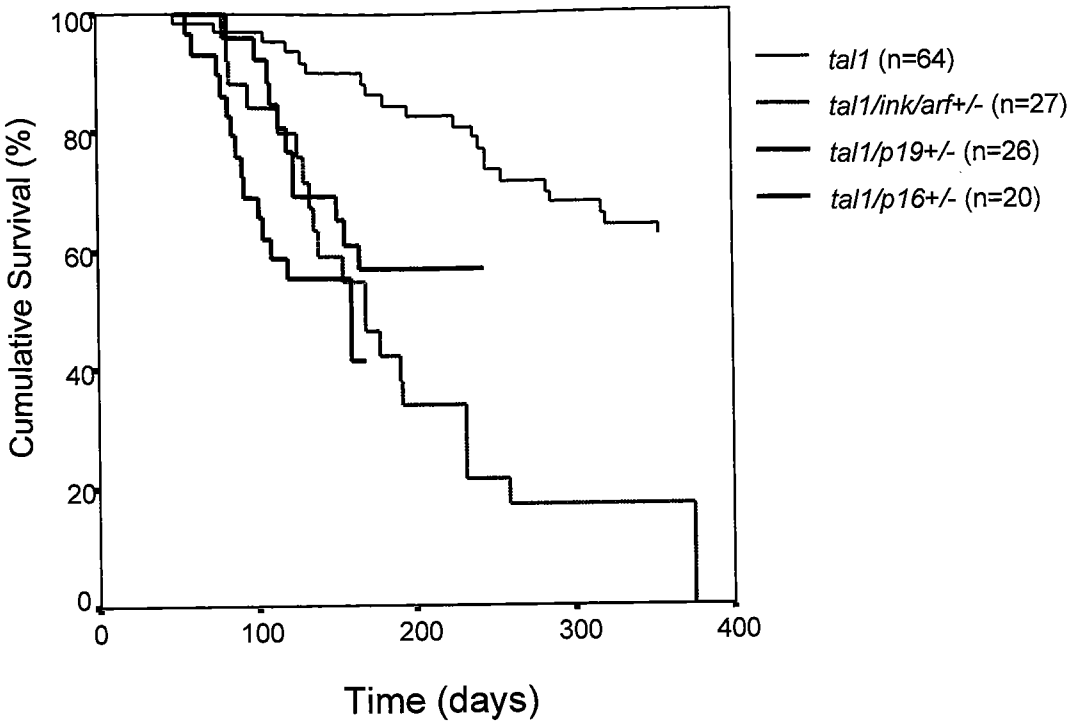

Figure 11. Disease acceleration in *tal1/p16^{ink4a}+/-* and *tal1/p19^{arf}+/-* mice. Kaplan-Meier survival plot of *tal1, tal1/ink4a/arf+/-, tal1/p16^{ink4a}+/-*, and *tal1/p19^{arf}+/-* mice is shown. Tarone-Ware statistical analysis demonstrates a highly statistically significant difference in survival between the *tal1* transgenic mice and the *tal1/p16^{ink4a}* mice (p =.0092), or the *tal1/p19^{arf}+/-* mice (p=0.00001)

Table 1. Immunophenotype of *tal1/ink/arf+/-, tal1/p16+/-, and tal1/p19+/-* tumors

Animal Number	Genotype	CD3	CD4	CD8	CD4, CD8	CD25	Phenotype	Survival (days)
2869	*tal1/ink/arf+/-*	9	1	98	1	25	CD8 SP	95
2902	*tal1/ink/arf+/-*	20	96	97	95	98	DP	168
2906	*tal1/ink/arf+/-*	22	75	88	72	88	DP	134
2912	*tal1/ink/arf+/-*	9	16	76	9	25	CD8 SP	177
2913	*tal1/ink/arf+/-*	10	98	98	97	98	DP	130
2914	*tal1/ink/arf+/-*	23	93	95	92	9	DP	139
3199	*tal1/ink/arf+/-*	99	99	0	0	65	CD4 SP	126
3470	*tal1/ink/arf+/-*	59	74	19	81	98	DP	82
3483	*tal1/ink/arf+/-*	52	24	96	23	99	CD8 SP	80
3569	*tal1/ink/arf+/-*	11	58	77	54	98	DP	81
3570	*tal1/ink/arf+/-*	6	48	93	47	99	DP, CD8 SP	83
4432	*tal1/p16+/-*	12	3	96	2	3	CD8 SP	115
4436	*tal1/p16+/-*	14	78	92	79	88	DP	109
4437	*tal1/p16+/-*	25	12	56	10	7	CD8 SP	123
4438	*tal1/p16+/-*	10	27	74	21	2	CD8 SP	123
4439	*tal1/p16+/-*	2	83	15	15	96	CD4SP	108
4442	*tal1/p16+/-*	10	5	92	4	4	CD8 SP	120
5406	*tal1/p16+/-*	17	10	96	9	4	CD8 SP	100
5409	*tal1/p16+/-*	27	30	71	2	6	CD8 SP	150
5415	*tal1/p16+/-*	8	5	98	4	5	CD8 SP	82
4393	*tal1/p19+/-*	54	5	88	5	99	CD8 SP	88
5129	*tal1/p19+/-*	91	16	85	15	83	CD8 SP	92
5131	*tal1/p19+/-*	72	98	98	98	98	DP	102
5138	*tal1/p19+/-*	20	34	67	1	3	CD8 SP	56
5519	*tal1/p19+/-*	42	42	82	38	92	CD8 SP, DP	79
5521	*tal1/p19+/-*	28	90	9	10	5	CD4 SP	109
5522	*tal1/p19+/-*	6	1	71	38	0	CD8 SP	82
5587	*tal1/p19+/-*	50	40	49	36	56	CD8 SP, DP	60
5588	*tal1/p19+/-*	98	65	25	18	53	CD4 SP	85

Tumors were stained with antibodies to CD3, CD4, CD8 and CD25 and analyzed by flow cytometry. Tumors were considered positive if >10% of the tumor stained for that antibody.

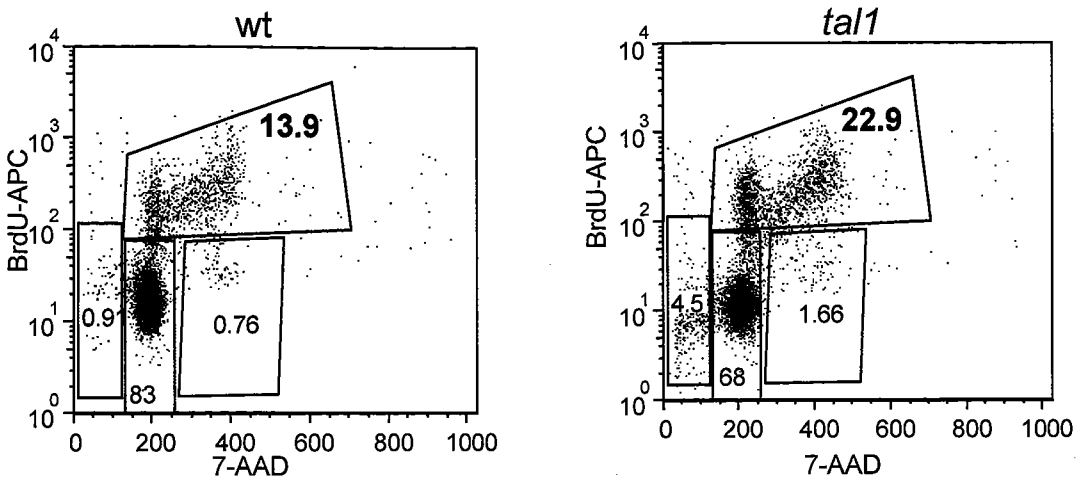

Figure 12. Increase in S phase cells in *tal1* premalignant thymus. To measure thymocyte proliferation, *in vivo* BrdU-incorporation analyses were performed on four-week old wild type and *tal1* mice. The mice were injected intraperitoneally twice with 1mg BrdU, and four hours later, the thymocytes were stained with an anti-BrdU antibody and analyzed by flow cytometry. *Tal1* thymocytes show a statistically significant increase in BrdU-positive cells compared to wild type ($p=0.0025$). A representative of five independent experiments is shown.

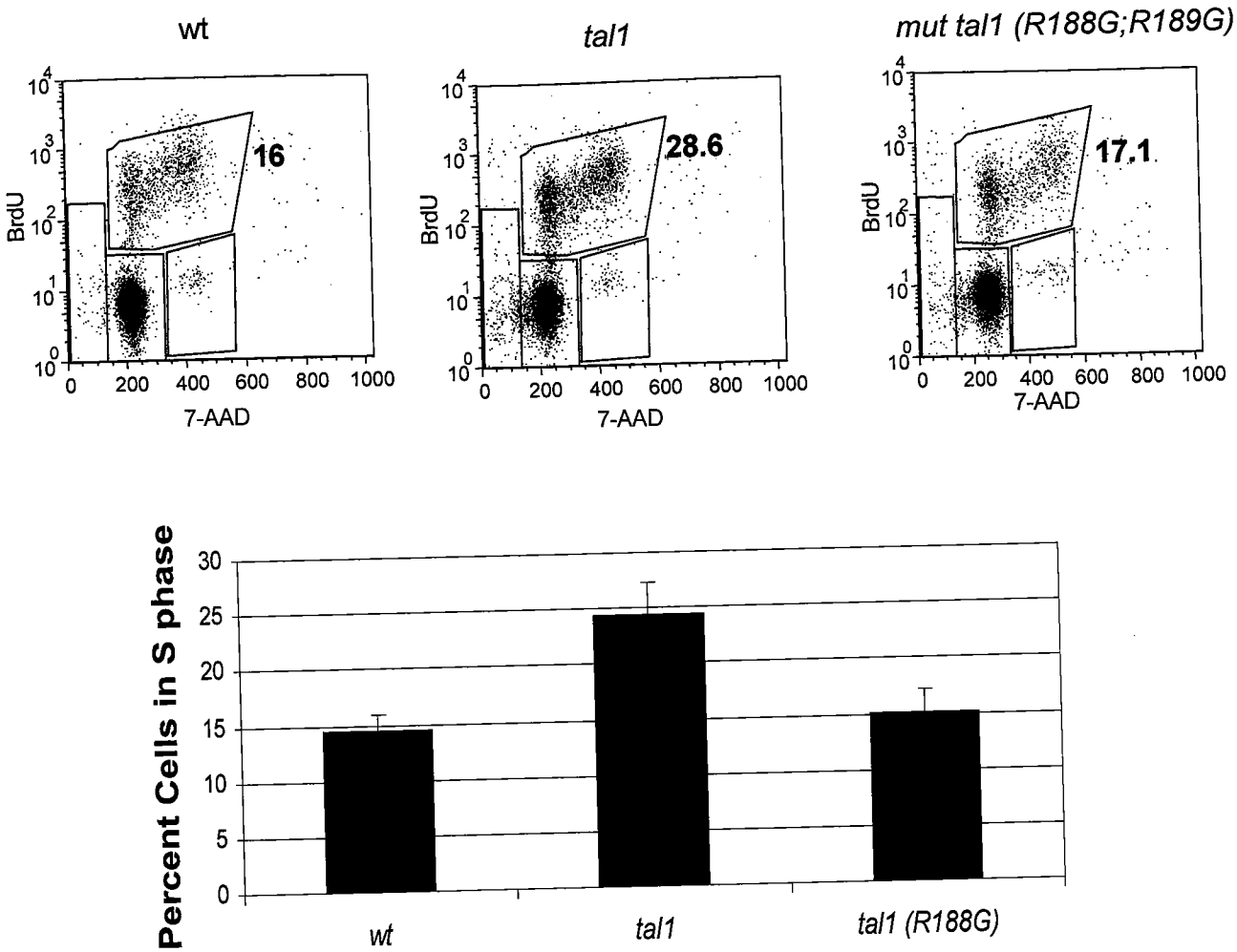

Figure 13. Increase in S-phase cells is observed in *tal1* transgenic mice but not in mice expressing a DNA binding mutant of mut tal1 (R188G;R189G). To determine if DNA-binding domain is essential for the increase in S-phase cells, *in vivo* BrdU-incorporation experiments were performed on wild type, *tal1* transgenic, and *tal1 R188G;R189G* transgenic mice. Mice were injected IP twice with 1 mg of BrdU and following a 4 hour rest, thymocytes were stained with antibodies to BrdU and analyzed by flow cytometry. *Mut tal1(R188G;R189G)* mice have decreased levels of BrdU-positive cells compared to *tal1* thymocytes (p=.02). Three wild type, three *tal1* and three *mut tal1(R188G;R189G)* transgenic animals were analyzed.

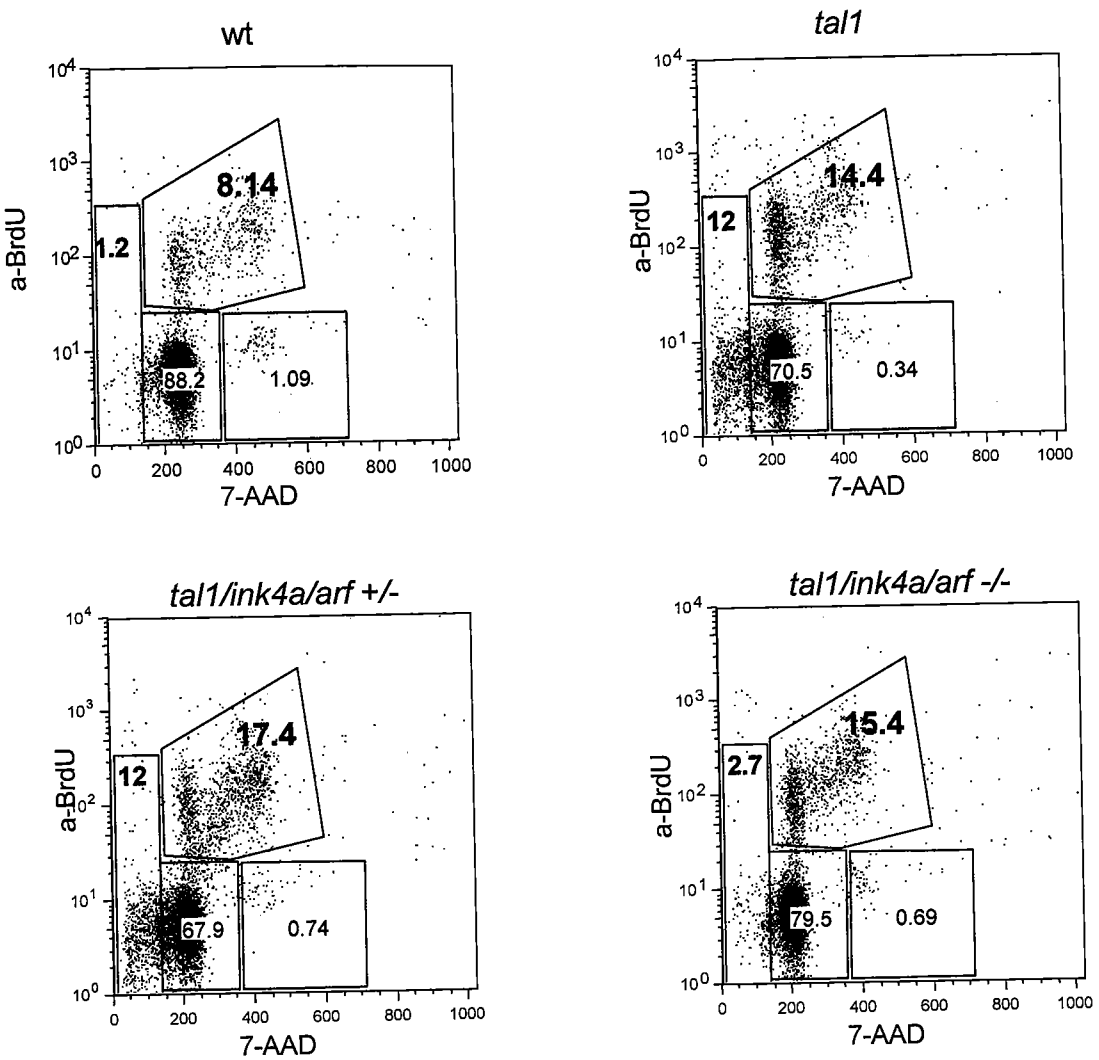

Figure 14. Thymocyte apoptosis in *tal1* but not *tal1/ink4a/arf-/-* thymocytes. To determine if Tal1 activates the $p19^{Arf}$-p53 pathway, *in vivo* BrdU-incorporation analyses were performed as described on wild type, *tal1*, *tal1/ink4a/arf+/-* and *tal1/ink4a/arf-/-* mice and analyzed by flow cytometry. The increase in S phase cells was accompanied by an increase in subG1 cells, and this Tal1-mediated increase in subG1 cells is not observed in the absence of the *ink4a/arf* allele. A representative of three independent experiments is shown.

Table 2: Genes Found Altered in *tal1* Thymocytes

Description of gene (accession number)	Fold change	p-value
CD5 antigen (NM_007650)	-5.4	0
Rag2 (NM_009020)	-4.8	9.05E-30
CD6 antigen (U12434)	-4.4	0
Bcl-X_L(NM_009743)	-4.4	1.36E-14
ROR-gamma (AJ132394)	-3.0	1.57E-23
CD4 antigen (NM_013488)	-2.9	1.31E-28
Id2 (NM_010496)	-2.8	1.80E-14
Bcl2 (NM_009741)	-2.8	0.00627
pre T-cell antigen receptor alpha (NM_011195)	-2.1	1.96E-08
Rag1 (NM_009019)	-1.8	6.46E-15
Myc (BC006728)	+2.0	1.20E-14
IL2R alpha (AF054581)	+2.5	2.52E-08
Deltex 1 (AB015422)	+3.3	4.92E-14
Cdk6 (NM_009873)	+3.7	0.00216
Wnt5b (NM_009525)	+8.9	0.00037

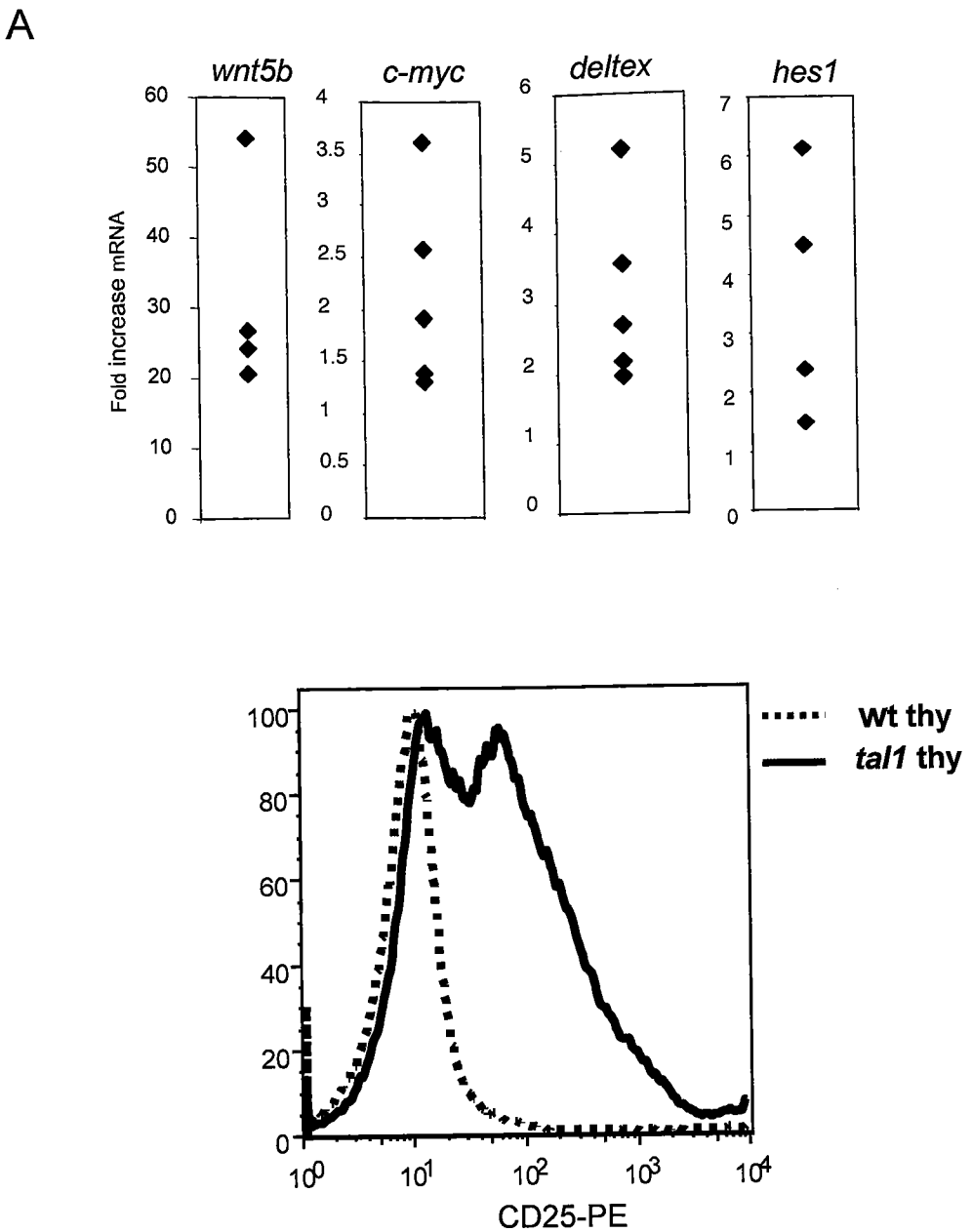

Figure 15. Activation of Notch and Wnt pathways in *tal1* premalignant thymocytes. A) Premalignant *tal1* thymocytes express increased levels of Wnt5b, c-Myc, Deltex and Hes1. To validate activation of Notch and Wnt pathways, real-time PCR was performed on 4 week old wild type and *tal1* thymoctyes. **B) *Tal1* thymocytes express increased levels of CD25.** To assay CD25 levels, wild type and *tal1* premalignant thymocytes were stained with anti-CD25-PE, stained and analyzed by flow cytometry. **C) Increased CD25 expression is seen in all subsets of Tal1 thymocytes** (continued on page 82). Wild type and *tal1* thymocytes were stained with CD4, CD8, CD25, and analyzed by flow cytometry to determine CD25 expression within DN, SP, and DP subsets.

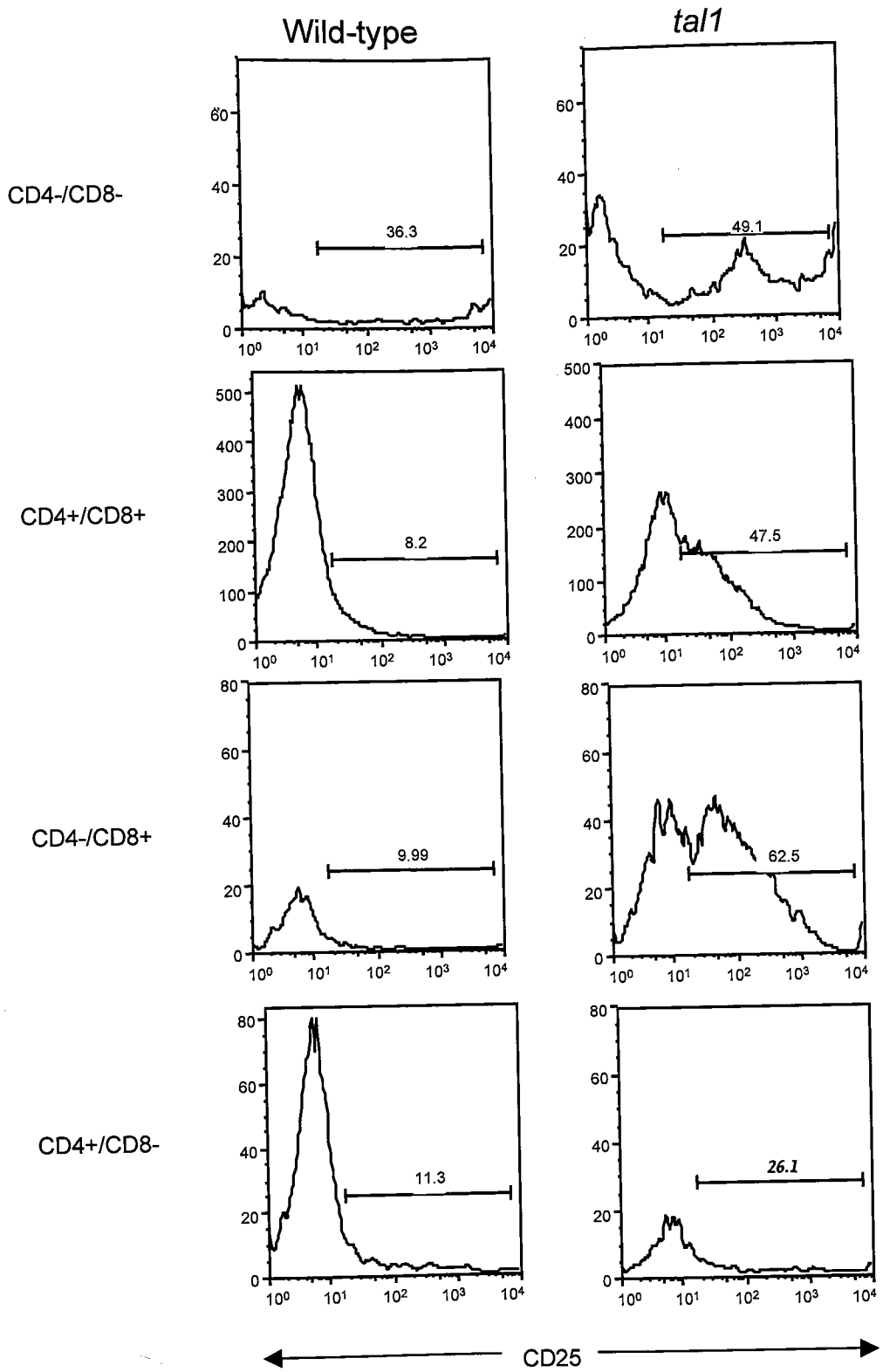
Wild-type
tal1
CD4-/CD8-
CD4+/CD8+
CD4-/CD8+
CD4+/CD8-
36.3
49.1
8.2
47.5
9.99
62.5
11.3
26.1
CD25

CHAPTER IV

ACTIVATION OF THE NOTCH1 PATHWAY COMMON IN *TAL1*-MEDIATED LEUKEMOGENISIS IN THE MOUSE

Introduction

Tal1 is a bHLH transcription factor that is found misexpressed in the thymus in 60% of T-cell acute lymphoblastic leukemia (T-ALL) patients (Bash et al., 1995). Significantly, TAL1-expressing T-ALL patients exhibit a less favorable prognosis, with a five year survival of 43%, indicating additional therapies are crucial for TAL1 leukemic patients (Ferrando et al., 2002). To model the misexpression of TAL1, we previously generated *lck-tal1* transgenic mice, which develop T cell leukemia with a long latency of 350 days, signifying that additional genetic events are required (Kelliher et al., 1996).

Notch1 is a member of an evolutionarily conserved family of proteins essential for cell fate determination. Notch1 is a transmembrane receptor that binds to ligands of the Jagged- and Delta- family. Upon ligand binding, two successive cleavage events occur, which allow the intracellular domain of Notch1 ($Notch^{IC}$) to translocate to the nucleus (De Strooper et al., 1999). Within the nucleus, $Notch^{IC}$ binds to and displaces the corepressors from CSL/RBP-Jκ, thereby relieving transcriptional repression (Kurooka and Honjo, 2000; Oswald et al., 2001). $Notch^{IC}$ then recruits Mastermind (MAML), and the coactivators p300, GCN5, and PCAF to activate transcription of target genes such as Hes1, Deltex, and preT-alpha (Deftos et al., 1998; Kurooka and Honjo, 2000; Oswald et al., 2001).

Notch1 was first implicated in leukemogenesis through the t(7;9)(q34;q34.3) translocation, which juxtaposes the *NOTCH1* gene to the TCRβ locus (Ellisen et al., 1991). This translocation, associated with less than 1% of T cell leukemic patients (Ma et al., 1999), leads to a truncated, constitutively active allele capable of signaling in a ligand-independent manner. The leukemogenic properties of this constitutively active

Notch^{IC} protein has been demonstrated *in vitro*, in bone marrow transplantation experiments in mice, and in Notch^{IC}-expressing transgenic mice (Capobianco et al., 1997; Deftos et al., 2000; Pear et al., 1996; Robey et al., 1996). A recent study demonstrates *NOTCH1* activation and HES1 expression, in all leukemic samples tested (Chiaramonte et al., 2003). In addition, 56% of T-ALL patients and specifically 39% of TAL1-expressing patients exhibit mutations within the heterodimerization (HD) and/or PEST domains of NOTCH1 (Weng et al., 2004). Together these studies suggest that activating NOTCH1 mutations may be an important event in T cell leukemogenesis.

In this study, we used retroviral insertional mutagenesis to identify genes that cooperate with Tal1 to induce leukemia in mice. Interestingly, 32% of infected tumors harbored Moloney Murine Leukemia Virus (MoMLV) integrations in the midregion of the *notch1* gene, which would lead to constitutive active allele. The tumors remain dependent on Notch1 signaling as Notch1 target genes, Hes1 and Deltex, remain expressed. Consistent with Tal1 cooperating with Notch1 activation in leukemogenesis, spontaneous *tal1* tumors also commonly activate the Notch1 pathway, as observed through increased levels of cleaved intracellular Notch, and the induction of Notch target genes. In addition, Notch1 activation in *tal1* tumor cell lines frequently conferred sensitivity to γ-secretase inhibitors. Additionally, mutational analysis of Notch1 in *tal1* tumors revealed frequent mutations in the HD and/or PEST domains.

To identify Notch^{IC} target genes responsible for G_0/G_1 arrest and apoptosis, we developed a doxycycline (dox)-regulated Notch^{IC} leukemic cell line by converting to culture tumors arising in *Eμ/tTA/Notch^{IC}/tal1* triple transgenic mice. Doxycycline treatment results in an increase in subG_1 and G_0/G_1 cells, indicating Notch provides both

a proliferative and an anti-apoptotic response in leukemic cells. We performed microarray analysis on this conditional Notch^{IC} T-ALL cell line to determine the Notch^{IC} target genes that may contribute to leukemogenesis. In addition to the regulation of many known Notch target genes, new putative target genes were identified. Interestingly, Ingenuity pathway analysis and quantitative real-time PCR demonstrated activation of the c-Myc pathway in the presence of Notch^{IC}. The activation of Myc provides insight as to how Notch^{IC} may contribute to leukemogenesis

Results

The Notch1 locus is a common insertion site in MoMLV-infected *mut tal1 (R188G;R189G)* tumors.

To identify oncogenes that cooperate with Tal1, we performed retroviral insertional mutagenesis. Wild type, *tal1,* or *mut tal1 (R188G;R189G)* transgenic neonates were injected with 50μl of Moloney Murine Leukemia Virus (MoMLV) in the presence of 8μg/ml polybrene. As expected, infection with MoMLV greatly accelerates the rate of disease, with a median survival latency of 81 days for *tal1* mice and 61 days for *mut tal1 (R188G;R189G)* mice (Figure 16A and data not shown). In addition, MoMLV-infected *tal1* mice and *mut tal1 (R188G;R189G)* mice both develop leukemia with complete penetrance. Moreover, MoMLV-infected wild type mice also develop disease with a median survival of approximately 180 days, which is significantly longer than MoMLV-infected *tal1* or *mut tal1 (R188G;R189G)* mice (Feldman et al., 2000).

We utilized inverse PCR (IPCR) to clone the region adjacent to the MoMLV integration in the genome. Subsequent sequence analysis of one cloned genomic clone determined that MoMLV integrated into intron 28 of the *notch1* gene, likely resulting in a constitutively active intracellular Notch1 protein. The previous connection between NOTCH1 activation and leukemia prompted us to further investigate *notch1* in Tal1-mediated leukemia. To determine the prevalence of *notch1* integrations in MoMLV-infected *mut tal1 R188G;R189G* tumors, we performed Southern blot screening on the remaining MoMLV-infected tumors. We digested genomic DNA isolated from MoMLV-infected *mut tal1 R188G;R189G* tumors with *EcoRV,* transferred to a

membrane, and probed with a *notch1* cDNA probe. The probe contains *notch1* cDNA exons 22-26, or cluster region I, which has previously been shown to be a common site of integrations in retroviral mutagenesis in *MMTV^{D}/myc* and *e2A/pbx1* transgenic mice (Feldman et al., 2000; Girard et al., 1996). Thirty-two percent (8/25) of the MoMLV-infected *mut tal1R188G;R189G* tumors contained integrations in the cluster region I of the *notch1* locus (Figure 16B). Surprisingly, additional Southern blot screening showed 0/18 tumors contained MoMLV integrations in the 3' cluster region II, which deletes negative regulatory the PEST domain (Figure 16B). This suggests that during MoMLV-induced *tal1* leukemogenesis, there appears to be a preferential activation of Notch1 by MoMLV integration into the midregion of the *notch1*, rather than the 3' PEST domain.

To determine if integration of MoMLV into the *notch1* allele increased intracellular Notch1 levels, we performed Western blot analysis on MoMLV-infected *mut tal1 R188G;R189G* tumors (Figure 16C). Tumors that contain *notch1* integrations (lanes 2, 5, and 6) display increased levels of Notch^{IC} compared to wild type thymocytes (lane 8) or MoMLV-infected tumors without Notch1 integrations (lanes 1, 3, 4, and 7). Yet, not all *mut tal1* tumors containing MoMLV integrations in *notch1* overexpressed Notch1^{IC}. To further determine if the Notch1 pathway was activated in these tumors, we examined expression of known Notch1 target genes, Hes1 and Deltex by performing RT-PCR. Compared to wild type thymocytes and premalignant *tal1* thymocytes, MoMLV-infected *mut tal1 R188G;R189G* tumors exhibited increased levels of Hes1 and Deltex expression, suggesting that tumors remain dependent on Notch1 signaling (Figure 16D).

Notch1 activation is common in spontaneous *tal1* tumors

Notch1 has been previously identified as a common retroviral integration site (CIS) (Shen et al., 2003; Suzuki et al., 2002). Therefore, to determine if the *notch1* integrations contributed to Tal1-mediated leukemia or were only identified through this locus being a CIS, we next wanted to determine if tumors that spontaneously arise in the *tal1* transgenic mice also exhibit Notch1 activation. To assay activation of the Notch1 pathway, we performed RT-PCR on 12 *tal1* tumor cell lines, assaying for Hes1 and Deltex expression. Ten *tal1* tumor cell lines (83%) demonstrated increased levels of Hes1 and Deltex, signifying that Notch1 is commonly activated in *tal1* tumors (Figure 17A and data not shown). The *tal1* tumor cell lines remain dependent on Notch1 signaling since pharmacologic inhibition of Notch1 with γ-secretase inhibitors results in G_0/G_1 arrest and apoptosis. In fact, 12/18 (67%) of the *tal1* tumor cell lines display sensitivity to DAPT, a γ-secretase inhibitor (Figure 17B). To confirm that γ-secretase inhibitor treatment interferes with Notch1 signaling in the *tal1* T-ALL lines, we assayed Hes1 and Deltex expression by RT-PCR following DAPT treatment. There is a significant reduction of Hes1 and Deltex expression levels following a 24h DAPT treatment, and following a 48h DAPT treatment, negligible levels of Hes1 and Deltex remain (Figure 17C). Strikingly, Western blot analysis demonstrated increased levels of $Notch^{IC}$ in 100 percent (18/18) of *tal1* tumor cell lines examined , and a 48h DAPT treatment in the *tal1* T-ALL lines significantly decreased $Notch^{IC}$ protein levels (Figure 18A and B). The Western blot also demonstrates $Notch^{IC}$ running with greater mobility in some *tal1* T-ALL lines, which is consistent with the presence of truncations of the PEST domain (asterisk in Figure 18A).

Together, this data indicates that activation of the Notch^{IC} pathway is a common secondary event in spontaneous *tal1* tumors.

Development of Dox-regulated Notch1 T-ALL line

Although some Notch1 target genes have been identified, the target genes are likely to be cell-type specific, and remain unclear for leukemic cells. To identify the signal Notch1 activation provides during leukemogenesis, we developed a dox-regulated Notch^{IC} T-ALL cell line. To develop this system, we mated the *tal1* transgenic mice to *Eμ/tTA/Notch^{IC}* bitransgenic mice, isolated tumors arising in the *Eμ/tTA/Notch^{IC}/tal1* mice, and adapted them to culture. Tumors isolated from *tal1* mice readily adapt to cell culture; 89% (8/9) of *tal1* tumors rapidly convert to culture (Kelliher et al., 1996). Conversely, of 14 *Eμ/tTA/Notch^{IC}/tal1* tumors isolated, only one tumor successfully converted to culture and confirmed responsive to doxycycline. Western blot analysis of the dox-regulated Notch^{IC} T-ALL line demonstrates that following 24 hr dox treatment, Notch^{IC} levels decrease to levels seen in wild type thymocytes (Figure 19A). Two additional *Eμ/tTA/Notch^{IC}/tal1* tumors also converted to culture, but failed to regulate Notch^{IC} in a dox-dependent manner (data not shown).

To confirm the Notch^{IC} signaling pathway was intact in this cell line and functioning in a dox-dependent manner, we performed RT-PCR to assay Hes1 and Deltex expression levels following dox treatment. There is a significant reduction of Hes1 and Deltex expression levels following an 18h dox treatment and a complete absence following 24h dox treatment (Figure 19B). This indicates the dox-regulated Notch^{IC} T-ALL cell line regulates the Notch^{IC} signaling pathway in a dox-dependent manner.

Phenotype of Dox-regulated Notch1 T-ALL line

Human leukemic T-ALL cell lines exhibit both a G_1 arrest and an increase in apoptosis following pharmacologic inhibition of Notch1 pathway by treatment with γ-secretase inhibitors (Weng et al., 2004; Weng et al., 2003). To test the possibility that $Notch^{IC}$ expression is providing either an anti-apoptotic and/or proliferative signal, we performed cell cycle analysis of the dox-regulated $Notch^{IC}$ T-ALL cell line in the presence and absence of doxycycline. Following 24h dox treatment, there was no significant change in cell cycle profiles (data not shown). However, following 72h dox treatment, there is a statistically significant increase in cells in the $subG_1$ phase of the cell cycle, indicating an increase in cells undergoing apoptosis ($p=0.0009$) (Figure 20A). In addition, the dox-treated cells demonstrate a G_0/G_1 cell cycle arrest. After electronically gating out $subG_1$ cells, a 22% increase in cells in G_0/G_1 phase of the cell cycle is observed ($p<0.002$) (Figure 20B). This demonstrates that $Notch^{IC}$ is providing both a proliferative and an anti-apoptotic signal in this conditional $Notch^{IC}$ system. The cell cycle profile following a 72h dox treatment is similar to cell cycle profiles observed following treatment with the γ-secretase inhibitor, DAPT, in sensitive mouse and human T-ALL cell lines (Figure 17B and (Weng et al., 2003)).

Notch1 signaling is essential for normal development of T lymphocytes. In addition to influencing αβ versus γδ T cell development, overexpression of $Notch^{IC}$ also promotes the maturation of CD4+ and CD8+ SP thymocytes (Deftos et al., 2000; Robey et al., 1996; Washburn et al., 1997). To test the possibility that $Notch^{IC}$ expression alters CD4 and CD8 co-receptor expression in our system, we assayed CD4 and CD8

expression following a 72h doxycycline treatment. We observe a significant increase in the mean fluorescence intensity (MFI) of CD4-FITC following dox treatment, indicating $Notch^{IC}$ expression is associated with decreased expression of the co-receptor CD4 ($p=0.001$) (Figure 21A; MFI=8.2±1.52 for –dox compared to MFI=19.03±1.03 for +dox). The repression of CD4 may be explained by the induction of the Notch1 target gene, Hes1, which binds to the CD4 silencer in to repress CD4 transcription (Allen et al., 2001). Alternatively, the inhibition of E2A by Notch may indirectly decrease the transcription of CD4, an E2A target gene (Bain et al., 1997; Sawada and Littman, 1993; Zhuang et al., 1996). Conversely, we observe no significant change in CD8 expression levels following dox treatment, indicating $Notch^{IC}$ does not affect CD8 expression (Figure 21A).

Thymocytes from $Notch1^{IC}$ and $Notch3^{IC}$ transgenic mice exhibit increased levels of CD25, the high-affinity IL-2Rα, indicating that inappropriate $Notch^{IC}$ signaling either induces or fails to repress CD25 (Bellavia et al., 2000; Deftos and Bevan, 2000). Additionally, expression of $Notch1^{IC}$ in CD4+ SP T cells induces all chains of the IL-2R complex and enhances proliferation (Adler et al., 2003). Consistent with these results, the immunophenotype of the *Eu/tTA/NotchIC/tal1* tumors were either CD8+ SP or DP and expressed moderate to high levels of CD25 (data not shown). To determine if $Notch^{IC}$ regulates CD25 expression in the dox-regulated $Notch^{IC}$ T-ALL cell line, we stained cells with antibodies against CD25 and performed FACS analysis. The expression of CD25 decreases drastically in the absence of $Notch^{IC}$ signaling, displaying over an 11-fold decrease in the MFI of CD25-PE following a 48h dox treatment (Figure

21B). Furthermore, pharmacologic inhibition of Notch^{IC} in *tal1* cell lines with DAPT treatment also resulted in a decrease in CD25 expression levels (data not shown).

Notch^{IC} target genes in T-ALL cell line

To determine what signal Notch^{IC} is providing during leukemogenesis, we performed an Affymetrix microarray experiment comparing Notch^{IC} T-ALL line. Following a 24h mock or doxycycline (2μg/ml) treatment of the dox-responsive Notch1^{IC} cell line, RNA was isolated from and hybridized Affymetrix 430A 2.0 microarrays, which contain 14,000 genes. The Rosetta Resolver System was used for normalization and statistical analysis. To narrow down the data set, we utilized a cut off p-value of <0.005, and greater than a 2.5 fold change. A partial list of putative and known Notch1^{IC} target genes is shown in Table 4, and a more comprehensive list can be found in Supplemental Data 2. As expected, with continuous expression of Notch^{IC}, many known Notch1 target genes are expressed at high levels: Hes1, Deltex, IL2Rα, and pre-Tα receptor (Adler et al., 2003; Deftos et al., 2000) (Table 1). In addition, multiple genes implicated in Notch1 signaling were also found upregulated in the absence of doxycycline, for example, Notch3, Adam19 (Meltrin β), and members of the Interferon 200 gene family (Table 1) (Adler et al., 2003; Deftos et al., 2000; Huang et al., 2004). In addition, the array demonstrates an increase in IL-10 levels but not IL-4, both of which are reported upregulated following Notch^{IC} activation by Jagged1 (Amsen et al., 2004).

Expression of Notch^{IC} in this dox-regulated T-ALL cell line appears to induce multiple genes implicated in regulation of Notch1 signaling. For example, Deltex is highly expressed in the absence of doxycycline, and has been proposed to antagonize or

promote Notch1 function depending on the model system (Izon et al., 2002; Matsuno et al., 1995). In addition, $Notch^{IC}$ induces expression of both Nf2r2 (nuclear receptor subfamily 2, group 2) and Nrarp (notch regulated ankryin repeat protein). Nrarp inhibits Notch function in a CSL-dependent manner, and is capable of inhibiting thymocyte development *in vivo* (Krebs et al., 2001; Yun and Bevan, 2003). Nf2r2 has recently been implicated in the inhibition of $Notch1^{IC}$ function in angiogenesis (Gridley, 2001; You et al., 2005). Together, this suggests that $Notch^{IC}$ may induce genes that negatively regulate its transcriptional activity or function.

Ingenuity pathway analysis revealed c-Myc was transcriptionally activated and many downstream c-Myc target genes were either induced or repressed upon Notch1 activation (Table 4). Furthermore, quantitative real-time PCR demonstrated c-Myc mRNA transcripts are elevated 10-fold in the presence $Notch^{IC}$ compared to when $Notch^{IC}$ is suppressed by a 24h dox treatment ($10.03\pm.007$, $p=.002$, data not shown). Consistent with this, Satoh et. al. demonstrated ectopic expression of Notch1 induced c-Myc expression in HSC, and Notch1/CSL activated the c-Myc promoter in a reporter assay (Satoh et al., 2004).

Discussion

Retroviral insertional Mutagenesis (RIM) demonstrates that expression of Tal1 cooperates with Notch1 activation to induce T-ALL. We observed MoMLV integrations in the *notch1* allele in (8/35) MoMLV-infected *mut tal1 (R188G;R189G)* tumors. All of the *notch1* integrations were found in cluster region I, which contains the LNR and EGFR repeats. Conversely, no integrations were observed in cluster region II, located within the PEST domain. Previous retroviral insertional mutagenesis screens of both *E2A-Pbx1* and *MMTV^{D}/myc* transgenic mice detected MoMLV integrations in *notch1,* indicating that similar to human T-ALL patients, activation of Notch1 is common during T cell leukemogenesis in the mouse (Feldman et al., 2000; Girard et al., 1996; Weng et al., 2004). However, Notch1 has been previously identified as a common integration site (CIS) during retroviral Insertional Mutagenesis (RIM)(Shen et al., 2003; Suzuki et al., 2002).

Interestingly, activation of Notch1 is also common in spontaneous *tal1* tumors. This confirms that the identification of notch1 integrations cooperate with Tal1 in leukemogenesis, and is not a consequence of being a CIS. All *tal1* T-ALL lines tested express increased levels of cleaved Notch1 protein, and 80% show activation of Notch1 pathway through upregulation of Hes1 and Deltex. This is consistent with the high percentage of *tal1* tumor cell lines that display sensitivity to γ-secretase inhibitors. Furthermore, recent evidence revealed over 74% of *tal1* primary tumors contain mutations in either the HD domain or PEST deletions in Notch1. Interestingly, the majority of mutations observed in *tal1* tumors are in the PEST domain, ultimately leading to a premature stop and truncation of the PEST domain.

A percentage of the *tal1* tumor cell lines exhibit sensitivity to γ-secretase inhibitors without harboring Notch1 mutations. This result suggests additional members of the Notch1 signaling pathway may be mutated. For example, mutations within the LNR domain could result in increased Notch1 activity. Point mutations in the LNR domain of *C. Elegans lin-12* induces a gain of function phenotype, or deletion of the LNR domain induces Notch1 activation (Greenwald and Seydoux, 1990; Rand et al., 2000). In addition, 5' deletions of *notch1* lead to transcriptional initiation at cryptic start sites and result in alternate transcripts, likely resulting in Notch1 proteins lacking the extracellular domains and thereby signaling in a ligand-independent manner (Tsuji et al., 2003). Additionally, mutations in the other members of the Notch1 signaling pathway could result in Notch1 activation. For example, inactivating mutations in the Notch1 E3 ligases, Sel-10 or Itch, could result in increased stability and therefore enhanced signaling. Similarly, mutation of other negative regulators, Numb or Nrarp, could also result in Notch1 activation. Furthermore, increased concentrations of ligand, or mutations in proteins modulating Notch1 response to ligand binding, such as the Fringe family of glycosyltransferases, may also result in Notch1 activation. Another potential way to induce Notch activation may be the deletion of microRNAs (miRNAs). A recent discovery suggests miRNAs may regulate Drosophila Notch and Notch target genes; ectopic expression of Notch target-regulating miRNAs results in a Notch loss of function phenotype (Lai et al., 2005). A link between deletion of miRNA clusters and human leukemia has previously been demonstrated; the loss of miR-15a/miR-16 cluster is associated with B-CLL and mantel cell lymphoma (Calin et al., 2002; Juliusson et al., 1990; Stilgenbauer et al., 1998). miR-34 was computationally determined to regulate

vertebrate Notch1 and Delta (Lewis et al., 2003). Therefore, the loss of miR34 may be another potential mechanism to induce Notch activity.

This dox-regulated Notch^{IC} T-ALL line provides multiple advantages over other experimental systems to examine the function of Notch1 in leukemogenesis. For example, although γ-secretase inhibitors are commonly used to inhibit the cleavage and activation of Notch (De Strooper et al., 1999), they do not specifically inhibit Notch signaling. γ secretase inhibitors also inhibit the well characterized cleavage of amyloid precursor protein, ErbB4, CD44, Growth hormone receptor, and N- and E-cadherins (Cowan et al., 2005; Haas et al., 2005; Lammich et al., 2002; Ni et al., 2001). This growing list of transmembrane proteins cleaved by γ secretases complicates the interpretation of analyses performed on cells treated with γ-secretase inhibitors. However, doxycycline treatment of this conditional Notch^{IC} cell line specifically inhibits Notch^{IC} expression levels. Therefore, this system provides an opportunity to identify Notch1-specific genes.

Another advantage of this dox-regulated T-ALL system is illustrated by the fact that Notch1 signaling differs depending on cell type and context. For example, Notch1 signaling leads to growth arrest and differentiation in keratinocytes, but induces S-phase induction in rat kidney epithelial cells (Rangarajan et al., 2001; Ronchini and Capobianco, 2001). Therefore, to determine the signal Notch1 activation provides during leukemogenesis, it is essential to interrogate Notch1 signaling in the appropriate cell type. Therefore this T-ALL cell provides the ideal context to investigate the function of Notch1 in leukemogenesis.

Microarray analysis on this dox-regulated Notch^{IC} T-ALL line demonstrated the upregulation of numerous known Notch^{IC} target genes, further validating the system. Nrarp, Notch3, Hes1, CD25, ADAM19, Deltex, IL10, IRF4, Egr1, and preTα have been shown in different cell systems to be Notch1-regulated genes (Adler et al., 2003; Amsen et al., 2004; Deftos et al., 2000; Huang et al., 2004). Ingenuity pathway analysis illustrated the alteration of various c-Myc-induced genes: Mina, Srm, Adm, Ly6a, Gadd45γ, and Fabp4. The increased levels of c-Myc transcript levels were further validated using quantitative real-time PCR. The regulation of c-Myc by Notch has been previously implicated in HSC cells (Satoh et al., 2004), and we have preliminary chromatin immunoprecipitation suggesting that Notch1^{IC} and CSL/RBP-Jk bound to the promoter regions of the *c-myc* promoter (Vishva Sharma, preliminary results). Additional preliminary data suggests that ectopic expression of c-Myc in the dox-regulated Notch^{IC} cell line may rescue some of the G_1 arrest and apoptosis following dox treatment.

NOTCH1 activation has been implicated in numerous types of cancers and treatment with GSI has been shown to induce apoptosis or differentiation *in vitro* and *in vivo*. Therefore, GSI may prove to be an effective adjuvant therapy for the various types of cancer. Fortunately, GSI are currently in phase I/II clinical trials for treatment of Alzheimer's patients and appear to have no severe toxicity. In addition, Drs. Miele and Nickoloff indicate that GSI may synergize with other chemotherapeutic agents such as cisplatin, MG132, or Paclitaxel, allowing lower doses of combined chemotherapeutic treatments, and therefore less severe side-effects (University of Illinois Technology Ref#CX063).

Recent mathematical analysis predicts that a minimum of 3 targeted drugs of different specificities should ultimately be used to prevent tumor resistance (Komarova and Wodarz, 2005). Therefore, additional Notch inhibitors need to be developed. Interestingly, imatinib has been shown to inhibit the cleavage of Amyloid-β (Aβ) peptides *in vitro*, but inhibiting Notch cleavage was not extensively examined. (Netzer et al., 2003). In addition, antisense Notch and anti-Notch monoclonal antibodies have been successfully used to inhibit Notch signaling *in vitro* (Garces et al., 1997; Weijzen et al., 2002; Yasutomo et al., 2000). Additionally, soluble Notch decoys have been described that sequester Notch ligands and therefore prevent ligand-receptor binding and Notch activation (Garces et al., 1997; Nickoloff et al., 2002). Another possible option is the development of a small molecule inhibitor that would bind intracellular Notch, inhibiting the Notch-CSL/RPB-Jκ interaction, or inhibiting the recruitment of Mastermind.

The high percentage of *tal1* tumor cells that contain *notch1* mutations (74%), and/or display sensitivity to γ-secretase inhibitor (GSI) treatment (67%), prompts us to determine if disease kinetics are altered when *tal1* transgenic mice are treated with γ-secretase inhibitors. Therefore, important ongoing experiments are to determine if *tal1* tumors regress following GSI treatment. It is expected from the high percent of *tal1* tumor cells that display sensitivity to GSI treatment *in vitro*, that upon GSI treatment of moribund *tal1* mice, disease will regress. It will be interesting to determine if the tumors regress through the induction of apoptosis or differentiation. Our *in vitro* data predicts *tal1* tumors may regress by undergoing apoptosis. Additionally, GSI treatment of malignant melanoma cell lines rapidly induced apoptosis (Qin et al., 2004). However, since Notch1 activation inhibits the differentiation of various cell types, inhibition of

Notch1 signaling may induce differentiation. Consistent with this, treatment of *Apc*^{min} mice displaying intestinal adenomas with GSI demonstrated a conversion from an undifferentiated epithelial cell to a more differentiated goblet cell (van Es et al., 2005). However, it is predicted that following GSI treatment, the *tal1* mice will not exhibit persistent resistance; *tal1* mice will likely reactivate Notch1 signaling and relapse. Consistent with this prediction, 100% of *Eμ/tTA/Notch*^{IC} T cell leukemias relapse following inactivation of Notch^{IC} by doxycycline treatment (Beverly et al., 2005).

Materials and Methods

Mice and Dox-regulated T-ALL cell line

For the retroviral insertional mutagenesis screen, wild type, *tal1* or *mut tal1 (R188G;R189G)* neonates were injected with 50µl Moloney Murine Leukemia Virus (gift from Dr. Rosenberg) and monitored daily for signs of disease. Kaplan-Meier analysis was performed comparing MoMLV-infected mice to uninfected *tal1* or *mut tal1 (R188G;R189G)* mice.

To develop a dox-regulated Notch^{IC} T-ALL line, a cohort of *Eμ/tTA/notch^{IC}/tal1* mice were aged and monitored for disease (*Eμ/tTA/notch^{IC}* mice gift from Dr. Capobianco). To convert primary tumors to culture, *Eμ/tTA/notch^{IC}/tal1* tumors were minced into a single-cell suspension using frosted slides and cultured in RPMI with 10% FBS, l-glutamine, Penicillin/Streptomycin, and 50µM β-mercaptoethanol. Primary tumor cells were plated at three concentrations in a 6-well plate: 5 X 10^6, 1 x10^7, and 2 x 10^7 cells per well. Tumor cells are left undisturbed for one week and subsequently fed 2-3 times weekly by the careful aspiration and addition of fresh media. When nonadherent cells became confluent, they were transitioned to a 60mm dish, and finally to a 10cm dish.

Inverse PCR and Southern Blot Analysis

Genomic DNA was isolated from MoMLV-infected *tal1* and *mut tal1 (R188G;R189G)* tumors. One microgram of DNA was digested overnight with *PstI*, heat-inactivated, and ligated in a total volume of 600µl overnight at 16°C. The ligation was ethanol precipitated and digested with *ClaI*. Following the *ClaI* digest, IPCR was performed using the Long Template Expand Kit (Roche, Indianapolis, IN) and primers to MoMLV LTR (5'-CTT-GTG-GTC-TCG-CTG-TTC-CTT-3') and to the region adjacent to the *PstI*

site within MoMLV (5'-TTA-AGC-TAG-CTT-GCC-AAA-CCT-ACA-GGT-3'). PCR products were electrophoresed on a 1% agarose gel, extracted, cloned into pCR4-TOPO (Invitrogen, Carlsbad, CA), and sequenced.

Genomic DNA was extracted from MoMLV-infected *tal1* tumors and uninfected *tal1* tumors. 15μg was digested overnight with *Eco RV* (*notch1* cluster region I) or *Asp 718* (*notch1* cluster region II) and electrophoresed on a 0.8% agarose-1X Tris-borate-EDTA gel, and transferred to a nylon membrane. The membrane was then probed with a cDNA probe corresponding to Notch1 cluster region I or cluster region II as in (Feldman et al., 2000).

Western Blot Analysis

Protein was isolated from MoMLV-infected tumors, and wild type thymocytes using RIPA buffer containing protease inhibitor tablets (Roche). Fifty micrograms of total protein was resolved on a 7.5% SDS-PAGE gel, transferred to a nitrocellulose membrane, and probed with polyclonal antibodies against full length Notch1 (a gift from Warren Pear), or an antibody specific for Notch1 activated by cleavage at Val 1744 (#2421, Cell Signaling Technology). Blots were stripped and reprobed with β-actin (A5441, Sigma, St. Louis, MO) to control for equal loading.

Flow Cytometry

Following 24h, 48h, 72h doxycycline treatment (2μg/ml), $Notch^{IC}$ T-ALL cell line was stained with CD25-PE, CD4-FITC, or CD8-PE (Pharmingen), fixed with 1% paraformaldehyde, and analyzed by flow cytometry. For cell cycle analysis, the cells were fixed overnight with 70% ethanol, stained with propidium iodide and analyzed for DNA content by flow cytometry. To test for sensitivity to γ-secretase inhibitor treatment,

$2x10^6$ *tal1* tumor cells were treated for 3 or 6 days with 1μM DAPT, fixed, and analyzed for DNA content by PI staining.

Microarray Analysis

The dox-regulated $Notch^{IC}$ T-ALL cell line was treated with doxycycline (2μg/ml) for 24h and RNA was extracted using Trizol reagent (Invitrogen, Carlsbad, CA), and purified using Qiagen RNeasy Mini Kit (Qiagen, Valencia, CA). RNA was hybridized to Affymetrix Mouse Genome 430A 2.0 arrays (Affymetrix, Santa Clara, CA). Data sets were analyzed using Rosetta Resolver, and Ingenuity software programs and analyzed by Manoj Bhasin (Dana Farber Cancer Institute).

RT-PCR

RNA was extracted using Trizol, and cDNA synthesized using Superscript First-Strand Synthesis System (Invitrogen). Deltex, Hes1 and Pre-Tα expression was assayed using primers as in (Deftos et al., 2000).

Real-time PCR

RNA was extracted using Trizol, and cDNA synthesized using Superscript First-Strand Synthesis System (Invitrogen). Primers to analyze c-myc expression (5'-CTG-TTT-GAA-GGC-TGG-ATT-TCC-T-3' and 5'-GTC-GTG-GCT-GTC-TGC-GG-3') were generated using Primer Express (Applied Biosystems). Relative quantities of mRNA expression were analyzed using QRT-PCR in the presence of SYBR green (Applied Biosystems ABI Prism 7300 Sequence Detection System, Applied Biosystems). For the normalization of each sample the expression level of the gene was divided by that of β-actin. The relative expression level was determined by comparing the normalized value

(/β-actin) to that in the reference sample (another normal tissue) included in the same reaction.

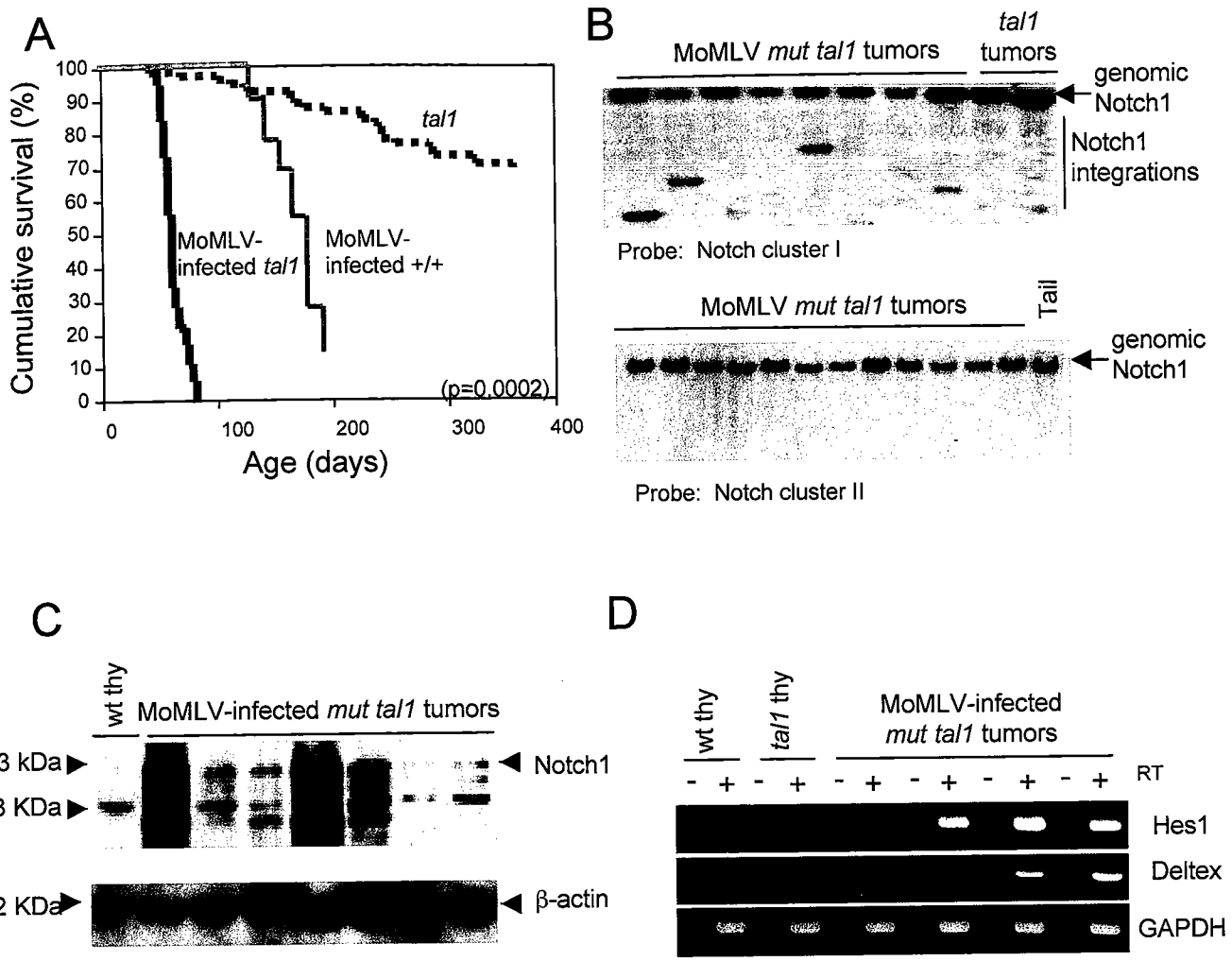

Figure 16. Notch1 activated in MoMLV-infected *mut tal1* tumors. A. Disease acceleration in MoMLV- infected *mut tal1* transgenic mice. Kaplan Meier survival plot of MoMLV- infected *mut tal1* transgenic mice. The cohort of *mut tal1* mice consisted of n=62 mice and the cohort of infected mice consisted of n=27 mice. MoMLV-infected FVB cohort consisted of n=10 (Feldman, Hampton et al. 2000) **B. The *notch1* locus is a common MoMLV- integration site in infected *mut tal1 (R188G;R189G)* tumors.** Genomic DNA from MoMLV-infected tumors (lanes 1-8) and from uninfected *tal1* tumors (lanes 9,10) was digested with *EcoRV* and hybridized with a probe to cluster region I of Notch1(Feldman, Hampton et al. 2000). **C. Notch1 activation in MoMLV-infected *tal1* and *mut tal1 (R188G;R189G)* tumors**. Lysates from tumors with MoMLV integrations in *notch1* (lanes 2,5,6) were probed with an anti-Notch1 antibody. Lanes 1,3,4,7 are from infected tumors with no detectable Notch1 integrations and lane 8 contains wild type thymus. **D. Hes1 and Deltex are expressed in tumors with MoMLV insertions in Notch1**. Hes1 and Deltex expression was examined in wt and *tal1* thymocytes and MoMLV-infected tumors with insertions in Notch1 using RT-PCR. GAPDH was used as an internal control.

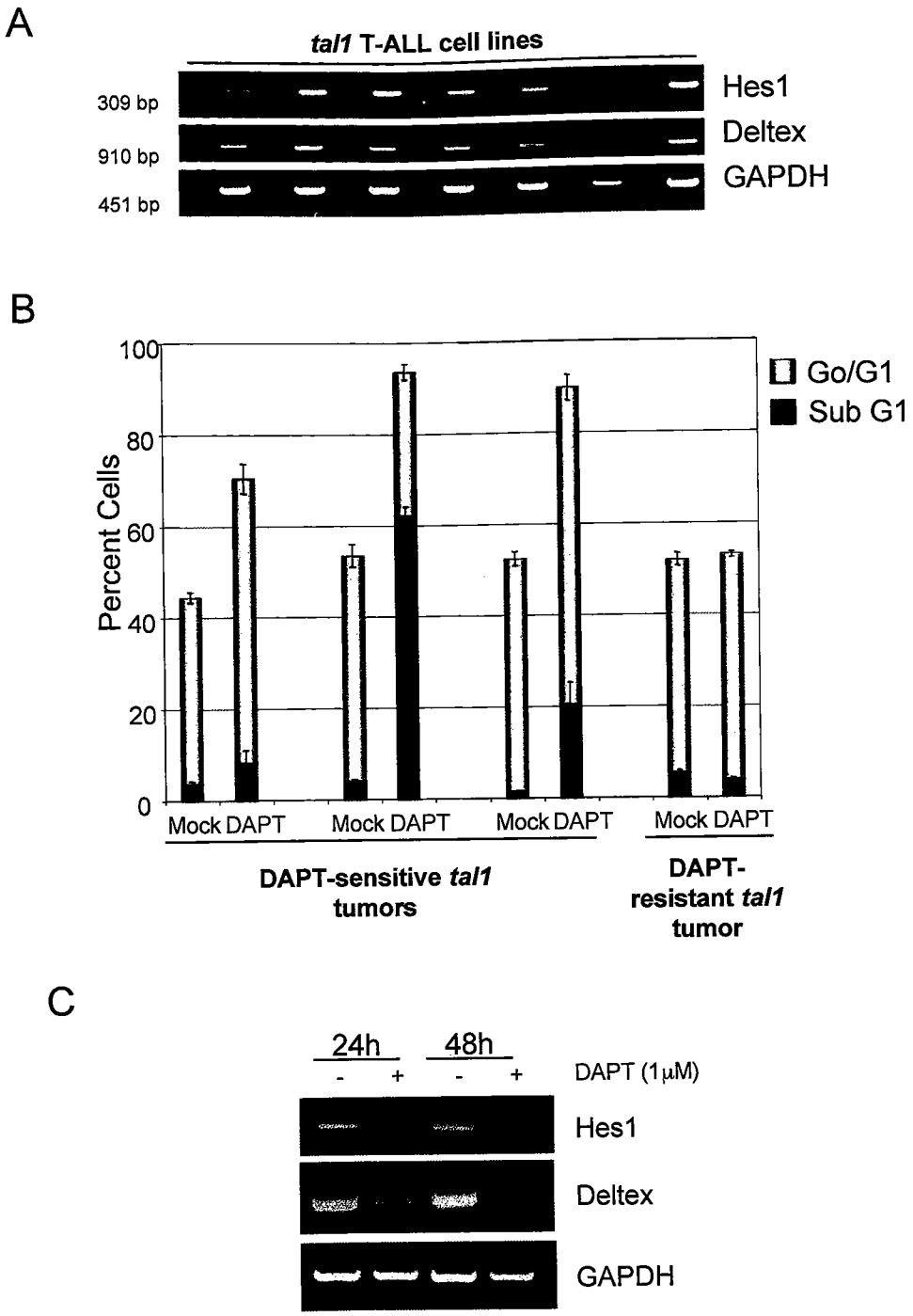

Figure 17. Tumor cell lines from spontaneous *tal1* tumors demonstrate Notch1 activation A) *tal1* tumor cell lines express Hes1 and Deltex. RT-PCR assaying Hes1, Deltex were performed on seven *tal1* cell lines. GAPDH was used as an internal control. **B) *Tal1* cell lines exhibit sensitivity to γ-secretase inhibitors.** 72h treatment of *tal1* cell lines with 1μM DAPT induced a G_1 arrest or apoptosis in *tal1* cell lines **C) DAPT treatment inhibits Notch^{IC} pathway in *tal1* T-ALL lines.** Notch1 target genes, Hes1 and Deltex, are assayed in *tal1* tumor cell lines by RT-PCR following18h and 24h DAPT treatment. GAPDH was used as an internal control.

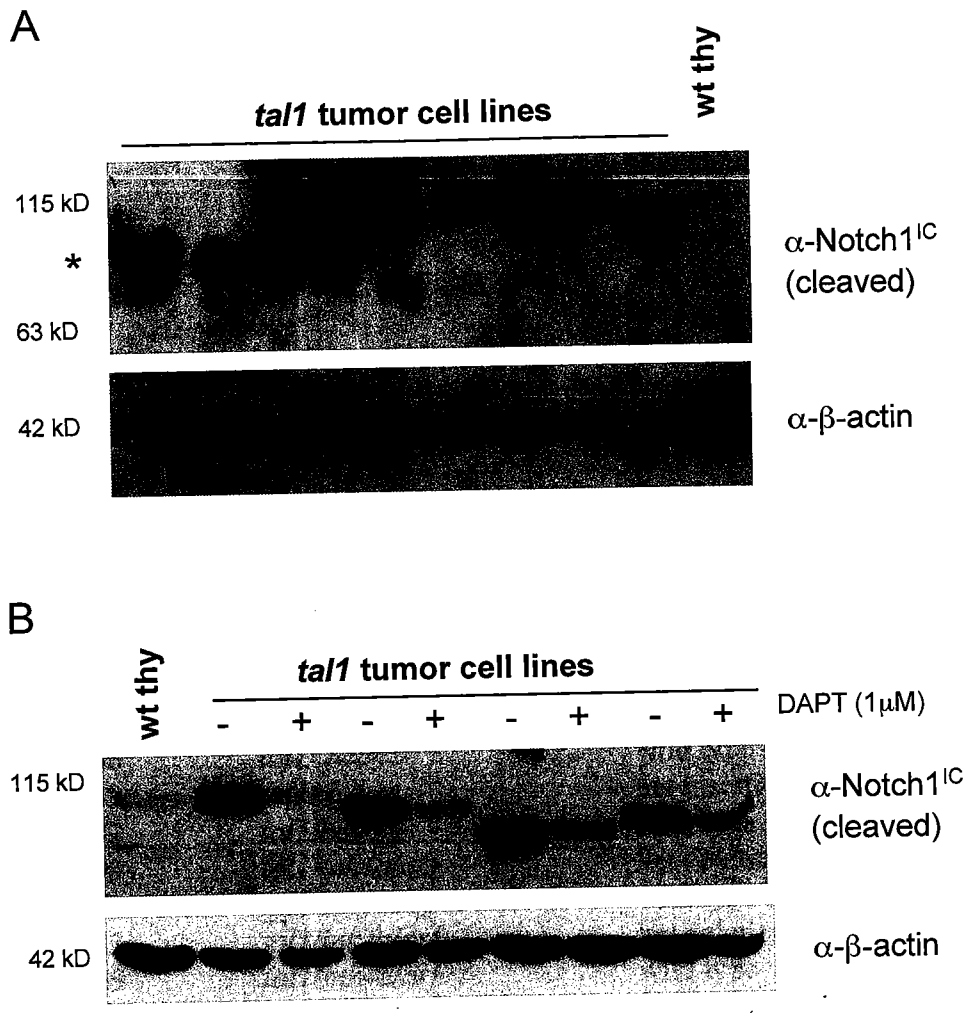

Figure 18. Spontaneous *tal1* tumors express cleaved Notch1. **A)** To examine *tal1* tumor cells for the presence of cleaved Notch1, tumor cell lysates were separated by SDS-PAGE electrophoresis, transferred to a membrane, and probed with antibodies to cleaved Notch1 and β-actin. **B)** *Tal1* tumor cell lystes from mock-treated and DAPT-treated *tal1* were separated by SDS-PAGE electrophoresis, transferred to a membrane, and probed with antibodies to cleaved Notch1 .

Table 3: Notch1 mutational analysis of *tal1*, *tal1/heb*+/-, and *tal1/ink4a/arf*+/- tumors

Tumor	Genotype	Notch1 status
5046	*tal1*/+	het insertion 2420
5151	*tal1*/+	het deletion 2492
5146	*tal1*/+	het deletion 2489
1444	*tal1*/+	het deletion 2360
5015	*tal1*/+	het insertion 2361
1330	*tal1*/+	wild type
5148	*tal1*/+	wild type
5188	*tal1*/+	het del 2360
1161	*tal1*/+	Q>stop 2419
5145	*tal1*/+	het insertion 2361
4862	*tal1*/+	het deletion 2488
1469	*tal1*/+	het insertion 2361
1011	*tal1*/+	Q>stop 2419
135	*tal1/heb*+/-	het insertion
756	*tal1/heb*+/-	wild type
720	*tal1/heb*+/-	het insertion
8998	*tal1/heb*+/-	Q>stop 2296
9450	*tal1/heb*+/-	het insertion 2420
9205	*tal1/heb*+/-	L>P 1668
9306	*tal1/ heb*+/-	wild type
6839	*tal1/ heb*+/-	het insertion 2360
8283	*tal1/heb*+/-	wild type
3199	*tal1/ink4a/arf*+/-	het deletion 2426
2871	*tal1/ink4a/arf*+/-	wild type
3483	*tal1/ink4a/arf*+/-	het deletion 2490
2869	*tal1/ink4a/arf*+/-	wild type
3460	*tal1/ink4a/arf*+/-	Q>stop 2382
3570	*tal1/ink4a/arf*+/-	wild type
2902	*tal1/ink4a/arf*+/-	het insertion 2474
3150	*tal1/ink4a/arf*+/-	het insertion/deletion 2356

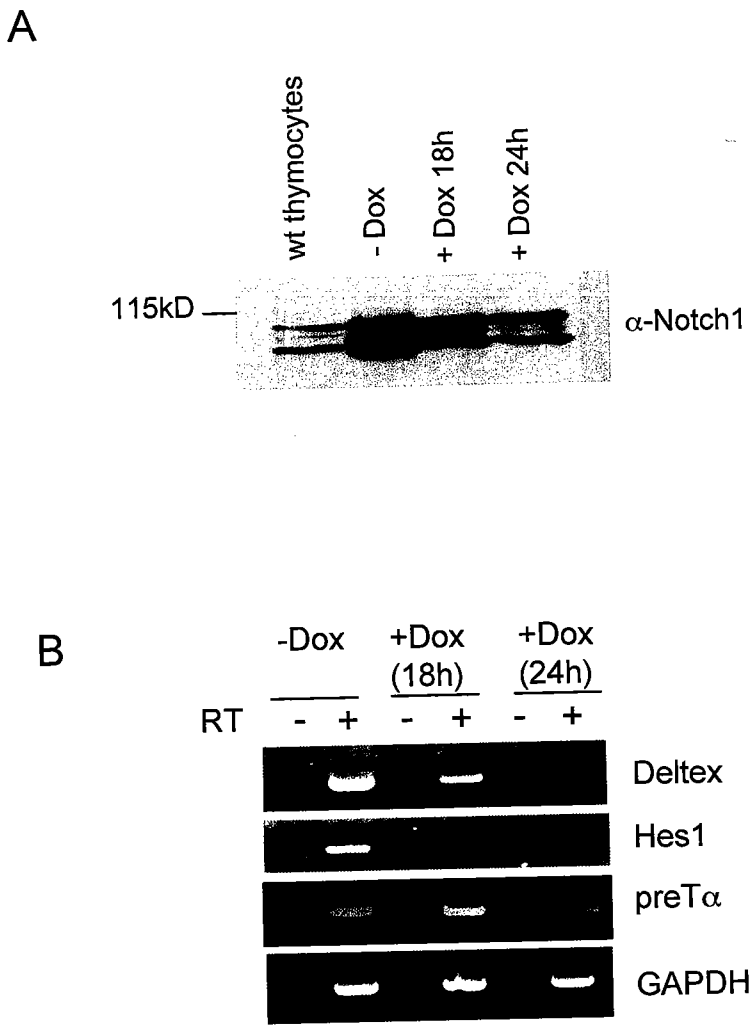

Figure 19. Mouse T-ALL cell line regulates Notch^{IC} expression in a doxycycline-responsive manner. A) Dox-regulated Notch^{IC} T-ALL line regulates Notch1 protein levels in a doxycycline-dependent manner. Fifty micrograms of protein isolated from wild-type thymocytes, and dox-regulated T-ALL cell line were left untreated or were treated with 2μg/ml doxycycline. Cell lysates were separated on a 7.5% SDS-PAGE gel and then probed with anti-Notch1 antibody. **B) Hes1 and Deltex expression regulated in a dox-dependent manner.** RT-PCR assaying Hes1, Deltex, and were performed in dox-regulated Notch^{IC} T-ALL line, following mock treatment or 18h and 24h dox (2μg/ml) treatment. GAPDH was used as an internal control.

A

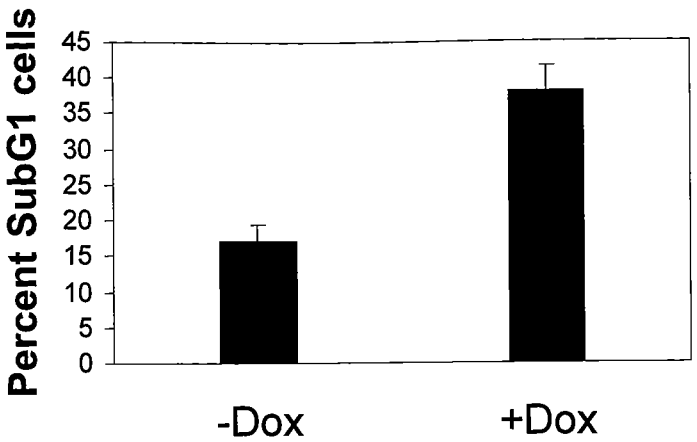

B

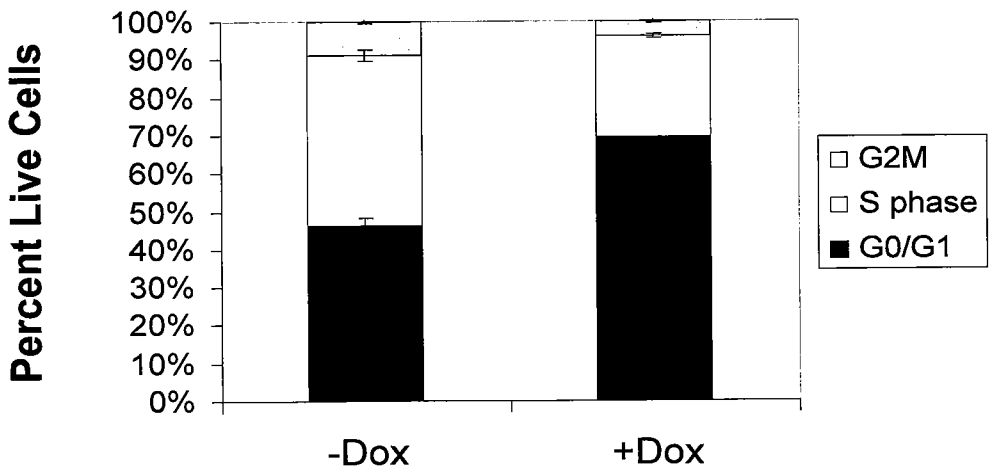

Figure 20. Notch^{IC} provides proliferative and anti-apoptotic signal in dox-regulated Notch^{IC} T-ALL line. A) Inhibition of Notch^{IC} signaling induces apoptosis. Following 72h dox treatment, cells were assayed for DNA content by staining with PI. Data is presented graphically as mean ± standard deviation. **B) Inhibition of Notch^{IC} signaling induces G_0/G_1 arrest.** Following 72h dox treatment, cells were assayed for DNA content by staining with PI. Cell cycle profiles were obtained following electronically gating out subG_1 cells and shown graphically as mean ± standard deviation.

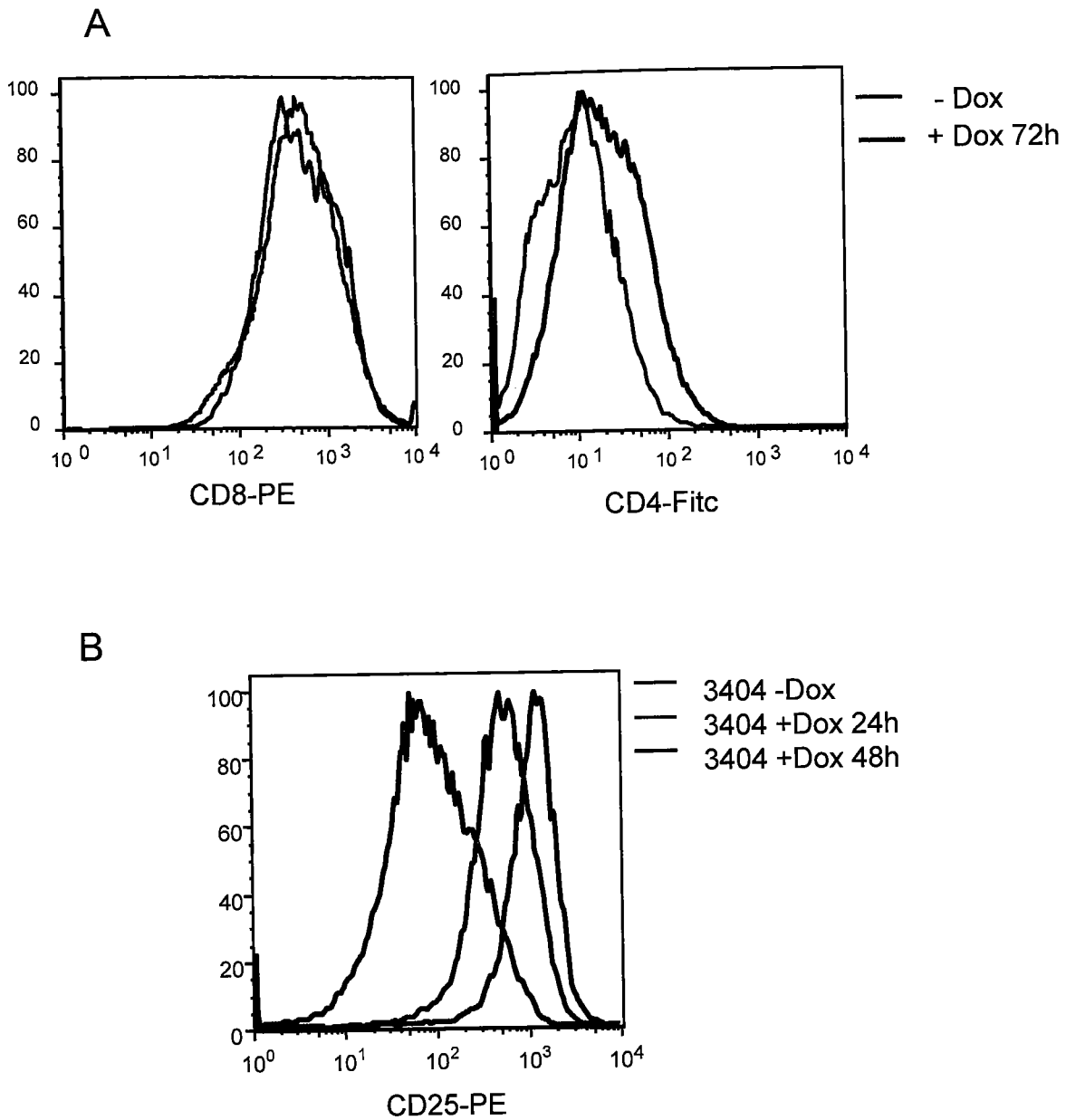

Figure 21. Constitutive Notch signaling alters expression of CD4 and IL2Rα. A) Notch signaling represses CD4 expression. Following a 72h with doxycycline (2μg/ml) treatment, Dox-responsive Notch^{IC} T-ALL cells were stained with CD8-PE and CD4-FITC and analyzed by flow cytometry. **B) Constitutive Notch^{IC} signaling induces CD25 expression.** Dox-responsive Notch^{IC} cells were treated for 24 and 48 with 2μg/ml Dox and assayed for CD25 expression levels by flow cytometry analysis.

Table 4. Genes activated or repressed by Notch1 in tumor cell line

Description of gene (accession number)	Fold change	P value
Bcl-XL (NM_009743)	-9.1	1.10E-04
CD4 antigen (NM_013488)	-6.2	2.50E-09
B-cell leukemia/lymphoma 6 (U41465)	-4.5	3.42E-03
Interferon gamma receptor 1 (NM_010511)	-4.3	1.44E-39
RAR-related orphan receptor gamma (AJ132394)	-3.6	4.46E-13
T-cell receptor alpha chain (U95921)	-3.2	1.66E-32
Notch-regulated ankyrin repeat protein (BI696369)	+3.0	1.48E-03
Notch gene homolog 3 (Drosophila) (NM_008716)	+3.0	1.13E-20
Notch gene homolog (Drosophila)1 (NM_008714)	+3.3	5.88E-35
Interferon regulatory factor 4 (U34307)	+4	3.39E-25
Interferon activated gene 203 (M74124)	+4.4	4.37E-02
hairy/enhancer-of-split related with YRPW motif-like (BG695100)	+4.6	3.90E-24
Early growth restonse 1 (NM_007913)	+5.3	0.00E+00
IL2 receptor alpha (AF054581)	+6.5	0.00E+00
pre T-cell antigen receptor alpha (NM_011195)	+6.9	0.00E+00
Interferon activated gene 202B (NM_011940)	+8.4	0.00E+00
a disintegrin and metalloproteinase domain 19 (NM_009616)	+9.8	0.00E+00
Nr2f2 (AI463873)	+10.8	5.69E-03
Deltex 1 homolog (Drosophila) (AB015422)	+11.3	0.00E+00
Interleukin 10 (NM_010548)	+13.0	6.49E-26
hairy and enhancer of split 1 (BC018375)	+13.9	1.28E-35

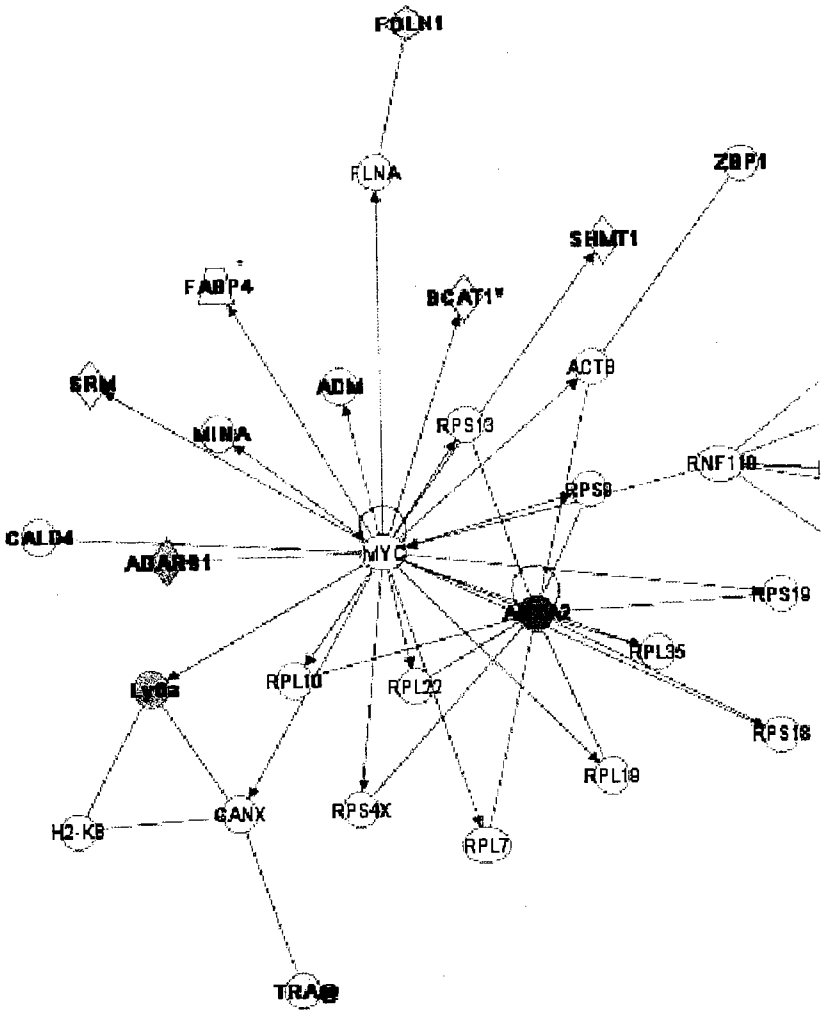

Figure 22. Notch signaling regulates multiple Myc target genes. Ingenuity pathway analysis demonstrates that constitutive Notch signaling alters the expression of multiple Myc target genes. Shades of green indicated are either induced whereas shades of red indicate genes are repressed .

Table 5. Myc target genes altered upon conditional Notch1 activation in mouse T-ALL cell line

Symbol	Gene Description	Fold Change	p-value
Mina	myc induced nuclear antigen	+10.8	1.39E-03
Fabp4	fatty acid binding protein 4	+5.4	2.00E-02
Adm	adrenomedullin	+5.4	2.10E-03
Gadd45g	growth arrest and DNA-damage 45 gamma	+4.9	1.19E-10
Cald1	caldesmon 1	+4.1	2.70E-02
Srm	spermidine synthase	+3.9	2.00E-02
Bcat1	branched chain aminotransferase 1	+3.1	1.37E-09
Shmt	serine hydroxymethyl transferase 1	+2.3	2.50E-09
Zbp1	Z-DNA binding protein 1	-3.8	1.50E-02
Folh1	folate hydrolase	-4.4	1.90E-02
Adarb1	adenosine deaminase, RNA-specific, B1	-5.4	3.30E-02
Ly6a	lymphocyte antigen 6 complex, locus A	-5.9	8.50E-12
Anxa2	annexin A2	-7.8	5.90E-03

CHAPTER V

DISCUSSION

Our laboratory has previously illustrated that misexpression of Tal1 in thymocytes results in thymocyte differentiation arrest *in vivo* and apoptosis *in vitro* (O'Neil et al., 2001; O'Neil et al., 2004). However, the work presented in this thesis demonstrates an additional function for Tal1 in cell cycle regulation in thymocytes (Chapter III). Using *in vivo* bromodoxyuridine (BrdU)-incorporation analysis, we have shown premalignant *tal1* thymocytes exhibit a 70% increase of cells in S phase of the cell cycle. Therefore, in addition to inducing a thymocyte differentiation arrest, Tal1 likely contributes to leukemogenesis by inappropriately inducing S phase progression. The S phase induction appears dependent of a functional DNA-binding domain, as *mut tal1 (R188G;R189G)* mice do not exhibit the induction of S phase. This result suggests that a Tal1/E47 or Tal1/Heb target gene is responsible for the S phase induction. Microarray analysis revealed activation of the Notch and Wnt receptor pathways in *tal1* premalignant thymocytes. Wnt5b and the Wnt target gene, c-Myc, were upregulated in addition to Notch target genes, Deltex, CD25, and Hes1. Since activation of Wnt and Notch pathways have been suggested to induce proliferation and confer self-renewal capacity of hematopoetic stem cells (Reya et al., 2003; Varnum-Finney et al., 2000), their induction may contribute to Tal1-mediated leukemogenesis.

Similar to the misexpression of other proliferative oncogenes, Tal1 inappropriately induces S-phase progression, and is associated with an increase in apoptosis. *In vivo*-BrdU analysis of *tal1* thymocytes demonstrates a 5-10-fold increase in subG$_1$ cells, which appears dependent on p19^{Arf}. This increased apoptosis may explain why although *tal1* mice exhibit an increase in proliferation, they display an 2-fold decrease in overall thymic cellularity (O'Neil et al., 2004). Therefore, it is likely that

mutation of apoptotic pathways would cooperate with *tal1* in leukemogenesis; consistent with this hypothesis, *tal1/p53+/-* mice display disease acceleration(Condorelli et al., 1996)

The ability of Tal1 to promote S-phase induction and apoptosis is reminiscent of ectopic expression of c-Myc (Askew et al., 1991; Evan et al., 1992). Similar to the S phase induction observed in *tal1* thymocytes (Figure 12), *in vivo* BrdU-incorporation analysis of *Eμ-Myc* transgenic mice revealed a 2- to 4-fold increase in BrdU-positive lymphocytes (Baudino et al., 2003). Interestingly, both Affymetrix microarray and real-time PCR analysis performed on premalignant *tal1* thymocytes demonstrate a modest increase in c-Myc expression. Perhaps Tal1 indirectly promotes S phase induction and the subsequent apoptosis by upregulating c-Myc expression. It will be interesting to determine if Tal1 directly induces c-Myc expression, and future experiments should include chromatin immunoprecipitation experiments to determine if Tal1/E47 or Tal1/Heb heterodimers can be detected at the E-boxes within the *c-myc* promoter. Alternatively, E2a inhibition may also be causing the Myc induction. Consistent, *e2a*-deficient tumors exhibit amplification of chromosome 15, which contains *c-myc* (Bain et al., 1997). Additionally, *tal1/lmo1* tumors show increased expression of c-Myc (Chervinsky et al., 1999), and spectral karyotyping indicates 20% of *tal1* tumors exhibit a gain of chromosome 15 (unpublished data). Furthermore, *tal1* transgenic mice display dramatically accelerated disease progression when crossed to *casein kinase II (CK2)* transgenic mice (Kelliher et al., 1996). CK2 is a serine/threonine kinase that has been shown to phosphorylate and stabilize c-Myc (Channavajhala and Seldin, 2002). Thus, multiple leukemic models exhibit modest induction of Myc, suggesting that this increased

dosage of c-Myc may be important for leukemogenesis. Therefore, it is tempting to hypothesize that an additional role for Tal1 in leukemogenesis is the induction of c-Myc. Nonetheless, combined transgenic expression of Tal1 and c-Myc fail to cooperate in vivo, as no disease acceleration is observed in *Eμ/tTA/Myc/tal1* triple transgenic mouse (data not shown). However, it remains possible that Tal1 and Myc cooperate in leukemogenesis, as the experiment may be flawed since Myc and Tal1 expression may not have been overlapping.

The *lck-tal1* transgenic mice develop leukemia with a long latency and incomplete penetrance, indicating additional mutations are essential in leukemogenesis. It has been previously shown that the deletion of the *INK4A/ARF*, which encodes the tumor suppressors $p16^{INK4a}$ and $p14^{ARF}$, is a common event in human TAL1-expressing leukemic patients (Ferrando et al., 2002). In addition, although the most frequent mutation disrupting the *INK4A/ARF* allele is deletion of exon 2, a common exon to both $p16^{INK4a}$ and $p14^{ARF}$, additional leukemic patients display the loss of either $p14^{ARF}$ or $p16^{INK4A}$ (Batova et al., 1997; Drexler, 1998; Gardie et al., 1998). Although, the overall contribution of each tumor suppressor to T cell leukemogenesis remains unclear, the common viewpoint is loss of $p16^{Ink4a}$ is the important genetic mutation in leukemogenesis. This thesis provides genetic evidence confirming Tal1 expression cooperates with the loss of the *ink4a/arf* allele *in vivo; tal1/ink4a/arf*+/- mice display accelerated leukemogenesis with an increased penetrance (Chapter III). The cooperation of Tal1 and loss of *ink4a/arf* allele indicates that disruption of Tal1-mediated apoptosis may be an important event in leukemogenesis. Consistent with this hypothesis, *tal1/p53*+/- mice display disease acceleration(Condorelli et al., 1996).

A subset of *tal1/ink4a/arf*+/- tumors undergoes LOH, as indicated by loss of the shared exon 2, while another subset demonstrates evidence of $p16^{ink4A}$ promoter methylation. Although this analysis implicates that loss of either $p16^{Ink4a}$ or $p19^{Arf}$ may cooperate with Tal1, their relative contribution remained unclear. To determine whether Tal1 preferentially cooperates with loss of $p16^{Ink4a}$ or $p19^{Arf}$, we generated both *tal1/*$p16^{ink4a}$+/- and *tal1/*$p19^{arf}$+/- mice, and observed similar disease acceleration, indicating Tal1 cooperates with loss of either $p16^{Ink4a}$ or $p19^{Arf}$. This demonstrates for the first time that the loss of $p19^{Arf}$ contributes to Tal1-mediated leukemogenesis.

The cooperation of Tal1 with the loss of $p19^{Arf}$ is consistent with Tal1-induced proliferation and apoptosis. Similar to the mechanism delineated in Eμ-Myc-induced lymphoma (Eischen et al., 1999), disruption of the $p19^{arf}$-Mdm2-p53 pathway in *tal1* thymocytes may prevent the Tal1-mediated apoptosis, thereby allowing pre-leukemic clones to survive. Conversely, the cooperation of Tal1 with loss of $p16^{Ink4a}$ reflects the common loss of $p16^{INK4A}$ observed in human leukemias. This cooperation may be due to increased proliferative signal or effects of $p16^{Ink4a}$ loss on senescence.

Additionally, my thesis research has identified Notch1 activation as a common secondary event that occurs during leukemogenesis. By performing RIM, we determined activation of the Notch1 signaling pathway may cooperate with Tal1 in leukemogenesis (Chapter IV). Specifically, 32% of MoMLV-infected *mut tal1(R188G;R189G)* tumors exhibit MoMLV integrations between exons 22-26 of *notch1*, presumably creating an allele capable of ligand-independent signaling. Conversely, MoMLV-infected *mut tal1 (R188G;R189G)* tumors lacked MoMLV integrations in the 3' of *notch1*, resulting in the loss of the negative-regulatory PEST domain, and the subsequent enhanced stability of

$Notch^{IC}$. The majority of tumors exhibiting *notch1* integrations continue to express Notch1, Deltex, and Hes1, indicating the tumors remain dependent of Notch1 signaling.

Significantly, a study revealed over 50% of human T-ALL patients exhibit mutations in the HD and PEST domains of *NOTCH1* (Weng et al., 2004). In fact, 43% of T-ALL patients contain mutations in the HD domain, which are hypothesized to destabilize the NEC/NTM interaction and confer greater susceptibility to γ-secretase cleavage (Figure 23) (Weng et al., 2004). An additional 30% of T-ALL patients demonstrate an insertion/deletion into the PEST domain. Of these patients, 18% contain both HD and PEST mutations together in *cis* (Weng et al., 2004).

Concurrent with this clinical finding, we demonstrate spontaneous *tal1* tumors also exhibit frequent Notch1 activation. In fact, the vast majority of *tal1* tumor cell lines express cleaved Notch1, and continue to express Notch1 target genes, Hes1 and Deltex, indicating the tumors remain dependent on Notch1 signaling. Furthermore, *tal1* tumors exhibit a G_1 arrest and/or apoptosis following treatment with γ-secretase inhibitors (GSI). Consistent with the widespread Notch1 activation in *tal1* tumors, we observe mutations in the HD and/or PEST domains of *notch1 in* 25/35 (71%) of *tal1* tumors examined. However, no *tal1* tumors exhibit mutations in *notch2, 3,* or, *4*, suggesting Notch1 activation may preferentially contribute to Tal1-mediated leukemogenesis. Interestingly, transgenic mice expressing both BHLHB1 and LMO2, two proteins that inhibit E2a function, develop T cell tumors exhibiting Notch1 activation, as revealed by GSI-sensitivity and *notch1* mutations (Lin et al., 2005). However, lymphomas arising in mice deficient for various combinations of *rag2, H2AX,* or *p53-/-* demonstrate a greatly reduced frequency of Notch1 activation (O'Neil, unpublished data). Additional

mutational analysis for other transgenic mouse models that display E2a inhibition should be performed, but together these data suggests that inhibition of E2a may cooperate with Notch activation in leukemogenesis.

Although the vast majority of the *tal1* tumors exhibit Notch1 activation, we still do not understand the signal Notch1 provides leukemic cells. To try to elucidate this signal, I generated a doxycycline-responsive Notch^{IC} cell line. Treatment of the dox-responsive Notch^{IC} cell line resulted in a decrease in the expression of Notch1 and Notch target genes as early as 24h following dox treatment. Additionally, a 72h dox treatment induces both a G_1 arrest and an accumulation of subG_1 cells, indicating that Notch^{IC} is providing both a proliferative and anti-apoptotic signal. Performing gene expression profiling revealed the dox-mediated regulation of numerous Notch1 target genes, including: Hes1, Deltex, CD25, Nrarp, IL10, IRF4, Egr1, and ADAM 19. This analysis also provides a list of new Notch1 target genes, which are currently undergoing further validation. Significantly, we observe the upregulation of c-Myc in the dox-responsive cell line, and we have preliminary evidence of partial rescue following ectopic expression of c-Myc. However, it is unlikely that one gene will fully rescue Notch^{IC} induced effects. We are in the process of performing additional microarray analysis on GSI-treated *tal1* tumor cell lines. Since GSI treatment is not Notch-specific, the comparison of gene profiling from GSI-treated tumors to the dox-responsive cell line will allow us to establish which targets in the GSI-microarray are Notch-specific. Additionally, these comparisons will allow us to elucidate what genes are globally affected by Notch activation in leukemia. Although this strategy will likely illuminate important Notch^{IC}

targets in leukemogenesis, it is predicted that in other malignancies, the $Notch^{IC}$ targets will vastly differ.

In summary, my thesis work has revealed a novel function for Tal1 in leukemia; expression of Tal1 in thymoyctes promotes an S phase induction and is associated with an increase in apoptosis. *Tal1* transgenic mice develop disease with a long latency and incomplete penetrance, indicating additional genetic events are essential for leukemogenesis. In my thesis work I have identified two secondary mutations that cooperate with Tal1: the loss of either $p16^{Ink4a}$ or $p19^{Arf}$, and the activation of the Notch1 signaling pathway. In the process of identifying cooperating mutations, I modified the *tal1* transgenic mouse model to more closely resemble human T-ALL. *Tal1/ink/arf*+/- mice exhibit the two most common mutations observed in human T-ALL, and develop leukemia with a complete penetrance. Therefore, this mouse model is amenable to testing potential therapeutic compounds, such as GSI or HDAC inhibitors *in vivo*. Additionally, it can be used to develop therapeutic agents for T-ALL patients displaying both TAL1 overexpression and loss of *INK4A/ARF*, a specific subset of patients given a poor prognosis.

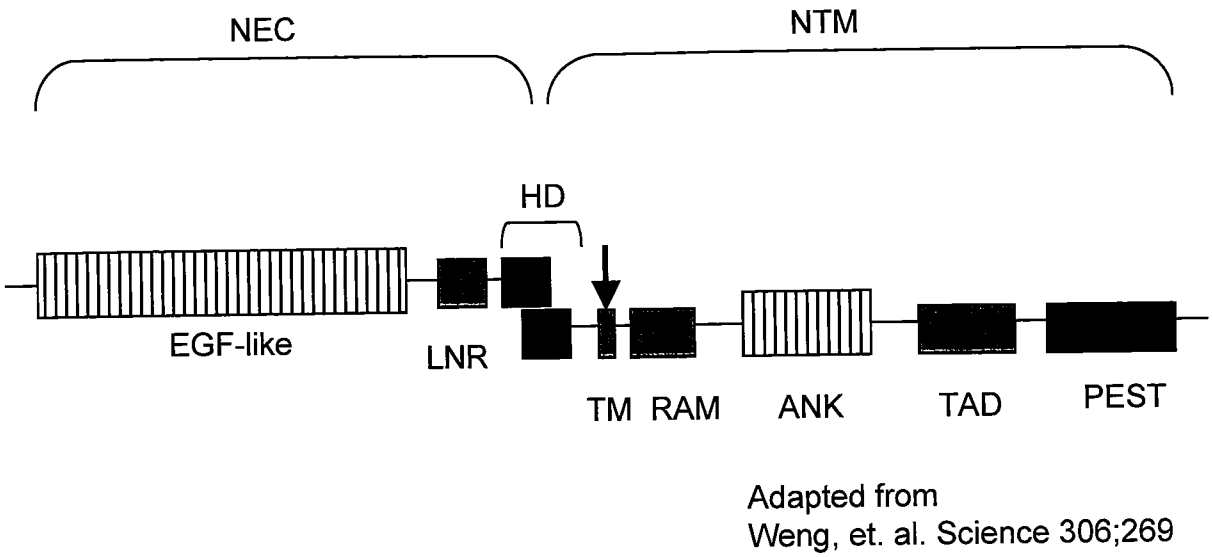

Figure 24. Schematic of *NOTCH1* mutations observed in T-ALL. Domains of NOTCH1 exhibiting frequent mutations in T-ALL are identified (red). HD mutations lead to increased $NOTCH^{IC}$ production due to increased susceptibility to γ-secretase cleavage. PEST mutations result in PEST deletion and increase $NOTCH^{IC}$ stability. Red arrow signifies site of γ-secretase cleavage

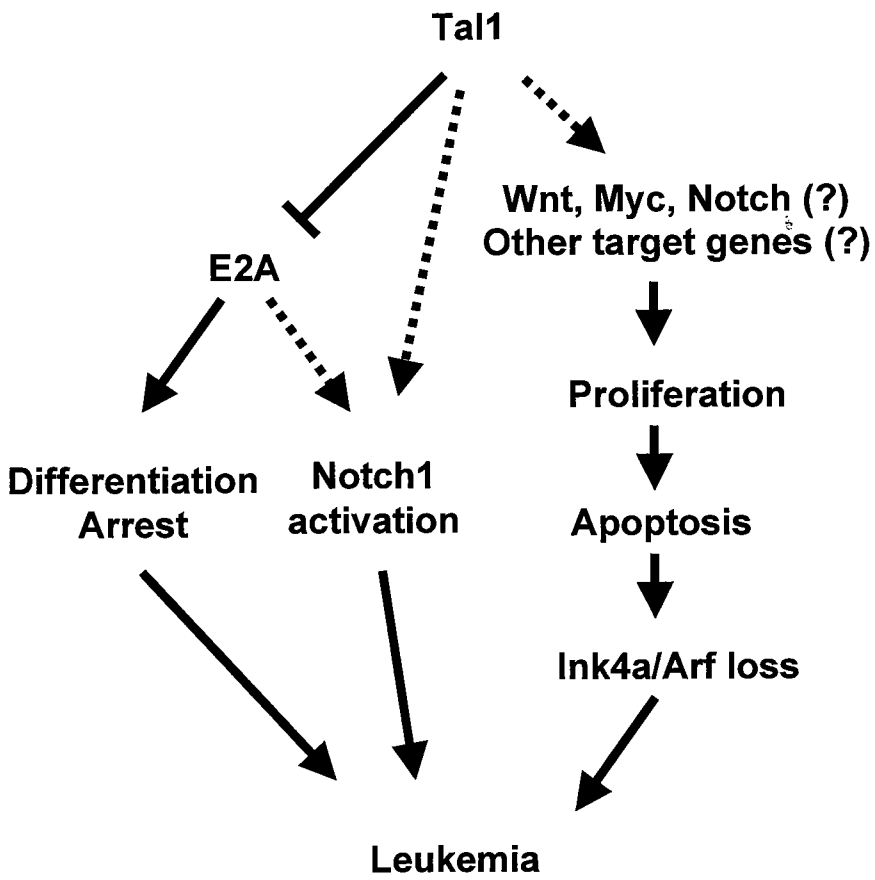

Figure 24. Proposed model of Tal1-mediated leukemogenesis. We have previously demonstrated that Tal1 inhibits E2a function and induces a thymocyte differentiation arrest. This thesis demonstrates that Tal1 additionally promotes an S phase induction, and is associated with an increase in thymocyte apoptosis. Microarray analysis suggests the Wnt and Notch receptor pathways may contribute to the S phase induction. We demonstrate that loss of *ink4a/arf* locus cooperates with Tal1 in leukemogenesis, suggesting that disruption of this Tal1-mediated apoptosis is an important step in leukemogenesis. Finally, we demonstrate another important genetic event in Tal1-mediated leukemogenesis is Notch1 activation. Dotted lines indicate parts of the pathway that require additional investigation.

REFERENCES

Adams, J. M., Harris, A. W., Pinkert, C. A., Corcoran, L. M., Alexander, W. S., Cory, S., Palmiter, R. D., and Brinster, R. L. (1985). The c-myc oncogene driven by immunoglobulin enhancers induces lymphoid malignancy in transgenic mice. Nature *318*, 533-538.

Adler, S. H., Chiffoleau, E., Xu, L., Dalton, N. M., Burg, J. M., Wells, A. D., Wolfe, M. S., Turka, L. A., and Pear, W. S. (2003). Notch signaling augments T cell responsiveness by enhancing CD25 expression. J Immunol *171*, 2896-2903.

Alcalay, M., Zangrilli, D., Fagioli, M., Pandolfi, P. P., Mencarelli, A., Lo Coco, F., Biondi, A., Grignani, F., and Pelicci, P. G. (1992). Expression pattern of the RAR alpha-PML fusion gene in acute promyelocytic leukemia. Proc Natl Acad Sci U S A *89*, 4840-4844.

Allen, R. D., 3rd, Kim, H. K., Sarafova, S. D., and Siu, G. (2001). Negative regulation of CD4 gene expression by a HES-1-c-Myb complex. Mol Cell Biol *21*, 3071-3082.

Altura, R. A., Inukai, T., Ashmun, R. A., Zambetti, G. P., Roussel, M. F., and Look, A. T. (1998). The chimeric E2A-HLF transcription factor abrogates p53-induced apoptosis in myeloid leukemia cells. Blood *92*, 1397-1405.

Amsen, D., Blander, J. M., Lee, G. R., Tanigaki, K., Honjo, T., and Flavell, R. A. (2004). Instruction of distinct CD4 T helper cell fates by different notch ligands on antigen-presenting cells. Cell *117*, 515-526.

Anderson, G., Pongracz, J., Parnell, S., and Jenkinson, E. J. (2001). Notch ligand-bearing thymic epithelial cells initiate and sustain Notch signaling in thymocytes independently of T cell receptor signaling. Eur J Immunol *31*, 3349-3354.

Apelqvist, A., Li, H., Sommer, L., Beatus, P., Anderson, D. J., Honjo, T., Hrabe de Angelis, M., Lendahl, U., and Edlund, H. (1999). Notch signalling controls pancreatic cell differentiation. Nature *400*, 877-881.

Aplan, P. D., Jones, C. A., Chervinsky, D. S., Zhao, X., Ellsworth, M., Wu, C., McGuire, E. A., and Gross, K. W. (1997). An scl gene product lacking the transactivation domain induces bony abnormalities and cooperates with LMO1 to generate T-cell malignancies in transgenic mice. Embo J *16*, 2408-2419.

Aplan, P. D., Lombardi, D. P., Ginsberg, A. M., Cossman, J., Bertness, V. L., and Kirsch, I. R. (1990). Disruption of the human SCL locus by "illegitimate" V-(D)-J recombinase activity. Science *250*, 1426-1429.

Aplan, P. D., Lombardi, D. P., and Kirsch, I. R. (1991). Structural characterization of SIL, a gene frequently disrupted in T-cell acute lymphoblastic leukemia. Mol Cell Biol *11*, 5462-5469.

Aplan, P. D., Nakahara, K., Orkin, S. H., and Kirsch, I. R. (1992). The SCL gene product: a positive regulator of erythroid differentiation. Embo J *11*, 4073-4081.

Aronheim, A., Shiran, R., Rosen, A., and Walker, M. D. (1993). The E2A gene product contains two separable and functionally distinct transcription activation domains. Proc Natl Acad Sci U S A *90*, 8063-8067.

Artavanis-Tsakonas, S., Rand, M. D., and Lake, R. J. (1999). Notch signaling: cell fate control and signal integration in development. Science *284*, 770-776.

Askew, D. S., Ashmun, R. A., Simmons, B. C., and Cleveland, J. L. (1991). Constitutive c-myc expression in an IL-3-dependent myeloid cell line suppresses cell cycle arrest and accelerates apoptosis. Oncogene *6*, 1915-1922.

Aster, J. C., Xu, L., Karnell, F. G., Patriub, V., Pui, J. C., and Pear, W. S. (2000). Essential roles for ankyrin repeat and transactivation domains in induction of T-cell leukemia by notch1. Mol Cell Biol *20*, 7505-7515.

Atherton, G. T., Travers, H., Deed, R., and Norton, J. D. (1996). Regulation of cell differentiation in C2C12 myoblasts by the Id3 helix-loop-helix protein. Cell Growth Differ *7*, 1059-1066.

Bailey, A. M., and Posakony, J. W. (1995). Suppressor of hairless directly activates transcription of enhancer of split complex genes in response to Notch receptor activity. Genes Dev *9*, 2609-2622.

Bain, G., Cravatt, C. B., Loomans, C., Alberola-Ila, J., Hedrick, S. M., and Murre, C. (2001). Regulation of the helix-loop-helix proteins, E2A and Id3, by the Ras-ERK MAPK cascade. Nat Immunol *2*, 165-171.

Bain, G., Engel, I., Robanus Maandag, E. C., te Riele, H. P., Voland, J. R., Sharp, L. L., Chun, J., Huey, B., Pinkel, D., and Murre, C. (1997). E2A deficiency leads to abnormalities in alphabeta T-cell development and to rapid development of T-cell lymphomas. Mol Cell Biol *17*, 4782-4791.

Bain, G., Maandag, E. C., Izon, D. J., Amsen, D., Kruisbeek, A. M., Weintraub, B. C., Krop, I., Schlissel, M. S., Feeney, A. J., van Roon, M., and et al. (1994). E2A proteins are required for proper B cell development and initiation of immunoglobulin gene rearrangements. Cell *79*, 885-892.

Bain, G., Quong, M. W., Soloff, R. S., Hedrick, S. M., and Murre, C. (1999). Thymocyte maturation is regulated by the activity of the helix-loop-helix protein, E47. J Exp Med *190*, 1605-1616.

Bain, G., Romanow, W. J., Albers, K., Havran, W. L., and Murre, C. (1999). Positive and negative regulation of V(D)J recombination by the E2A proteins. J Exp Med *189*, 289-300.

Barndt, R., Dai, M. F., and Zhuang, Y. (1999). A novel role for HEB downstream or parallel to the pre-TCR signaling pathway during alpha beta thymopoiesis. J Immunol *163*, 3331-3343.

Barone, M. V., Pepperkok, R., Peverali, F. A., and Philipson, L. (1994). Id proteins control growth induction in mammalian cells. Proc Natl Acad Sci U S A *91*, 4985-4988.

Bash, R. O., Crist, W. M., Shuster, J. J., Link, M. P., Amylon, M., Pullen, J., Carroll, A. J., Buchanan, G. R., Smith, R. G., and Baer, R. (1993). Clinical features and outcome of T-cell acute lymphoblastic leukemia in childhood with respect to alterations at the TAL1 locus: a Pediatric Oncology Group study. Blood *81*, 2110-2117.

Bash, R. O., Hall, S., Timmons, C. F., Crist, W. M., Amylon, M., Smith, R. G., and Baer, R. (1995). Does activation of the TAL1 gene occur in a majority of patients with T-cell acute lymphoblastic leukemia? A pediatric oncology group study. Blood *86*, 666-676.

Bates, S., Phillips, A. C., Clark, P. A., Stott, F., Peters, G., Ludwig, R. L., and Vousden, K. H. (1998). p14ARF links the tumour suppressors RB and p53. Nature *395*, 124-125.

Batova, A., Diccianni, M. B., Yu, J. C., Nobori, T., Link, M. P., Pullen, J., and Yu, A. L. (1997). Frequent and selective methylation of p15 and deletion of both p15 and p16 in T-cell acute lymphoblastic leukemia. Cancer Res *57*, 832-836.

Baudino, T. A., Maclean, K. H., Brennan, J., Parganas, E., Yang, C., Aslanian, A., Lees, J. A., Sherr, C. J., Roussel, M. F., and Cleveland, J. L. (2003). Myc-mediated proliferation and lymphomagenesis, but not apoptosis, are compromised by E2f1 loss. Mol Cell *11*, 905-914.

Begley, C. G., Aplan, P. D., Davey, M. P., Nakahara, K., Tchorz, K., Kurtzberg, J., Hershfield, M. S., Haynes, B. F., Cohen, D. I., Waldmann, T. A., and et al. (1989). Chromosomal translocation in a human leukemic stem-cell line disrupts the T-cell antigen receptor delta-chain diversity region and results in a previously unreported fusion transcript. Proc Natl Acad Sci U S A *86*, 2031-2035.

Begley, C. G., Aplan, P. D., Denning, S. M., Haynes, B. F., Waldmann, T. A., and Kirsch, I. R. (1989). The gene SCL is expressed during early hematopoiesis and encodes a differentiation-related DNA-binding motif. Proc Natl Acad Sci U S A *86*, 10128-10132.

Bellavia, D., Campese, A. F., Alesse, E., Vacca, A., Felli, M. P., Balestri, A., Stoppacciaro, A., Tiveron, C., Tatangelo, L., Giovarelli, M., *et al.* (2000). Constitutive activation of NF-kappaB and T-cell leukemia/lymphoma in Notch3 transgenic mice. Embo J *19*, 3337-3348.

Bellavia, D., Campese, A. F., Checquolo, S., Balestri, A., Biondi, A., Cazzaniga, G., Lendahl, U., Fehling, H. J., Hayday, A. C., Frati, L., *et al.* (2002). Combined expression of pTalpha and Notch3 in T cell leukemia identifies the requirement of preTCR for leukemogenesis. Proc Natl Acad Sci U S A *99*, 3788-3793.

Ben-Arie, N., Bellen, H. J., Armstrong, D. L., McCall, A. E., Gordadze, P. R., Guo, Q., Matzuk, M. M., and Zoghbi, H. Y. (1997). Math1 is essential for genesis of cerebellar granule neurons. Nature *390*, 169-172.

Benezra, R., Davis, R. L., Lockshon, D., Turner, D. L., and Weintraub, H. (1990). The protein Id: a negative regulator of helix-loop-helix DNA binding proteins. Cell *61*, 49-59.

Bessho, Y., and Kageyama, R. (2003). Oscillations, clocks and segmentation. Curr Opin Genet Dev *13*, 379-384.

Bettenhausen, B., Hrabe de Angelis, M., Simon, D., Guenet, J. L., and Gossler, A. (1995). Transient and restricted expression during mouse embryogenesis of Dll1, a murine gene closely related to Drosophila Delta. Development *121*, 2407-2418.

Beverly, L. J., and Capobianco, A. J. (2003). Perturbation of Ikaros isoform selection by MLV integration is a cooperative event in Notch(IC)-induced T cell leukemogenesis. Cancer Cell *3*, 551-564.

Beverly, L. J., Felsher, D. W., and Capobianco, A. J. (2005). Suppression of p53 by Notch in lymphomagenesis: implications for initiation and regression. Cancer Res *65*, 7159-7168.

Bigas, A., Martin, D. I., and Milner, L. A. (1998). Notch1 and Notch2 inhibit myeloid differentiation in response to different cytokines. Mol Cell Biol *18*, 2324-2333.

Borg, A., Johannsson, U., Johannsson, O., Hakansson, S., Westerdahl, J., Masback, A., Olsson, H., and Ingvar, C. (1996). Novel germline p16 mutation in familial malignant melanoma in southern Sweden. Cancer Res *56*, 2497-2500.

Brambillasca, F., Mosna, G., Colombo, M., Rivolta, A., Caslini, C., Minuzzo, M., Giudici, G., Mizzi, L., Biondi, A., and Privitera, E. (1999). Identification of a novel molecular partner of the E2A gene in childhood leukemia. Leukemia *13*, 369-375.

Brou, C., Logeat, F., Gupta, N., Bessia, C., LeBail, O., Doedens, J. R., Cumano, A., Roux, P., Black, R. A., and Israel, A. (2000). A novel proteolytic cleavage involved in Notch signaling: the role of the disintegrin-metalloprotease TACE. Mol Cell *5*, 207-216.

Brown, L., Cheng, J. T., Chen, Q., Siciliano, M. J., Crist, W., Buchanan, G., and Baer, R. (1990). Site-specific recombination of the tal-1 gene is a common occurrence in human T cell leukemia. Embo J *9*, 3343-3351.

Calin, G. A., Dumitru, C. D., Shimizu, M., Bichi, R., Zupo, S., Noch, E., Aldler, H., Rattan, S., Keating, M., Rai, K., *et al.* (2002). Frequent deletions and down-regulation of micro- RNA genes miR15 and miR16 at 13q14 in chronic lymphocytic leukemia. Proc Natl Acad Sci U S A *99*, 15524-15529.

Capobianco, A. J., Zagouras, P., Blaumueller, C. M., Artavanis-Tsakonas, S., and Bishop, J. M. (1997). Neoplastic transformation by truncated alleles of human NOTCH1/TAN1 and NOTCH2. Mol Cell Biol *17*, 6265-6273.

Carlesso, N., Aster, J. C., Sklar, J., and Scadden, D. T. (1999). Notch1-induced delay of human hematopoietic progenitor cell differentiation is associated with altered cell cycle kinetics. Blood *93*, 838-848.

Cayuela, J. M., Gardie, B., and Sigaux, F. (1997). Disruption of the multiple tumor suppressor gene MTS1/p16(INK4a)/CDKN2 by illegitimate V(D)J recombinase activity in T-cell acute lymphoblastic leukemias. Blood *90*, 3720-3726.

Cayuela, J. M., Hebert, J., and Sigaux, F. (1995). Homozygous MTS1 (p16INK4A) deletion in primary tumor cells of 163 leukemic patients. Blood *85*, 854.

Cayuela, J. M., Madani, A., Sanhes, L., Stern, M. H., and Sigaux, F. (1996). Multiple tumor-suppressor gene 1 inactivation is the most frequent genetic alteration in T-cell acute lymphoblastic leukemia. Blood *87*, 2180-2186.

Channavajhala, P., and Seldin, D. C. (2002). Functional interaction of protein kinase CK2 and c-Myc in lymphomagenesis. Oncogene *21*, 5280-5288.

Chen, J., Jackson, P. K., Kirschner, M. W., and Dutta, A. (1995). Separate domains of p21 involved in the inhibition of Cdk kinase and PCNA. Nature *374*, 386-388.

Cheng, J. T., Hsu, H. L., Hwang, L. Y., and Baer, R. (1993). Products of the TAL1 oncogene: basic helix-loop-helix proteins phosphorylated at serine residues. Oncogene *8*, 677-683.

Chervinsky, D. S., Zhao, X. F., Lam, D. H., Ellsworth, M., Gross, K. W., and Aplan, P. D. (1999). Disordered T-cell development and T-cell malignancies in SCL LMO1 double-transgenic mice: parallels with E2A-deficient mice. Mol Cell Biol *19*, 5025-5035.

Chiaramonte, R., Calzavara, E., Balordi, F., Sabbadini, M., Capello, D., Gaidano, G., Serra, A., Comi, P., and Sherbet, G. V. (2003). Differential regulation of Notch signal transduction in leukaemia and lymphoma cells in culture. J Cell Biochem *88*, 569-577.

Chilcote, R. R., Brown, E., and Rowley, J. D. (1985). Lymphoblastic leukemia with lymphomatous features associated with abnormalities of the short arm of chromosome 9. N Engl J Med *313*, 286-291.

Choi, J. K., Shen, C. P., Radomska, H. S., Eckhardt, L. A., and Kadesch, T. (1996). E47 activates the Ig-heavy chain and TdT loci in non-B cells. Embo J *15*, 5014-5021.

Chu, C., and Kohtz, D. S. (2001). Identification of the E2A gene products as regulatory targets of the G1 cyclin-dependent kinases. J Biol Chem *276*, 8524-8534.

Condorelli, G. L., Facchiano, F., Valtieri, M., Proietti, E., Vitelli, L., Lulli, V., Huebner, K., Peschle, C., and Croce, C. M. (1996). T-cell-directed TAL-1 expression induces T-cell malignancies in transgenic mice. Cancer Res *56*, 5113-5119.

Condorelli, G. L., Tocci, A., Botta, R., Facchiano, F., Testa, U., Vitelli, L., Valtieri, M., Croce, C. M., and Peschle, C. (1997). Ectopic TAL-1/SCL expression in phenotypically normal or leukemic myeloid precursors: proliferative and antiapoptotic effects coupled with a differentiation blockade. Mol Cell Biol *17*, 2954-2969.

Conlon, R. A., Reaume, A. G., and Rossant, J. (1995). Notch1 is required for the coordinate segmentation of somites. Development *121*, 1533-1545.

Conradt, B., and Horvitz, H. R. (1998). The C. elegans protein EGL-1 is required for programmed cell death and interacts with the Bcl-2-like protein CED-9. Cell *93*, 519-529.

Coppola, J. A., and Cole, M. D. (1986). Constitutive c-myc oncogene expression blocks mouse erythroleukaemia cell differentiation but not commitment. Nature *320*, 760-763.

Cowan, J. W., Wang, X., Guan, R., He, K., Jiang, J., Baumann, G., Black, R. A., Wolfe, M. S., and Frank, S. J. (2005). Growth hormone receptor is a target for presenilin-dependent gamma-secretase cleavage. J Biol Chem *280*, 19331-19342.

de Stanchina, E., McCurrach, M. E., Zindy, F., Shieh, S. Y., Ferbeyre, G., Samuelson, A. V., Prives, C., Roussel, M. F., Sherr, C. J., and Lowe, S. W. (1998). E1A signaling to p53 involves the p19(ARF) tumor suppressor. Genes Dev *12*, 2434-2442.

De Strooper, B. (2003). Aph-1, Pen-2, and Nicastrin with Presenilin generate an active gamma-Secretase complex. Neuron *38*, 9-12.

De Strooper, B., Annaert, W., Cupers, P., Saftig, P., Craessaerts, K., Mumm, J. S., Schroeter, E. H., Schrijvers, V., Wolfe, M. S., Ray, W. J., *et al.* (1999). A presenilin-1-dependent gamma-secretase-like protease mediates release of Notch intracellular domain. Nature *398*, 518-522.

Deed, R. W., Hara, E., Atherton, G. T., Peters, G., and Norton, J. D. (1997). Regulation of Id3 cell cycle function by Cdk-2-dependent phosphorylation. Mol Cell Biol *17*, 6815-6821.

Deftos, M. L., and Bevan, M. J. (2000). Notch signaling in T cell development. Curr Opin Immunol *12*, 166-172.

Deftos, M. L., He, Y. W., Ojala, E. W., and Bevan, M. J. (1998). Correlating notch signaling with thymocyte maturation. Immunity *9*, 777-786.

Deftos, M. L., Huang, E., Ojala, E. W., Forbush, K. A., and Bevan, M. J. (2000). Notch1 signaling promotes the maturation of CD4 and CD8 SP thymocytes. Immunity *13*, 73-84.

DeGregori, J., Kowalik, T., and Nevins, J. R. (1995). Cellular targets for activation by the E2F1 transcription factor include DNA synthesis- and G1/S-regulatory genes. Mol Cell Biol *15*, 4215-4224.

Desprez, P. Y., Hara, E., Bissell, M. J., and Campisi, J. (1995). Suppression of mammary epithelial cell differentiation by the helix-loop-helix protein Id-1. Mol Cell Biol *15*, 3398-3404.

Devaraj, P. E., Foroni, L., Sekhar, M., Butler, T., Wright, F., Mehta, A., Samson, D., Prentice, H. G., Hoffbrand, A. V., and Secker-Walker, L. M. (1994). E2A/HLF fusion cDNAs and the use of RT-PCR for the detection of minimal residual disease in t(17;19)(q22;p13) acute lymphoblastic leukemia. Leukemia *8*, 1131-1138.

Diaz, M. O., Ziemin, S., Le Beau, M. M., Pitha, P., Smith, S. D., Chilcote, R. R., and Rowley, J. D. (1988). Homozygous deletion of the alpha- and beta 1-interferon genes in human leukemia and derived cell lines. Proc Natl Acad Sci U S A *85*, 5259-5263.

Dmitrovsky, E., Kuehl, W. M., Hollis, G. F., Kirsch, I. R., Bender, T. P., and Segal, S. (1986). A transfected c-myc oncogene inhibits mouse erythroleukemic differentiation. Curr Top Microbiol Immunol *132*, 327-330.

Doerfler, P., Shearman, M. S., and Perlmutter, R. M. (2001). Presenilin-dependent gamma-secretase activity modulates thymocyte development. Proc Natl Acad Sci U S A *98*, 9312-9317.

Domen, J., Gandy, K. L., and Weissman, I. L. (1998). Systemic overexpression of BCL-2 in the hematopoietic system protects transgenic mice from the consequences of lethal irradiation. Blood *91*, 2272-2282.

Drexler, H. G. (1998). Review of alterations of the cyclin-dependent kinase inhibitor INK4 family genes p15, p16, p18 and p19 in human leukemia-lymphoma cells. Leukemia *12*, 845-859.

Duncan, A. W., Rattis, F. M., DiMascio, L. N., Congdon, K. L., Pazianos, G., Zhao, C., Yoon, K., Cook, J. M., Willert, K., Gaiano, N., and Reya, T. (2005). Integration of Notch and Wnt signaling in hematopoietic stem cell maintenance. Nat Immunol *6*, 314-322.

Duronio, R. J., and O'Farrell, P. H. (1995). Developmental control of the G1 to S transition in Drosophila: cyclin Eis a limiting downstream target of E2F. Genes Dev *9*, 1456-1468.

Eischen, C. M., Weber, J. D., Roussel, M. F., Sherr, C. J., and Cleveland, J. L. (1999). Disruption of the ARF-Mdm2-p53 tumor suppressor pathway in Myc-induced lymphomagenesis. Genes Dev *13*, 2658-2669.

el-Deiry, W. S., Harper, J. W., O'Connor, P. M., Velculescu, V. E., Canman, C. E., Jackman, J., Pietenpol, J. A., Burrell, M., Hill, D. E., Wang, Y., and et al. (1994). WAF1/CIP1 is induced in p53-mediated G1 arrest and apoptosis. Cancer Res *54*, 1169-1174.

Ellenberger, T., Fass, D., Arnaud, M., and Harrison, S. C. (1994). Crystal structure of transcription factor E47: E-box recognition by a basic region helix-loop-helix dimer. Genes Dev *8*, 970-980.

Ellis, R. E., and Horvitz, H. R. (1991). Two C. elegans genes control the programmed deaths of specific cells in the pharynx. Development *112*, 591-603.

Ellisen, L. W., Bird, J., West, D. C., Soreng, A. L., Reynolds, T. C., Smith, S. D., and Sklar, J. (1991). TAN-1, the human homolog of the Drosophila notch gene, is broken by chromosomal translocations in T lymphoblastic neoplasms. Cell *66*, 649-661.

Elwood, N. J., Zogos, H., Pereira, D. S., Dick, J. E., and Begley, C. G. (1998). Enhanced megakaryocyte and erythroid development from normal human CD34(+) cells: consequence of enforced expression of SCL. Blood *91*, 3756-3765.

Ema, M., Faloon, P., Zhang, W. J., Hirashima, M., Reid, T., Stanford, W. L., Orkin, S., Choi, K., and Rossant, J. (2003). Combinatorial effects of Flk1 and Tal1 on vascular and hematopoietic development in the mouse. Genes Dev *17*, 380-393.

Engel, I., Johns, C., Bain, G., Rivera, R. R., and Murre, C. (2001). Early thymocyte development is regulated by modulation of E2A protein activity. J Exp Med *194*, 733-745.

Engel, I., and Murre, C. (1999). Ectopic expression of E47 or E12 promotes the death of E2A-deficient lymphomas. Proc Natl Acad Sci U S A *96*, 996-1001.

Engel, I., and Murre, C. (2004). E2A proteins enforce a proliferation checkpoint in developing thymocytes. Embo J *23*, 202-211.

Espinosa, L., Ingles-Esteve, J., Aguilera, C., and Bigas, A. (2003). Phosphorylation by glycogen synthase kinase-3 beta down-regulates Notch activity, a link for Notch and Wnt pathways. J Biol Chem *278*, 32227-32235.

Evan, G. I., Wyllie, A. H., Gilbert, C. S., Littlewood, T. D., Land, H., Brooks, M., Waters, C. M., Penn, L. Z., and Hancock, D. C. (1992). Induction of apoptosis in fibroblasts by c-myc protein. Cell *69*, 119-128.

Feldman, B. J., Hampton, T., and Cleary, M. L. (2000). A carboxy-terminal deletion mutant of Notch1 accelerates lymphoid oncogenesis in E2A-PBX1 transgenic mice. Blood *96*, 1906-1913.

Ferrando, A. A., Herblot, S., Palomero, T., Hansen, M., Hoang, T., Fox, E. A., and Look, A. T. (2004). Biallelic transcriptional activation of oncogenic transcription factors in T-cell acute lymphoblastic leukemia. Blood *103*, 1909-1911.

Ferrando, A. A., Neuberg, D. S., Staunton, J., Loh, M. L., Huard, C., Raimondi, S. C., Behm, F. G., Pui, C. H., Downing, J. R., Gilliland, D. G., *et al.* (2002). Gene expression

signatures define novel oncogenic pathways in T cell acute lymphoblastic leukemia. Cancer Cell *1*, 75-87.

Fitzgerald, T. J., Neale, G. A., Raimondi, S. C., and Goorha, R. M. (1991). c-tal, a helix-loop-helix protein, is juxtaposed to the T-cell receptor-beta chain gene by a reciprocal chromosomal translocation: t(1;7)(p32;q35). Blood *78*, 2686-2695.

Fonjallaz, P., Ossipow, V., Wanner, G., and Schibler, U. (1996). The two PAR leucine zipper proteins, TEF and DBP, display similar circadian and tissue-specific expression, but have different target promoter preferences. Embo J *15*, 351-362.

Francke, U., and Kung, F. (1976). Sporadic bilateral retinoblastoma and 13q- chromosomal deletion. Med Pediatr Oncol *2*, 379-385.

Fre, S., Huyghe, M., Mourikis, P., Robine, S., Louvard, D., and Artavanis-Tsakonas, S. (2005). Notch signals control the fate of immature progenitor cells in the intestine. Nature *435*, 964-968.

Friend, S. H., Bernards, R., Rogelj, S., Weinberg, R. A., Rapaport, J. M., Albert, D. M., and Dryja, T. P. (1986). A human DNA segment with properties of the gene that predisposes to retinoblastoma and osteosarcoma. Nature *323*, 643-646.

Galceran, J., Sustmann, C., Hsu, S. C., Folberth, S., and Grosschedl, R. (2004). LEF1-mediated regulation of Delta-like1 links Wnt and Notch signaling in somitogenesis. Genes Dev *18*, 2718-2723.

Garces, C., Ruiz-Hidalgo, M. J., de Mora, J. F., Park, C., Miele, L., Goldstein, J., Bonvini, E., Porras, A., and Laborda, J. (1997). Notch-1 controls the expression of fatty acid-activated transcription factors and is required for adipogenesis. J Biol Chem *272*, 29729-29734.

Gardie, B., Cayuela, J. M., Martini, S., and Sigaux, F. (1998). Genomic alterations of the p19ARF encoding exons in T-cell acute lymphoblastic leukemia. Blood *91*, 1016-1020.

Georgantas, R. W., 3rd, Tanadve, V., Malehorn, M., Heimfeld, S., Chen, C., Carr, L., Martinez-Murillo, F., Riggins, G., Kowalski, J., and Civin, C. I. (2004). Microarray and serial analysis of gene expression analyses identify known and novel transcripts overexpressed in hematopoietic stem cells. Cancer Res *64*, 4434-4441.

German, M. S., Blanar, M. A., Nelson, C., Moss, L. G., and Rutter, W. J. (1991). Two related helix-loop-helix proteins participate in separate cell-specific complexes that bind the insulin enhancer. Mol Endocrinol *5*, 292-299.

Girard, L., Hanna, Z., Beaulieu, N., Hoemann, C. D., Simard, C., Kozak, C. A., and Jolicoeur, P. (1996). Frequent provirus insertional mutagenesis of Notch1 in thymomas of MMTVD/myc transgenic mice suggests a collaboration of c-myc and Notch1 for oncogenesis. Genes Dev *10*, 1930-1944.

Goardon, N., Schuh, A., Hajar, I., Ma, X., Jouault, H., Dzierzak, E., Romeo, P. H., and Maouche-Chretien, L. (2002). Ectopic expression of TAL-1 protein in Ly-6E.1-htal-1 transgenic mice induces defects in B- and T-lymphoid differentiation. Blood *100*, 491-500.

Godbout, R., Dryja, T. P., Squire, J., Gallie, B. L., and Phillips, R. A. (1983). Somatic inactivation of genes on chromosome 13 is a common event in retinoblastoma. Nature *304*, 451-453.

Green, A. R., and Begley, C. G. (1992). SCL and related hemopoietic helix-loop-helix transcription factors. Int J Cell Cloning *10*, 269-276.

Green, A. R., DeLuca, E., and Begley, C. G. (1991). Antisense SCL suppresses self-renewal and enhances spontaneous erythroid differentiation of the human leukaemic cell line K562. Embo J *10*, 4153-4158.

Greenwald, I. (1998). LIN-12/Notch signaling: lessons from worms and flies. Genes Dev *12*, 1751-1762.

Greenwald, I., and Rubin, G. M. (1992). Making a difference: the role of cell-cell interactions in establishing separate identities for equivalent cells. Cell *68*, 271-281.

Greenwald, I., and Seydoux, G. (1990). Analysis of gain-of-function mutations of the lin-12 gene of Caenorhabditis elegans. Nature *346*, 197-199.

Gridley, T. (2001). Notch signaling during vascular development. Proc Natl Acad Sci U S A *98*, 5377-5378.

Guan, K. L., Jenkins, C. W., Li, Y., Nichols, M. A., Wu, X., O'Keefe, C. L., Matera, A. G., and Xiong, Y. (1994). Growth suppression by p18, a p16INK4/MTS1- and p14INK4B/MTS2-related CDK6 inhibitor, correlates with wild-type pRb function. Genes Dev *8*, 2939-2952.

Guillemot, F., Lo, L. C., Johnson, J. E., Auerbach, A., Anderson, D. J., and Joyner, A. L. (1993). Mammalian achaete-scute homolog 1 is required for the early development of olfactory and autonomic neurons. Cell *75*, 463-476.

Guo, S. X., Taki, T., Ohnishi, H., Piao, H. Y., Tabuchi, K., Bessho, F., Hanada, R., Yanagisawa, M., and Hayashi, Y. (2000). Hypermethylation of p16 and p15 genes and RB protein expression in acute leukemia. Leuk Res *24*, 39-46.

Haas, I. G., Frank, M., Veron, N., and Kemler, R. (2005). Presenilin-dependent processing and nuclear function of gamma-protocadherins. J Biol Chem *280*, 9313-9319.

Hacker, C., Kirsch, R. D., Ju, X. S., Hieronymus, T., Gust, T. C., Kuhl, C., Jorgas, T., Kurz, S. M., Rose-John, S., Yokota, Y., and Zenke, M. (2003). Transcriptional profiling identifies Id2 function in dendritic cell development. Nat Immunol *4*, 380-386.

Hadland, B. K., Manley, N. R., Su, D., Longmore, G. D., Moore, C. L., Wolfe, M. S., Schroeter, E. H., and Kopan, R. (2001). Gamma -secretase inhibitors repress thymocyte development. Proc Natl Acad Sci U S A *98*, 7487-7491.

Haidar, M. A., Cao, X. B., Manshouri, T., Chan, L. L., Glassman, A., Kantarjian, H. M., Keating, M. J., Beran, M. S., and Albitar, M. (1995). p16INK4A and p15INK4B gene deletions in primary leukemias. Blood *86*, 311-315.

Hall, M. A., Curtis, D. J., Metcalf, D., Elefanty, A. G., Sourris, K., Robb, L., Gothert, J. R., Jane, S. M., and Begley, C. G. (2003). The critical regulator of embryonic hematopoiesis, SCL, is vital in the adult for megakaryopoiesis, erythropoiesis, and lineage choice in CFU-S12. Proc Natl Acad Sci U S A *100*, 992-997.

Hamada, Y., Kadokawa, Y., Okabe, M., Ikawa, M., Coleman, J. R., and Tsujimoto, Y. (1999). Mutation in ankyrin repeats of the mouse Notch2 gene induces early embryonic lethality. Development *126*, 3415-3424.

Han, W., Ye, Q., and Moore, M. A. (2000). A soluble form of human Delta-like-1 inhibits differentiation of hematopoietic progenitor cells. Blood *95*, 1616-1625.

Hannon, G. J., and Beach, D. (1994). p15INK4B is a potential effector of TGF-beta-induced cell cycle arrest. Nature *371*, 257-261.

Hansson, A., Manetopoulos, C., Jonsson, J. I., and Axelson, H. (2003). The basic helix-loop-helix transcription factor TAL1/SCL inhibits the expression of the p16INK4A and pTalpha genes. Biochem Biophys Res Commun *312*, 1073-1081.

Hara, E., Yamaguchi, T., Nojima, H., Ide, T., Campisi, J., Okayama, H., and Oda, K. (1994). Id-related genes encoding helix-loop-helix proteins are required for G1 progression and are repressed in senescent human fibroblasts. J Biol Chem *269*, 2139-2145.

Hardy, R. R., and Hayakawa, K. (2001). B cell development pathways. Annu Rev Immunol *19*, 595-621.

Harper, J. W., Adami, G. R., Wei, N., Keyomarsi, K., and Elledge, S. J. (1993). The p21 Cdk-interacting protein Cip1 is a potent inhibitor of G1 cyclin-dependent kinases. Cell *75*, 805-816.

Harrison, C. J. (2001). Acute lymphoblastic leukaemia. Best Pract Res Clin Haematol *14*, 593-607.

Hatta, Y., Hirama, T., Miller, C. W., Yamada, Y., Tomonaga, M., and Koeffler, H. P. (1995). Homozygous deletions of the p15 (MTS2) and p16 (CDKN2/MTS1) genes in adult T-cell leukemia. Blood *85*, 2699-2704.

He, J., Allen, J. R., Collins, V. P., Allalunis-Turner, M. J., Godbout, R., Day, R. S., 3rd, and James, C. D. (1994). CDK4 amplification is an alternative mechanism to p16 gene homozygous deletion in glioma cell lines. Cancer Res *54*, 5804-5807.

He, T. C., Sparks, A. B., Rago, C., Hermeking, H., Zawel, L., da Costa, L. T., Morin, P. J., Vogelstein, B., and Kinzler, K. W. (1998). Identification of c-MYC as a target of the APC pathway. Science *281*, 1509-1512.

Hebert, J., Cayuela, J. M., Berkeley, J., and Sigaux, F. (1994). Candidate tumor-suppressor genes MTS1 (p16INK4A) and MTS2 (p15INK4B) display frequent homozygous deletions in primary cells from T- but not from B-cell lineage acute lymphoblastic leukemias. Blood *84*, 4038-4044.

Hecht, F., and Hecht, B. K. (1986). Chromosome 9 in acute lymphoblastic leukemia: breaks in band 9p21-22 and a fragile site. Cancer Genet Cytogenet *21*, 1-3.

Heemskerk, M. H., Blom, B., Nolan, G., Stegmann, A. P., Bakker, A. Q., Weijer, K., Res, P. C., and Spits, H. (1997). Inhibition of T cell and promotion of natural killer cell development by the dominant negative helix loop helix factor Id3. J Exp Med *186*, 1597-1602.

Henthorn, P., Kiledjian, M., and Kadesch, T. (1990). Two distinct transcription factors that bind the immunoglobulin enhancer microE5/kappa 2 motif. Science *247*, 467-470.

Herblot, S., Steff, A. M., Hugo, P., Aplan, P. D., and Hoang, T. (2000). SCL and LMO1 alter thymocyte differentiation: inhibition of E2A-HEB function and pre-T alpha chain expression. Nat Immunol *1*, 138-144.

Hirai, H., Roussel, M. F., Kato, J. Y., Ashmun, R. A., and Sherr, C. J. (1995). Novel INK4 proteins, p19 and p18, are specific inhibitors of the cyclin D-dependent kinases CDK4 and CDK6. Mol Cell Biol *15*, 2672-2681.

Hitzler, J. K., Soares, H. D., Drolet, D. W., Inaba, T., O'Connel, S., Rosenfeld, M. G., Morgan, J. I., and Look, A. T. (1999). Expression patterns of the hepatic leukemia factor gene in the nervous system of developing and adult mice. Brain Res *820*, 1-11.

Hoang, T., Paradis, E., Brady, G., Billia, F., Nakahara, K., Iscove, N. N., and Kirsch, I. R. (1996). Opposing effects of the basic helix-loop-helix transcription factor SCL on erythroid and monocytic differentiation. Blood *87*, 102-111.

Honda, H., Inaba, T., Suzuki, T., Oda, H., Ebihara, Y., Tsuiji, K., Nakahata, T., Ishikawa, T., Yazaki, Y., and Hirai, H. (1999). Expression of E2A-HLF chimeric protein induced T-cell apoptosis, B-cell maturation arrest, and development of acute lymphoblastic leukemia. Blood *93*, 2780-2790.

Horvitz, H. R. (1999). Genetic control of programmed cell death in the nematode Caenorhabditis elegans. Cancer Res *59*, 1701s-1706s.

Hrabe de Angelis, M., McIntyre, J., 2nd, and Gossler, A. (1997). Maintenance of somite borders in mice requires the Delta homologue DII1. Nature *386*, 717-721.

Hsieh, J. J., Zhou, S., Chen, L., Young, D. B., and Hayward, S. D. (1999). CIR, a corepressor linking the DNA binding factor CBF1 to the histone deacetylase complex. Proc Natl Acad Sci U S A *96*, 23-28.

Huang, S., and Brandt, S. J. (2000). mSin3A regulates murine erythroleukemia cell differentiation through association with the TAL1 (or SCL) transcription factor. Mol Cell Biol *20*, 2248-2259.

Huang, S., Qiu, Y., Shi, Y., Xu, Z., and Brandt, S. J. (2000). P/CAF-mediated acetylation regulates the function of the basic helix-loop-helix transcription factor TAL1/SCL. Embo J *19*, 6792-6803.

Huang, S., Qiu, Y., Stein, R. W., and Brandt, S. J. (1999). p300 functions as a transcriptional coactivator for the TAL1/SCL oncoprotein. Oncogene *18*, 4958-4967.

Huang, Y. H., Li, D., Winoto, A., and Robey, E. A. (2004). Distinct transcriptional programs in thymocytes responding to T cell receptor, Notch, and positive selection signals. Proc Natl Acad Sci U S A *101*, 4936-4941.

Huang, Z., Nie, L., Xu, M., and Sun, X. H. (2004). Notch-induced E2A degradation requires CHIP and Hsc70 as novel facilitators of ubiquitination. Mol Cell Biol *24*, 8951-8962.

Hunger, S. P. (1996). Chromosomal translocations involving the E2A gene in acute lymphoblastic leukemia: clinical features and molecular pathogenesis. Blood *87*, 1211-1224.

Hunger, S. P., Devaraj, P. E., Foroni, L., Secker-Walker, L. M., and Cleary, M. L. (1994). Two types of genomic rearrangements create alternative E2A-HLF fusion proteins in t(17;19)-ALL. Blood *83*, 2970-2977.

Hunger, S. P., Ohyashiki, K., Toyama, K., and Cleary, M. L. (1992). Hlf, a novel hepatic bZIP protein, shows altered DNA-binding properties following fusion to E2A in t(17;19) acute lymphoblastic leukemia. Genes Dev *6*, 1608-1620.

Huppert, S. S., Le, A., Schroeter, E. H., Mumm, J. S., Saxena, M. T., Milner, L. A., and Kopan, R. (2000). Embryonic lethality in mice homozygous for a processing-deficient allele of Notch1. Nature *405*, 966-970.

Iavarone, A., Garg, P., Lasorella, A., Hsu, J., and Israel, M. A. (1994). The helix-loop-helix protein Id-2 enhances cell proliferation and binds to the retinoblastoma protein. Genes Dev *8*, 1270-1284.

Ikawa, T., Kawamoto, H., Wright, L. Y., and Murre, C. (2004). Long-term cultured E2A-deficient hematopoietic progenitor cells are pluripotent. Immunity *20*, 349-360.

Inaba, T., Inukai, T., Yoshihara, T., Seyschab, H., Ashmun, R. A., Canman, C. E., Laken, S. J., Kastan, M. B., and Look, A. T. (1996). Reversal of apoptosis by the leukaemia-associated E2A-HLF chimaeric transcription factor. Nature *382*, 541-544.

Inaba, T., Roberts, W. M., Shapiro, L. H., Jolly, K. W., Raimondi, S. C., Smith, S. D., and Look, A. T. (1992). Fusion of the leucine zipper gene HLF to the E2A gene in human acute B-lineage leukemia. Science *257*, 531-534.

Inukai, T., Inaba, T., Ikushima, S., and Look, A. T. (1998). The AD1 and AD2 transactivation domains of E2A are essential for the antiapoptotic activity of the chimeric oncoprotein E2A-HLF. Mol Cell Biol *18*, 6035-6043.

Inukai, T., Inoue, A., Kurosawa, H., Goi, K., Shinjyo, T., Ozawa, K., Mao, M., Inaba, T., and Look, A. T. (1999). SLUG, a ces-1-related zinc finger transcription factor gene with antiapoptotic activity, is a downstream target of the E2A-HLF oncoprotein. Mol Cell *4*, 343-352.

Ivanova, N. B., Dimos, J. T., Schaniel, C., Hackney, J. A., Moore, K. A., and Lemischka, I. R. (2002). A stem cell molecular signature. Science *298*, 601-604.

Izon, D. J., Aster, J. C., He, Y., Weng, A., Karnell, F. G., Patriub, V., Xu, L., Bakkour, S., Rodriguez, C., Allman, D., and Pear, W. S. (2002). Deltex1 redirects lymphoid progenitors to the B cell lineage by antagonizing Notch1. Immunity *16*, 231-243.

Jen, Y., Weintraub, H., and Benezra, R. (1992). Overexpression of Id protein inhibits the muscle differentiation program: in vivo association of Id with E2A proteins. Genes Dev *6*, 1466-1479.

Joutel, A., Corpechot, C., Ducros, A., Vahedi, K., Chabriat, H., Mouton, P., Alamowitch, S., Domenga, V., Cecillion, M., Marechal, E., *et al.* (1996). Notch3 mutations in CADASIL, a hereditary adult-onset condition causing stroke and dementia. Nature *383*, 707-710.

Juliusson, G., Oscier, D. G., Fitchett, M., Ross, F. M., Stockdill, G., Mackie, M. J., Parker, A. C., Castoldi, G. L., Guneo, A., Knuutila, S., and et al. (1990). Prognostic subgroups in B-cell chronic lymphocytic leukemia defined by specific chromosomal abnormalities. N Engl J Med *323*, 720-724.

Jundt, F., Anagnostopoulos, I., Forster, R., Mathas, S., Stein, H., and Dorken, B. (2002). Activated Notch1 signaling promotes tumor cell proliferation and survival in Hodgkin and anaplastic large cell lymphoma. Blood *99*, 3398-3403.

Kallianpur, A. R., Jordan, J. E., and Brandt, S. J. (1994). The SCL/TAL-1 gene is expressed in progenitors of both the hematopoietic and vascular systems during embryogenesis. Blood *83*, 1200-1208.

Kamb, A., Gruis, N. A., Weaver-Feldhaus, J., Liu, Q., Harshman, K., Tavtigian, S. V., Stockert, E., Day, R. S., 3rd, Johnson, B. E., and Skolnick, M. H. (1994). A cell cycle regulator potentially involved in genesis of many tumor types. Science *264*, 436-440.

Kamijo, T., Bodner, S., van de Kamp, E., Randle, D. H., and Sherr, C. J. (1999). Tumor spectrum in ARF-deficient mice. Cancer Res *59*, 2217-2222.

Kamijo, T., Zindy, F., Roussel, M. F., Quelle, D. E., Downing, J. R., Ashmun, R. A., Grosveld, G., and Sherr, C. J. (1997). Tumor suppression at the mouse INK4a locus mediated by the alternative reading frame product p19ARF. Cell *91*, 649-659.

Kamps, M. P., and Baltimore, D. (1993). E2A-Pbx1, the t(1;19) translocation protein of human pre-B-cell acute lymphocytic leukemia, causes acute myeloid leukemia in mice. Mol Cell Biol *13*, 351-357.

Kamps, M. P., Look, A. T., and Baltimore, D. (1991). The human t(1;19) translocation in pre-B ALL produces multiple nuclear E2A-Pbx1 fusion proteins with differing transforming potentials. Genes Dev *5*, 358-368.

Kamps, M. P., and Wright, D. D. (1994). Oncoprotein E2A-Pbx1 immortalizes a myeloid progenitor in primary marrow cultures without abrogating its factor-dependence. Oncogene *9*, 3159-3166.

Kamps, M. P., Wright, D. D., and Lu, Q. (1996). DNA-binding by oncoprotein E2a-Pbx1 is important for blocking differentiation but dispensable for fibroblast transformation. Oncogene *12*, 19-30.

Kao, H. Y., Ordentlich, P., Koyano-Nakagawa, N., Tang, Z., Downes, M., Kintner, C. R., Evans, R. M., and Kadesch, T. (1998). A histone deacetylase corepressor complex regulates the Notch signal transduction pathway. Genes Dev *12*, 2269-2277.

Kee, B. L., Bain, G., and Murre, C. (2002). IL-7Ralpha and E47: independent pathways required for development of multipotent lymphoid progenitors. Embo J *21*, 103-113.

Kee, B. L., and Murre, C. (1998). Induction of early B cell factor (EBF) and multiple B lineage genes by the basic helix-loop-helix transcription factor E12. J Exp Med *188*, 699-713.

Kee, B. L., Rivera, R. R., and Murre, C. (2001). Id3 inhibits B lymphocyte progenitor growth and survival in response to TGF-beta. Nat Immunol *2*, 242-247.

Kees, U. R., Burton, P. R., Lu, C., and Baker, D. L. (1997). Homozygous deletion of the p16/MTS1 gene in pediatric acute lymphoblastic leukemia is associated with unfavorable clinical outcome. Blood *89*, 4161-4166.

Kelliher, M. A., Seldin, D. C., and Leder, P. (1996). Tal-1 induces T cell acute lymphoblastic leukemia accelerated by casein kinase IIalpha. Embo J *15*, 5160-5166.

Khatib, Z. A., Matsushime, H., Valentine, M., Shapiro, D. N., Sherr, C. J., and Look, A. T. (1993). Coamplification of the CDK4 gene with MDM2 and GLI in human sarcomas. Cancer Res *53*, 5535-5541.

Kim, D., Peng, X. C., and Sun, X. H. (1999). Massive apoptosis of thymocytes in T-cell-deficient Id1 transgenic mice. Mol Cell Biol *19*, 8240-8253.

Koch, U., Lacombe, T. A., Holland, D., Bowman, J. L., Cohen, B. L., Egan, S. E., and Guidos, C. J. (2001). Subversion of the T/B lineage decision in the thymus by lunatic fringe-mediated inhibition of Notch-1. Immunity *15*, 225-236.

Koh, J., Enders, G. H., Dynlacht, B. D., and Harlow, E. (1995). Tumour-derived p16 alleles encoding proteins defective in cell-cycle inhibition. Nature *375*, 506-510.

Komarova, N. L., and Wodarz, D. (2005). Drug resistance in cancer: principles of emergence and prevention. Proc Natl Acad Sci U S A *102*, 9714-9719.

Kopan, R., Nye, J. S., and Weintraub, H. (1994). The intracellular domain of mouse Notch: a constitutively activated repressor of myogenesis directed at the basic helix-loop-helix region of MyoD. Development *120*, 2385-2396.

Kovar, H., Jug, G., Aryee, D. N., Zoubek, A., Ambros, P., Gruber, B., Windhager, R., and Gadner, H. (1997). Among genes involved in the RB dependent cell cycle regulatory cascade, the p16 tumor suppressor gene is frequently lost in the Ewing family of tumors. Oncogene *15*, 2225-2232.

Krebs, L. T., Deftos, M. L., Bevan, M. J., and Gridley, T. (2001). The Nrarp gene encodes an ankyrin-repeat protein that is transcriptionally regulated by the notch signaling pathway. Dev Biol *238*, 110-119.

Krebs, L. T., Xue, Y., Norton, C. R., Shutter, J. R., Maguire, M., Sundberg, J. P., Gallahan, D., Closson, V., Kitajewski, J., Callahan, R., *et al.* (2000). Notch signaling is essential for vascular morphogenesis in mice. Genes Dev *14*, 1343-1352.

Kreider, B. L., Benezra, R., Rovera, G., and Kadesch, T. (1992). Inhibition of myeloid differentiation by the helix-loop-helix protein Id. Science *255*, 1700-1702.

Kumano, K., Chiba, S., Kunisato, A., Sata, M., Saito, T., Nakagami-Yamaguchi, E., Yamaguchi, T., Masuda, S., Shimizu, K., Takahashi, T., *et al.* (2003). Notch1 but not Notch2 is essential for generating hematopoietic stem cells from endothelial cells. Immunity *18*, 699-711.

Kumano, K., Chiba, S., Shimizu, K., Yamagata, T., Hosoya, N., Saito, T., Takahashi, T., Hamada, Y., and Hirai, H. (2001). Notch1 inhibits differentiation of hematopoietic cells by sustaining GATA-2 expression. Blood *98*, 3283-3289.

Kunisch, M., Haenlin, M., and Campos-Ortega, J. A. (1994). Lateral inhibition mediated by the Drosophila neurogenic gene delta is enhanced by proneural proteins. Proc Natl Acad Sci U S A *91*, 10139-10143.

Kurooka, H., and Honjo, T. (2000). Functional interaction between the mouse notch1 intracellular region and histone acetyltransferases PCAF and GCN5. J Biol Chem *275*, 17211-17220.

Kurooka, H., Kuroda, K., and Honjo, T. (1998). Roles of the ankyrin repeats and C-terminal region of the mouse notch1 intracellular region. Nucleic Acids Res *26*, 5448-5455.

Lai, E. C., Tam, B., and Rubin, G. M. (2005). Pervasive regulation of Drosophila Notch target genes by GY-box-, Brd-box-, and K-box-class microRNAs. Genes Dev *19*, 1067-1080.

Lammich, S., Okochi, M., Takeda, M., Kaether, C., Capell, A., Zimmer, A. K., Edbauer, D., Walter, J., Steiner, H., and Haass, C. (2002). Presenilin-dependent intramembrane proteolysis of CD44 leads to the liberation of its intracellular domain and the secretion of an Abeta-like peptide. J Biol Chem *277*, 44754-44759.

Lasorella, A., Iavarone, A., and Israel, M. A. (1996). Id2 specifically alters regulation of the cell cycle by tumor suppressor proteins. Mol Cell Biol *16*, 2570-2578.

LeBrun, D. P., and Cleary, M. L. (1994). Fusion with E2A alters the transcriptional properties of the homeodomain protein PBX1 in t(1;19) leukemias. Oncogene *9*, 1641-1647.

Lee, J. E., Hollenberg, S. M., Snider, L., Turner, D. L., Lipnick, N., and Weintraub, H. (1995). Conversion of Xenopus ectoderm into neurons by NeuroD, a basic helix-loop-helix protein. Science *268*, 836-844.

Lee, M. H., Reynisdottir, I., and Massague, J. (1995). Cloning of p57KIP2, a cyclin-dependent kinase inhibitor with unique domain structure and tissue distribution. Genes Dev *9*, 639-649.

Lemercier, C., To, R. Q., Swanson, B. J., Lyons, G. E., and Konieczny, S. F. (1997). Mist1: a novel basic helix-loop-helix transcription factor exhibits a developmentally regulated expression pattern. Dev Biol *182*, 101-113.

Lewis, B. P., Shih, I. H., Jones-Rhoades, M. W., Bartel, D. P., and Burge, C. B. (2003). Prediction of mammalian microRNA targets. Cell *115*, 787-798.

Liao, E. C., Paw, B. H., Oates, A. C., Pratt, S. J., Postlethwait, J. H., and Zon, L. I. (1998). SCL/Tal-1 transcription factor acts downstream of cloche to specify hematopoietic and vascular progenitors in zebrafish. Genes Dev *12*, 621-626.

Lin, Y. W., Deveney, R., Barbara, M., Iscove, N. N., Nimer, S. D., Slape, C., and Aplan, P. D. (2005). OLIG2 (BHLHB1), a bHLH transcription factor, contributes to leukemogenesis in concert with LMO1. Cancer Res *65*, 7151-7158.

Lindsell, C. E., Shawber, C. J., Boulter, J., and Weinmaster, G. (1995). Jagged: a mammalian ligand that activates Notch1. Cell *80*, 909-917.

Logeat, F., Bessia, C., Brou, C., LeBail, O., Jarriault, S., Seidah, N. G., and Israel, A. (1998). The Notch1 receptor is cleaved constitutively by a furin-like convertase. Proc Natl Acad Sci U S A *95*, 8108-8112.

Look, A. T. (1997). Oncogenic transcription factors in the human acute leukemias. Science *278*, 1059-1064.

Lu, Q., and Kamps, M. P. (1997). Heterodimerization of Hox proteins with Pbx1 and oncoprotein E2a-Pbx1 generates unique DNA-binding specifities at nucleotides predicted to contact the N-terminal arm of the Hox homeodomain--demonstration of Hox-dependent targeting of E2a-Pbx1 in vivo. Oncogene *14*, 75-83.

Lu, Q., Wright, D. D., and Kamps, M. P. (1994). Fusion with E2A converts the Pbx1 homeodomain protein into a constitutive transcriptional activator in human leukemias carrying the t(1;19) translocation. Mol Cell Biol *14*, 3938-3948.

Lukas, J., Parry, D., Aagaard, L., Mann, D. J., Bartkova, J., Strauss, M., Peters, G., and Bartek, J. (1995). Retinoblastoma-protein-dependent cell-cycle inhibition by the tumour suppressor p16. Nature *375*, 503-506.

Luo, Y., Hurwitz, J., and Massague, J. (1995). Cell-cycle inhibition by independent CDK and PCNA binding domains in p21Cip1. Nature *375*, 159-161.

Ma, Q., Kintner, C., and Anderson, D. J. (1996). Identification of neurogenin, a vertebrate neuronal determination gene. Cell *87*, 43-52.

Ma, S. K., Wan, T. S., and Chan, L. C. (1999). Cytogenetics and molecular genetics of childhood leukemia. Hematol Oncol *17*, 91-105.

Ma, T., Van Tine, B. A., Wei, Y., Garrett, M. D., Nelson, D., Adams, P. D., Wang, J., Qin, J., Chow, L. T., and Harper, J. W. (2000). Cell cycle-regulated phosphorylation of p220(NPAT) by cyclin E/Cdk2 in Cajal bodies promotes histone gene transcription. Genes Dev *14*, 2298-2313.

Markus, M., and Benezra, R. (1999). Two isoforms of protein disulfide isomerase alter the dimerization status of E2A proteins by a redox mechanism. J Biol Chem *274*, 1040-1049.

Massari, M. E., and Murre, C. (2000). Helix-loop-helix proteins: regulators of transcription in eucaryotic organisms. Mol Cell Biol *20*, 429-440.

Matsuno, K., Diederich, R. J., Go, M. J., Blaumueller, C. M., and Artavanis-Tsakonas, S. (1995). Deltex acts as a positive regulator of Notch signaling through interactions with the Notch ankyrin repeats. Development *121*, 2633-2644.

McGill, M. A., and McGlade, C. J. (2003). Mammalian numb proteins promote Notch1 receptor ubiquitination and degradation of the Notch1 intracellular domain. J Biol Chem *278*, 23196-23203.

McHale, C. M., Wiemels, J. L., Zhang, L., Ma, X., Buffler, P. A., Feusner, J., Matthay, K., Dahl, G., and Smith, M. T. (2003). Prenatal origin of childhood acute myeloid leukemias harboring chromosomal rearrangements t(15;17) and inv(16). Blood *101*, 4640-4641.

Medema, R. H., Herrera, R. E., Lam, F., and Weinberg, R. A. (1995). Growth suppression by p16ink4 requires functional retinoblastoma protein. Proc Natl Acad Sci U S A *92*, 6289-6293.

Mellentin, J. D., Murre, C., Donlon, T. A., McCaw, P. S., Smith, S. D., Carroll, A. J., McDonald, M. E., Baltimore, D., and Cleary, M. L. (1989). The gene for enhancer binding proteins E12/E47 lies at the t(1;19) breakpoint in acute leukemias. Science *246*, 379-382.

Mellentin, J. D., Smith, S. D., and Cleary, M. L. (1989). lyl-1, a novel gene altered by chromosomal translocation in T cell leukemia, codes for a protein with a helix-loop-helix DNA binding motif. Cell *58*, 77-83.

Melnikova, I. N., and Christy, B. A. (1996). Muscle cell differentiation is inhibited by the helix-loop-helix protein Id3. Cell Growth Differ *7*, 1067-1079.

Melo, J. V., Gordon, D. E., Cross, N. C., and Goldman, J. M. (1993). The ABL-BCR fusion gene is expressed in chronic myeloid leukemia. Blood *81*, 158-165.

Metzstein, M. M., Hengartner, M. O., Tsung, N., Ellis, R. E., and Horvitz, H. R. (1996). Transcriptional regulator of programmed cell death encoded by Caenorhabditis elegans gene ces-2. Nature *382*, 545-547.

Mikkola, H. K., Klintman, J., Yang, H., Hock, H., Schlaeger, T. M., Fujiwara, Y., and Orkin, S. H. (2003). Haematopoietic stem cells retain long-term repopulating activity and multipotency in the absence of stem-cell leukaemia SCL/tal-1 gene. Nature *421*, 547-551.

Milner, L. A., Bigas, A., Kopan, R., Brashem-Stein, C., Bernstein, I. D., and Martin, D. I. (1996). Inhibition of granulocytic differentiation by mNotch1. Proc Natl Acad Sci U S A *93*, 13014-13019.

Milner, L. A., Kopan, R., Martin, D. I., and Bernstein, I. D. (1994). A human homologue of the Drosophila developmental gene, Notch, is expressed in CD34+ hematopoietic precursors. Blood *83*, 2057-2062.

Mitsumori, K., Shimo, T., Onodera, H., Takagi, H., Yasuhara, K., Tamura, T., Aoki, Y., Nagata, O., and Hirose, M. (2000). Modifying effects of ethinylestradiol but not methoxychlor on N-ethyl-N-nitrosourea-induced uterine carcinogenesis in heterozygous p53-deficient CBA mice. Toxicol Sci *58*, 43-49.

Moloney, D. J., Panin, V. M., Johnston, S. H., Chen, J., Shao, L., Wilson, R., Wang, Y., Stanley, P., Irvine, K. D., Haltiwanger, R. S., and Vogt, T. F. (2000). Fringe is a glycosyltransferase that modifies Notch. Nature *406*, 369-375.

Monica, K., LeBrun, D. P., Dedera, D. A., Brown, R., and Cleary, M. L. (1994). Transformation properties of the E2a-Pbx1 chimeric oncoprotein: fusion with E2a is essential, but the Pbx1 homeodomain is dispensable. Mol Cell Biol *14*, 8304-8314.

Morgan, T. H. (1917). The theory of a gene. Am Nat *51*, 513-544.

Mori, H., Colman, S. M., Xiao, Z., Ford, A. M., Healy, L. E., Donaldson, C., Hows, J. M., Navarrete, C., and Greaves, M. (2002). Chromosome translocations and covert leukemic clones are generated during normal fetal development. Proc Natl Acad Sci U S A *99*, 8242-8247.

Morrow, M. A., Mayer, E. W., Perez, C. A., Adlam, M., and Siu, G. (1999). Overexpression of the Helix-Loop-Helix protein Id2 blocks T cell development at multiple stages. Mol Immunol *36*, 491-503.

Motokura, T., Bloom, T., Kim, H. G., Juppner, H., Ruderman, J. V., Kronenberg, H. M., and Arnold, A. (1991). A novel cyclin encoded by a bcl1-linked candidate oncogene. Nature *350*, 512-515.

Mouthon, M. A., Bernard, O., Mitjavila, M. T., Romeo, P. H., Vainchenker, W., and Mathieu-Mahul, D. (1993). Expression of tal-1 and GATA-binding proteins during human hematopoiesis. Blood *81*, 647-655.

Murphy, S. B., Raimondi, S. C., Rivera, G. K., Crone, M., Dodge, R. K., Behm, F. G., Pui, C. H., and Williams, D. L. (1989). Nonrandom abnormalities of chromosome 9p in childhood acute lymphoblastic leukemia: association with high-risk clinical features. Blood *74*, 409-415.

Murre, C., McCaw, P. S., and Baltimore, D. (1989). A new DNA binding and dimerization motif in immunoglobulin enhancer binding, daughterless, MyoD, and myc proteins. Cell *56*, 777-783.

Murre, C., Voronova, A., and Baltimore, D. (1991). B-cell- and myocyte-specific E2-box-binding factors contain E12/E47-like subunits. Mol Cell Biol *11*, 1156-1160.

Naya, F. J., Huang, H. P., Qiu, Y., Mutoh, H., DeMayo, F. J., Leiter, A. B., and Tsai, M. J. (1997). Diabetes, defective pancreatic morphogenesis, and abnormal enteroendocrine differentiation in BETA2/neuroD-deficient mice. Genes Dev *11*, 2323-2334.

Nelson, C., Shen, L. P., Meister, A., Fodor, E., and Rutter, W. J. (1990). Pan: a transcriptional regulator that binds chymotrypsin, insulin, and AP-4 enhancer motifs. Genes Dev *4*, 1035-1043.

Netzer, W. J., Dou, F., Cai, D., Veach, D., Jean, S., Li, Y., Bornmann, W. G., Clarkson, B., Xu, H., and Greengard, P. (2003). Gleevec inhibits beta-amyloid production but not Notch cleavage. Proc Natl Acad Sci U S A *100*, 12444-12449.

Ni, C. Y., Murphy, M. P., Golde, T. E., and Carpenter, G. (2001). gamma -Secretase cleavage and nuclear localization of ErbB-4 receptor tyrosine kinase. Science *294*, 2179-2181.

Nickoloff, B. J., Qin, J. Z., Chaturvedi, V., Denning, M. F., Bonish, B., and Miele, L. (2002). Jagged-1 mediated activation of notch signaling induces complete maturation of human keratinocytes through NF-kappaB and PPARgamma. Cell Death Differ *9*, 842-855.

Nie, L., Xu, M., Vladimirova, A., and Sun, X. H. (2003). Notch-induced E2A ubiquitination and degradation are controlled by MAP kinase activities. Embo J *22*, 5780-5792.

O'Neil, J., Billa, M., Oikemus, S., and Kelliher, M. (2001). The DNA binding activity of TAL-1 is not required to induce leukemia/lymphoma in mice. Oncogene *20*, 3897-3905.

O'Neil, J., Shank, J., Cusson, N., Murre, C., and Kelliher, M. (2004). TAL1/SCL induces leukemia by inhibiting the transcriptional activity of E47/HEB. Cancer Cell *5*, 587-596.

O'Riordan, M., and Grosschedl, R. (1999). Coordinate regulation of B cell differentiation by the transcription factors EBF and E2A. Immunity *11*, 21-31.

Ohnishi, H., Kawamura, M., Ida, K., Sheng, X. M., Hanada, R., Nobori, T., Yamamori, S., and Hayashi, Y. (1995). Homozygous deletions of p16/MTS1 gene are frequent but mutations are infrequent in childhood T-cell acute lymphoblastic leukemia. Blood *86*, 1269-1275.

Ohyashiki, K., Fujieda, H., Miyauchi, J., Ohyashiki, J. H., Tauchi, T., Saito, M., Nakazawa, S., Abe, K., Yamamoto, K., Clark, S. C., and et al. (1991). Establishment of a novel heterotransplantable acute lymphoblastic leukemia cell line with a t(17;19) chromosomal translocation the growth of which is inhibited by interleukin-3. Leukemia *5*, 322-331.

Oka, C., Nakano, T., Wakeham, A., de la Pompa, J. L., Mori, C., Sakai, T., Okazaki, S., Kawaichi, M., Shiota, K., Mak, T. W., and Honjo, T. (1995). Disruption of the mouse RBP-J kappa gene results in early embryonic death. Development *121*, 3291-3301.

Okuda, M., Horn, H. F., Tarapore, P., Tokuyama, Y., Smulian, A. G., Chan, P. K., Knudsen, E. S., Hofmann, I. A., Snyder, J. D., Bove, K. E., and Fukasawa, K. (2000).

Nucleophosmin/B23 is a target of CDK2/cyclin E in centrosome duplication. Cell *103*, 127-140.

Okuda, T., Shurtleff, S. A., Valentine, M. B., Raimondi, S. C., Head, D. R., Behm, F., Curcio-Brint, A. M., Liu, Q., Pui, C. H., Sherr, C. J., and et al. (1995). Frequent deletion of p16INK4a/MTS1 and p15INK4b/MTS2 in pediatric acute lymphoblastic leukemia. Blood *85*, 2321-2330.

Olson, E. N. (1990). MyoD family: a paradigm for development? Genes Dev *4*, 1454-1461.

Ordentlich, P., Lin, A., Shen, C. P., Blaumueller, C., Matsuno, K., Artavanis-Tsakonas, S., and Kadesch, T. (1998). Notch inhibition of E47 supports the existence of a novel signaling pathway. Mol Cell Biol *18*, 2230-2239.

Oswald, F., Tauber, B., Dobner, T., Bourteele, S., Kostezka, U., Adler, G., Liptay, S., and Schmid, R. M. (2001). p300 acts as a transcriptional coactivator for mammalian Notch-1. Mol Cell Biol *21*, 7761-7774.

Pagliuca, A., Gallo, P., De Luca, P., and Lania, L. (2000). Class A helix-loop-helix proteins are positive regulators of several cyclin-dependent kinase inhibitors' promoter activity and negatively affect cell growth. Cancer Res *60*, 1376-1382.

Palmero, I., Pantoja, C., and Serrano, M. (1998). p19ARF links the tumour suppressor p53 to Ras. Nature *395*, 125-126.

Park, S. T., Nolan, G. P., and Sun, X. H. (1999). Growth inhibition and apoptosis due to restoration of E2A activity in T cell acute lymphoblastic leukemia cells. J Exp Med *189*, 501-508.

Pear, W. S., Aster, J. C., Scott, M. L., Hasserjian, R. P., Soffer, B., Sklar, J., and Baltimore, D. (1996). Exclusive development of T cell neoplasms in mice transplanted with bone marrow expressing activated Notch alleles. J Exp Med *183*, 2283-2291.

Peverali, F. A., Ramqvist, T., Saffrich, R., Pepperkok, R., Barone, M. V., and Philipson, L. (1994). Regulation of G1 progression by E2A and Id helix-loop-helix proteins. Embo J *13*, 4291-4301.

Pinto, D., Gregorieff, A., Begthel, H., and Clevers, H. (2003). Canonical Wnt signals are essential for homeostasis of the intestinal epithelium. Genes Dev *17*, 1709-1713.

Polesskaya, A., Seale, P., and Rudnicki, M. A. (2003). Wnt signaling induces the myogenic specification of resident CD45+ adult stem cells during muscle regeneration. Cell *113*, 841-852.

Pollak, C., and Hagemeijer, A. (1987). Abnormalities of the short arm of chromosome 9 with partial loss of material in hematological disorders. Leukemia *1*, 541-548.

Polyak, K., Kato, J. Y., Solomon, M. J., Sherr, C. J., Massague, J., Roberts, J. M., and Koff, A. (1994). p27Kip1, a cyclin-Cdk inhibitor, links transforming growth factor-beta and contact inhibition to cell cycle arrest. Genes Dev *8*, 9-22.

Pomerantz, J., Schreiber-Agus, N., Liegeois, N. J., Silverman, A., Alland, L., Chin, L., Potes, J., Chen, K., Orlow, I., Lee, H. W., *et al.* (1998). The Ink4a tumor suppressor gene product, p19Arf, interacts with MDM2 and neutralizes MDM2's inhibition of p53. Cell *92*, 713-723.

Porcher, C., Swat, W., Rockwell, K., Fujiwara, Y., Alt, F. W., and Orkin, S. H. (1996). The T cell leukemia oncoprotein SCL/tal-1 is essential for development of all hematopoietic lineages. Cell *86*, 47-57.

Prabhu, S., Ignatova, A., Park, S. T., and Sun, X. H. (1997). Regulation of the expression of cyclin-dependent kinase inhibitor p21 by E2A and Id proteins. Mol Cell Biol *17*, 5888-5896.

Pui, J. C., Allman, D., Xu, L., DeRocco, S., Karnell, F. G., Bakkour, S., Lee, J. Y., Kadesch, T., Hardy, R. R., Aster, J. C., and Pear, W. S. (1999). Notch1 expression in early lymphopoiesis influences B versus T lineage determination. Immunity *11*, 299-308.

Qin, J. Z., Stennett, L., Bacon, P., Bodner, B., Hendrix, M. J., Seftor, R. E., Seftor, E. A., Margaryan, N. V., Pollock, P. M., Curtis, A., *et al.* (2004). p53-independent NOXA induction overcomes apoptotic resistance of malignant melanomas. Mol Cancer Ther *3*, 895-902.

Qiu, L., Joazeiro, C., Fang, N., Wang, H. Y., Elly, C., Altman, Y., Fang, D., Hunter, T., and Liu, Y. C. (2000). Recognition and ubiquitination of Notch by Itch, a hect-type E3 ubiquitin ligase. J Biol Chem *275*, 35734-35737.

Quelle, D. E., Cheng, M., Ashmun, R. A., and Sherr, C. J. (1997). Cancer-associated mutations at the INK4a locus cancel cell cycle arrest by p16INK4a but not by the alternative reading frame protein p19ARF. Proc Natl Acad Sci U S A *94*, 669-673.

Quelle, D. E., Zindy, F., Ashmun, R. A., and Sherr, C. J. (1995). Alternative reading frames of the INK4a tumor suppressor gene encode two unrelated proteins capable of inducing cell cycle arrest. Cell *83*, 993-1000.

Quong, M. W., Harris, D. P., Swain, S. L., and Murre, C. (1999). E2A activity is induced during B-cell activation to promote immunoglobulin class switch recombination. Embo J *18*, 6307-6318.

Quong, M. W., Massari, M. E., Zwart, R., and Murre, C. (1993). A new transcriptional-activation motif restricted to a class of helix-loop-helix proteins is functionally conserved in both yeast and mammalian cells. Mol Cell Biol *13*, 792-800.

Radtke, F., Wilson, A., Mancini, S. J., and MacDonald, H. R. (2004). Notch regulation of lymphocyte development and function. Nat Immunol *5*, 247-253.

Radtke, F., Wilson, A., Stark, G., Bauer, M., van Meerwijk, J., MacDonald, H. R., and Aguet, M. (1999). Deficient T cell fate specification in mice with an induced inactivation of Notch1. Immunity *10*, 547-558.

Raimondi, S. C., Privitera, E., Williams, D. L., Look, A. T., Behm, F., Rivera, G. K., Crist, W. M., and Pui, C. H. (1991). New recurring chromosomal translocations in childhood acute lymphoblastic leukemia. Blood *77*, 2016-2022.

Rand, M. D., Grimm, L. M., Artavanis-Tsakonas, S., Patriub, V., Blacklow, S. C., Sklar, J., and Aster, J. C. (2000). Calcium depletion dissociates and activates heterodimeric notch receptors. Mol Cell Biol *20*, 1825-1835.

Rangarajan, A., Talora, C., Okuyama, R., Nicolas, M., Mammucari, C., Oh, H., Aster, J. C., Krishna, S., Metzger, D., Chambon, P., *et al.* (2001). Notch signaling is a direct determinant of keratinocyte growth arrest and entry into differentiation. Embo J *20*, 3427-3436.

Rao, L., Debbas, M., Sabbatini, P., Hockenbery, D., Korsmeyer, S., and White, E. (1992). The adenovirus E1A proteins induce apoptosis, which is inhibited by the E1B 19-kDa and Bcl-2 proteins. Proc Natl Acad Sci U S A *89*, 7742-7746.

Rebay, I., Fleming, R. J., Fehon, R. G., Cherbas, L., Cherbas, P., and Artavanis-Tsakonas, S. (1991). Specific EGF repeats of Notch mediate interactions with Delta and Serrate: implications for Notch as a multifunctional receptor. Cell *67*, 687-699.

Rechsteiner, M. (1988). Regulation of enzyme levels by proteolysis: the role of pest regions. Adv Enzyme Regul *27*, 135-151.

Reifenberger, G., Reifenberger, J., Ichimura, K., Meltzer, P. S., and Collins, V. P. (1994). Amplification of multiple genes from chromosomal region 12q13-14 in human malignant gliomas: preliminary mapping of the amplicons shows preferential involvement of CDK4, SAS, and MDM2. Cancer Res *54*, 4299-4303.

Reya, T., Duncan, A. W., Ailles, L., Domen, J., Scherer, D. C., Willert, K., Hintz, L., Nusse, R., and Weissman, I. L. (2003). A role for Wnt signalling in self-renewal of haematopoietic stem cells. Nature *423*, 409-414.

Rida, P. C., Le Minh, N., and Jiang, Y. J. (2004). A Notch feeling of somite segmentation and beyond. Dev Biol *265*, 2-22.

Riechmann, V., van Cruchten, I., and Sablitzky, F. (1994). The expression pattern of Id4, a novel dominant negative helix-loop-helix protein, is distinct from Id1, Id2 and Id3. Nucleic Acids Res *22*, 749-755.

Robb, L., Lyons, I., Li, R., Hartley, L., Kontgen, F., Harvey, R. P., Metcalf, D., and Begley, C. G. (1995). Absence of yolk sac hematopoiesis from mice with a targeted disruption of the scl gene. Proc Natl Acad Sci U S A *92*, 7075-7079.

Robb, L., Rasko, J. E., Bath, M. L., Strasser, A., and Begley, C. G. (1995). scl, a gene frequently activated in human T cell leukaemia, does not induce lymphomas in transgenic mice. Oncogene *10*, 205-209.

Robbins, J., Blondel, B. J., Gallahan, D., and Callahan, R. (1992). Mouse mammary tumor gene int-3: a member of the notch gene family transforms mammary epithelial cells. J Virol *66*, 2594-2599.

Robey, E., Chang, D., Itano, A., Cado, D., Alexander, H., Lans, D., Weinmaster, G., and Salmon, P. (1996). An activated form of Notch influences the choice between CD4 and CD8 T cell lineages. Cell *87*, 483-492.

Ronchini, C., and Capobianco, A. J. (2001). Induction of cyclin D1 transcription and CDK2 activity by Notch(ic): implication for cell cycle disruption in transformation by Notch(ic). Mol Cell Biol *21*, 5925-5934.

Sarmento, L. M., Huang, H., Limon, A., Gordon, W., Fernandes, J., Tavares, M. J., Miele, L., Cardoso, A. A., Classon, M., and Carlesso, N. (2005). Notch1 modulates timing of G1-S progression by inducing SKP2 transcription and p27Kip1 degradation. J Exp Med *202*, 157-168.

Satoh, Y., Matsumura, I., Tanaka, H., Ezoe, S., Sugahara, H., Mizuki, M., Shibayama, H., Ishiko, E., Ishiko, J., Nakajima, K., and Kanakura, Y. (2004). Roles for c-Myc in self-renewal of hematopoietic stem cells. J Biol Chem *279*, 24986-24993.

Sawada, S., and Littman, D. R. (1993). A heterodimer of HEB and an E12-related protein interacts with the CD4 enhancer and regulates its activity in T-cell lines. Mol Cell Biol *13*, 5620-5628.

Schlissel, M., Voronova, A., and Baltimore, D. (1991). Helix-loop-helix transcription factor E47 activates germ-line immunoglobulin heavy-chain gene transcription and rearrangement in a pre-T-cell line. Genes Dev *5*, 1367-1376.

Schmidt, E. E., Ichimura, K., Reifenberger, G., and Collins, V. P. (1994). CDKN2 (p16/MTS1) gene deletion or CDK4 amplification occurs in the majority of glioblastomas. Cancer Res *54*, 6321-6324.

Schulze, A., Zerfass, K., Spitkovsky, D., Middendorp, S., Berges, J., Helin, K., Jansen-Durr, P., and Henglein, B. (1995). Cell cycle regulation of the cyclin A gene promoter is mediated by a variant E2F site. Proc Natl Acad Sci U S A *92*, 11264-11268.

Serrano, M., Hannon, G. J., and Beach, D. (1993). A new regulatory motif in cell-cycle control causing specific inhibition of cyclin D/CDK4. Nature *366*, 704-707.

Serrano, M., Lee, H., Chin, L., Cordon-Cardo, C., Beach, D., and DePinho, R. A. (1996). Role of the INK4a locus in tumor suppression and cell mortality. Cell *85*, 27-37.

Sharpless, N. E., Bardeesy, N., Lee, K. H., Carrasco, D., Castrillon, D. H., Aguirre, A. J., Wu, E. A., Horner, J. W., and DePinho, R. A. (2001). Loss of p16Ink4a with retention of p19Arf predisposes mice to tumorigenesis. Nature *413*, 86-91.

Shawber, C., Nofziger, D., Hsieh, J. J., Lindsell, C., Bogler, O., Hayward, D., and Weinmaster, G. (1996). Notch signaling inhibits muscle cell differentiation through a CBF1-independent pathway. Development *122*, 3765-3773.

Shen, C. P., and Kadesch, T. (1995). B-cell-specific DNA binding by an E47 homodimer. Mol Cell Biol *15*, 4518-4524.

Shen, H., Suzuki, T., Munroe, D. J., Stewart, C., Rasmussen, L., Gilbert, D. J., Jenkins, N. A., and Copeland, N. G. (2003). Common sites of retroviral integration in mouse hematopoietic tumors identified by high-throughput, single nucleotide polymorphism-based mapping and bacterial artificial chromosome hybridization. J Virol *77*, 1584-1588.

Shen, J., Bronson, R. T., Chen, D. F., Xia, W., Selkoe, D. J., and Tonegawa, S. (1997). Skeletal and CNS defects in Presenilin-1-deficient mice. Cell *89*, 629-639.

Shojaei, F., Trowbridge, J., Gallacher, L., Yuefei, L., Goodale, D., Karanu, F., Levac, K., and Bhatia, M. (2005). Hierarchical and ontogenic positions serve to define the molecular basis of human hematopoietic stem cell behavior. Dev Cell *8*, 651-663.

Shoji, W., Yamamoto, T., and Obinata, M. (1994). The helix-loop-helix protein Id inhibits differentiation of murine erythroleukemia cells. J Biol Chem *269*, 5078-5084.

Simpson, P. (1990). Lateral inhibition and the development of the sensory bristles of the adult peripheral nervous system of Drosophila. Development *109*, 509-519.

Singh, N., Phillips, R. A., Iscove, N. N., and Egan, S. E. (2000). Expression of notch receptors, notch ligands, and fringe genes in hematopoiesis. Exp Hematol *28*, 527-534.

Sloan, S. R., Shen, C. P., McCarrick-Walmsley, R., and Kadesch, T. (1996). Phosphorylation of E47 as a potential determinant of B-cell-specific activity. Mol Cell Biol *16*, 6900-6908.

Smith, K. S., Rhee, J. W., and Cleary, M. L. (2002). Transformation of bone marrow B-cell progenitors by E2a-Hlf requires coexpression of Bcl-2. Mol Cell Biol *22*, 7678-7687.

Smith, K. S., Rhee, J. W., Naumovski, L., and Cleary, M. L. (1999). Disrupted differentiation and oncogenic transformation of lymphoid progenitors in E2A-HLF transgenic mice. Mol Cell Biol *19*, 4443-4451.

Somers, K. D., Cartwright, S. L., and Schechter, G. L. (1990). Amplification of the int-2 gene in human head and neck squamous cell carcinomas. Oncogene *5*, 915-920.

Song, S., Cooperman, J., Letting, D. L., Blobel, G. A., and Choi, J. K. (2004). Identification of cyclin D3 as a direct target of E2A using DamID. Mol Cell Biol *24*, 8790-8802.

Stilgenbauer, S., Nickolenko, J., Wilhelm, J., Wolf, S., Weitz, S., Dohner, K., Boehm, T., Dohner, H., and Lichter, P. (1998). Expressed sequences as candidates for a novel tumor suppressor gene at band 13q14 in B-cell chronic lymphocytic leukemia and mantle cell lymphoma. Oncogene *16*, 1891-1897.

Su, Y. A., Lee, M. M., Hutter, C. M., and Meltzer, P. S. (1997). Characterization of a highly conserved gene (OS4) amplified with CDK4 in human sarcomas. Oncogene *15*, 1289-1294.

Sun, X. H. (1994). Constitutive expression of the Id1 gene impairs mouse B cell development. Cell *79*, 893-900.

Sun, X. H., and Baltimore, D. (1991). An inhibitory domain of E12 transcription factor prevents DNA binding in E12 homodimers but not in E12 heterodimers. Cell *64*, 459-470.

Suzuki, T., Shen, H., Akagi, K., Morse, H. C., Malley, J. D., Naiman, D. Q., Jenkins, N. A., and Copeland, N. G. (2002). New genes involved in cancer identified by retroviral tagging. Nat Genet *32*, 166-174.

Swiatek, P. J., Lindsell, C. E., del Amo, F. F., Weinmaster, G., and Gridley, T. (1994). Notch1 is essential for postimplantation development in mice. Genes Dev *8*, 707-719.

Sykes, D. B., and Kamps, M. P. (2004). E2a/Pbx1 induces the rapid proliferation of stem cell factor-dependent murine pro-T cells that cause acute T-lymphoid or myeloid leukemias in mice. Mol Cell Biol *24*, 1256-1269.

Takahashi, M., Iijima, T., Suzuki, K., Ando-Lu, J., Yoshida, M., Kitamura, T., Nishiyama, K., Miyajima, K., and Maekawa, A. (1996). Rapid and high yield induction of endometrial adenocarcinomas in CD-1 mice by a single intrauterine administration of N-ethyl-N-nitrosourea combined with chronic 17 beta-estradiol treatment. Cancer Lett *104*, 7-12.

Takeuchi, A., Yamasaki, S., Takase, K., Nakatsu, F., Arase, H., Onodera, M., and Saito, T. (2001). E2A and HEB activate the pre-TCR alpha promoter during immature T cell development. J Immunol *167*, 2157-2163.

Talora, C., Campese, A. F., Bellavia, D., Pascucci, M., Checquolo, S., Groppioni, M., Frati, L., von Boehmer, H., Gulino, A., and Screpanti, I. (2003). Pre-TCR-triggered ERK signalling-dependent downregulation of E2A activity in Notch3-induced T-cell lymphoma. EMBO Rep *4*, 1067-1072.

Taniguchi, Y., Furukawa, T., Tun, T., Han, H., and Honjo, T. (1998). LIM protein KyoT2 negatively regulates transcription by association with the RBP-J DNA-binding protein. Mol Cell Biol *18*, 644-654.

Tremblay, M., Herblot, S., Lecuyer, E., and Hoang, T. (2003). Regulation of pT alpha gene expression by a dosage of E2A, HEB, and SCL. J Biol Chem *278*, 12680-12687.

Tsuji, H., Ishii-Ohba, H., Ukai, H., Katsube, T., and Ogiu, T. (2003). Radiation-induced deletions in the 5' end region of Notch1 lead to the formation of truncated proteins and are involved in the development of mouse thymic lymphomas. Carcinogenesis *24*, 1257-1268.

Valge-Archer, V. E., Osada, H., Warren, A. J., Forster, A., Li, J., Baer, R., and Rabbitts, T. H. (1994). The LIM protein RBTN2 and the basic helix-loop-helix protein TAL1 are present in a complex in erythroid cells. Proc Natl Acad Sci U S A *91*, 8617-8621.

Valtieri, M., Tocci, A., Gabbianelli, M., Luchetti, L., Masella, B., Vitelli, L., Botta, R., Testa, U., Condorelli, G. L., and Peschle, C. (1998). Enforced TAL-1 expression stimulates primitive, erythroid and megakaryocytic progenitors but blocks the granulopoietic differentiation program. Cancer Res *58*, 562-569.

van Es, J. H., van Gijn, M. E., Riccio, O., van den Born, M., Vooijs, M., Begthel, H., Cozijnsen, M., Robine, S., Winton, D. J., Radtke, F., and Clevers, H. (2005). Notch/gamma-secretase inhibition turns proliferative cells in intestinal crypts and adenomas into goblet cells. Nature *435*, 959-963.

Varnum-Finney, B., Purton, L. E., Yu, M., Brashem-Stein, C., Flowers, D., Staats, S., Moore, K. A., Le Roux, I., Mann, R., Gray, G., *et al.* (1998). The Notch ligand, Jagged-1, influences the development of primitive hematopoietic precursor cells. Blood *91*, 4084-4091.

Varnum-Finney, B., Xu, L., Brashem-Stein, C., Nourigat, C., Flowers, D., Bakkour, S., Pear, W. S., and Bernstein, I. D. (2000). Pluripotent, cytokine-dependent, hematopoietic stem cells are immortalized by constitutive Notch1 signaling. Nat Med *6*, 1278-1281.

Visvader, J., Begley, C. G., and Adams, J. M. (1991). Differential expression of the LYL, SCL and E2A helix-loop-helix genes within the hemopoietic system. Oncogene *6*, 187-194.

Visvader, J. E., Fujiwara, Y., and Orkin, S. H. (1998). Unsuspected role for the T-cell leukemia protein SCL/tal-1 in vascular development. Genes Dev *12*, 473-479.

Wadman, I. A., Osada, H., Grutz, G. G., Agulnick, A. D., Westphal, H., Forster, A., and Rabbitts, T. H. (1997). The LIM-only protein Lmo2 is a bridging molecule assembling an erythroid, DNA-binding complex which includes the TAL1, E47, GATA-1 and Ldb1/NLI proteins. Embo J *16*, 3145-3157.

Washburn, T., Schweighoffer, E., Gridley, T., Chang, D., Fowlkes, B. J., Cado, D., and Robey, E. (1997). Notch activity influences the alphabeta versus gammadelta T cell lineage decision. Cell *88*, 833-843.

Watanabe, T., Kashida, Y., Yasuhara, K., Koujitani, T., Hirose, M., and Mitsumori, K. (2002). Rapid induction of uterine endometrial proliferative lesions in transgenic mice carrying a human prototype c-Ha-ras gene (rasH2 mice) given a single intraperitoneal injection of N-ethyl-N-nitrosourea. Cancer Lett *188*, 39-46.

Weijzen, S., Rizzo, P., Braid, M., Vaishnav, R., Jonkheer, S. M., Zlobin, A., Osborne, B. A., Gottipati, S., Aster, J. C., Hahn, W. C., *et al.* (2002). Activation of Notch-1 signaling maintains the neoplastic phenotype in human Ras-transformed cells. Nat Med *8*, 979-986.

Weng, A. P., Ferrando, A. A., Lee, W., Morris, J. P. t., Silverman, L. B., Sanchez-Irizarry, C., Blacklow, S. C., Look, A. T., and Aster, J. C. (2004). Activating mutations of NOTCH1 in human T cell acute lymphoblastic leukemia. Science *306*, 269-271.

Weng, A. P., Nam, Y., Wolfe, M. S., Pear, W. S., Griffin, J. D., Blacklow, S. C., and Aster, J. C. (2003). Growth suppression of pre-T acute lymphoblastic leukemia cells by inhibition of notch signaling. Mol Cell Biol *23*, 655-664.

Williams, D. L., Look, A. T., Melvin, S. L., Roberson, P. K., Dahl, G., Flake, T., and Stass, S. (1984). New chromosomal translocations correlate with specific immunophenotypes of childhood acute lymphoblastic leukemia. Cell *36*, 101-109.

Williams, M. E., Swerdlow, S. H., and Meeker, T. C. (1993). Chromosome t(11;14)(q13;q32) breakpoints in centrocytic lymphoma are highly localized at the bcl-1 major translocation cluster. Leukemia *7*, 1437-1440.

Wilson, A., MacDonald, H. R., and Radtke, F. (2001). Notch 1-deficient common lymphoid precursors adopt a B cell fate in the thymus. J Exp Med *194*, 1003-1012.

Won, K. A., and Reed, S. I. (1996). Activation of cyclin E/CDK2 is coupled to site-specific autophosphorylation and ubiquitin-dependent degradation of cyclin E. Embo J *15*, 4182-4193.

Wu, G., Lyapina, S., Das, I., Li, J., Gurney, M., Pauley, A., Chui, I., Deshaies, R. J., and Kitajewski, J. (2001). SEL-10 is an inhibitor of notch signaling that targets notch for ubiquitin-mediated protein degradation. Mol Cell Biol *21*, 7403-7415.

Wu, L., Sun, T., Kobayashi, K., Gao, P., and Griffin, J. D. (2002). Identification of a family of mastermind-like transcriptional coactivators for mammalian notch receptors. Mol Cell Biol *22*, 7688-7700.

Xia, Y., Brown, L., Yang, C. Y., Tsan, J. T., Siciliano, M. J., Espinosa, R., III, Le Beau, M. M., and Baer, R. J. (1991). TAL2, a helix-loop-helix gene activated by the (7;9)(q34;q32) translocation in human T-cell leukemia. Proc Natl Acad Sci U S A *88*, 11416-11420.

Xiong, Y., Zhang, H., and Beach, D. (1993). Subunit rearrangement of the cyclin-dependent kinases is associated with cellular transformation. Genes Dev *7*, 1572-1583.

Xue, Y., Gao, X., Lindsell, C. E., Norton, C. R., Chang, B., Hicks, C., Gendron-Maguire, M., Rand, E. B., Weinmaster, G., and Gridley, T. (1999). Embryonic lethality and vascular defects in mice lacking the Notch ligand Jagged1. Hum Mol Genet *8*, 723-730.

Yang, L. T., Nichols, J. T., Yao, C., Manilay, J. O., Robey, E. A., and Weinmaster, G. (2005). Fringe glycosyltransferases differentially modulate Notch1 proteolysis induced by Delta1 and Jagged1. Mol Biol Cell *16*, 927-942.

Yasutomo, K., Doyle, C., Miele, L., Fuchs, C., and Germain, R. N. (2000). The duration of antigen receptor signalling determines CD4+ versus CD8+ T-cell lineage fate. Nature *404*, 506-510.

Yoon, K., and Gaiano, N. (2005). Notch signaling in the mammalian central nervous system: insights from mouse mutants. Nat Neurosci *8*, 709-715.

Yoshida, M. C., Wada, M., Satoh, H., Yoshida, T., Sakamoto, H., Miyagawa, K., Yokota, J., Koda, T., Kakinuma, M., Sugimura, T., and et al. (1988). Human HST1 (HSTF1) gene maps to chromosome band 11q13 and coamplifies with the INT2 gene in human cancer. Proc Natl Acad Sci U S A *85*, 4861-4864.

Yoshihara, T., Inaba, T., Shapiro, L. H., Kato, J. Y., and Look, A. T. (1995). E2A-HLF-mediated cell transformation requires both the trans-activation domains of E2A and the leucine zipper dimerization domain of HLF. Mol Cell Biol *15*, 3247-3255.

You, L. R., Lin, F. J., Lee, C. T., DeMayo, F. J., Tsai, M. J., and Tsai, S. Y. (2005). Suppression of Notch signalling by the COUP-TFII transcription factor regulates vein identity. Nature *435*, 98-104.

Yu, Q., Erman, B., Park, J. H., Feigenbaum, L., and Singer, A. (2004). IL-7 receptor signals inhibit expression of transcription factors TCF-1, LEF-1, and RORgammat: impact on thymocyte development. J Exp Med *200*, 797-803.

Yu, Z. K., Gervais, J. L., and Zhang, H. (1998). Human CUL-1 associates with the SKP1/SKP2 complex and regulates p21(CIP1/WAF1) and cyclin D proteins. Proc Natl Acad Sci U S A *95*, 11324-11329.

Yukawa, K., Kikutani, H., Inomoto, T., Uehira, M., Bin, S. H., Akagi, K., Yamamura, K., and Kishimoto, T. (1989). Strain dependency of B and T lymphoma development in immunoglobulin heavy chain enhancer (E mu)-myc transgenic mice. J Exp Med *170*, 711-726.

Yun, T. J., and Bevan, M. J. (2003). Notch-regulated ankyrin-repeat protein inhibits Notch1 signaling: multiple Notch1 signaling pathways involved in T cell development. J Immunol *170*, 5834-5841.

Zhao, F., Vilardi, A., Neely, R. J., and Choi, J. K. (2001). Promotion of cell cycle progression by basic helix-loop-helix E2A. Mol Cell Biol *21*, 6346-6357.

Zhao, J., Dynlacht, B., Imai, T., Hori, T., and Harlow, E. (1998). Expression of NPAT, a novel substrate of cyclin E-CDK2, promotes S-phase entry. Genes Dev *12*, 456-461.

Zhou, M., Gu, L., Yeager, A. M., and Findley, H. W. (1997). Incidence and clinical significance of CDKN2/MTS1/P16ink4A and MTS2/P15ink4B gene deletions in childhood acute lymphoblastic leukemia. Pediatr Hematol Oncol *14*, 141-150.

Zhuang, Y., Cheng, P., and Weintraub, H. (1996). B-lymphocyte development is regulated by the combined dosage of three basic helix-loop-helix genes, E2A, E2-2, and HEB. Mol Cell Biol *16*, 2898-2905.

Zhuang, Y., Soriano, P., and Weintraub, H. (1994). The helix-loop-helix gene E2A is required for B cell formation. Cell *79*, 875-884.

Zindy, F., Eischen, C. M., Randle, D. H., Kamijo, T., Cleveland, J. L., Sherr, C. J., and Roussel, M. F. (1998). Myc signaling via the ARF tumor suppressor regulates p53-dependent apoptosis and immortalization. Genes Dev *12*, 2424-2433.

Zuniga-Pflucker, J. C., and Lenardo, M. J. (1996). Regulation of thymocyte development from immature progenitors. Curr Opin Immunol *8*, 215-224.

APPENDIX

MICROARRAY DATA

Supplemental Data 1: Genes Activated or Repressed in *tal1* thymocytes

Primary Sequence Name	Sequence Description	Accession #	Fold Change	p-value
Rsdr1-pending	retinal short-chain dehydrogenase/reductase 1	NM_011303	-22.86	3.99E-21
Irf6	interferon regulatory factor 6	NM_016851	-19.48	3.09E-08
Cldn4	claudin 4	NM_009903	-15.82	2.43E-06
Smoc1-pending	secreted modular calcium-binding protein 1	NM_022316	-12.60	7.20E-08
Klc3	kinesin light chain 3	BC017147	-12.54	3.56E-14
Gtf2h4	general transcription factor IIH, polypeptide 4	BE457600	-9.87	0.00205
Slc7a11	solute carrier family 7 (cationic amino acid, transporter, y+ system), member 11	NM_011990	-9.74	3.00E-08
Plxnd1	Plexin D1	BC019530	-9.64	7.01E-45
Idb3	inhibitor of DNA binding 3	NM_008321	-8.92	0
Olig3	oligodendrocyte transcription factor 3	NM_053008	-8.86	0.00049
Pip5k1a	phosphatidylinositol-4-phosphate 5-kinase, type 1a	NM_008846	-8.01	0.00134
Prodh	proline dehydrogenase	NM_011172	-7.84	3.01E-16
Tnfaip9	tumor necrosis factor, alpha-induced protein 9	NM_054098	-7.04	0.00184
Ntn1	netrin 1	BI143915	-6.67	1.18E-21
Art1	ADP-ribosyltransferase 1	U31510	-6.65	2.42E-09
Taa1	tumor-associated antigen 1	NM_009310	-6.60	9.44E-06
Insl5	insulin-like 5	NM_011831	-6.58	3.11E-16
Atp1b1	ATPase, Na+/K+ transporting, beta 1 polypeptide	NM_009721	-6.45	3.27E-39
Atp1b1	ATPase, Na+/K+ transporting, beta 1 polypeptide	AV152334	-6.08	0
Tgfb1i4	TGF beta 1 induced transcript 4	AU016382	-5.93	4.22E-32
F13a1	coagulation factor XIII, A1 subunit	NM_028784	-5.91	0
Zdhhc14	zinc finger, DHHC domain containing 14	BC021423	-5.83	2.92E-10
Tcra-V8	T-cell receptor alpha, variable 8	M31649	-5.82	0.00033
Zdhhc14	ESTs	AV223474	-5.79	2.67E-41
Igh-VJ558	immunoglobulin heavy chain (J558 family)	NM_134051	-5.78	2.08E-26
Lox	lysyl oxidase	BB820958	-5.66	0.00325
Tilz1b	TSC22-related inducible leucine zipper 1b (Tilz1b)	AF201285	-5.57	7.85E-30
Igh-VJ558	immunoglobulin heavy chain (J558 family)	BC019425	-5.49	1.41E-29
Zdhhc14	ESTs	BB318221	-5.42	0
Cd5	CD5 antigen	NM_007650	-5.39	0
Zdhhc14	ESTs	AV361868	-5.33	6.79E-41
Tgfb1i4	TGF beta 1 induced transcript 4	BB357514	-5.32	6.26E-31
Centd1	ESTs	AV375176	-5.10	8.69E-44
Tec	cytoplasmic tyrosine kinase, Dscr28C related	NM_013689	-5.10	1.87E-23
Map4k5	MAP kinase kinase kinase kinase 5	BC002309	-5.08	4.81E-09
Vamp1	Mus musculus adult male cerebellum cDNA	AK018783	-5.03	2.71E-08
Atp1b1	ATPase, Na+/K+ transporting, beta 1 polypeptide	BC027319	-5.03	4.71E-30
Egr2	early growth response 2	X06746	-4.98	7.88E-19

Il4ra	interleukin 4 receptor, alpha	AF000304	-4.97	4.34E-11
Tns	tensin	NM_027884	-4.97	0.0007
Rag2	recombination activating gene 2	NM_009020	-4.87	9.05E-30
Mmp14	matrix metalloproteinase 14 (membrane-inserted)	NM_008608	-4.86	5.37E-06
Igh-VJ558	Mus 10 day old male pancreas cDNA	AK007826	-4.85	1.08E-28
Cacna1c	CA channel, voltage-dependent, L type, alpha 1C	NM_009781	-4.68	9.74E-06
Tgfb1i4	TGF beta 1 induced transcript 4	AU016382	-4.67	1.20E-09
P2rx1	purinergic receptor P2X, ligand-gated ion channel 1	NM_008771	-4.67	2.55E-21
Il4ra	interleukin 4 receptor, alpha	NM_010557	-4.60	5.47E-24
Ankrd6	ankyrin repeat domain 6	BM199504	-4.47	2.74E-11
Gtf2h4	general transcription factor IIH, polypeptide 4	NM_010364	-4.43	2.64E-39
Cd6	CD6 antigen	U12434	-4.42	0
P2rx1	Mus musculus 10 day old male pancreas cDNA	AK007650	-4.37	3.35E-16
Epha2	Eph receptor A2	NM_010139	-4.31	5.19E-08
Cxxc5	Mus musculus adult male testis cDNA	AK015150	-4.23	2.31E-09
Bcl2l	Bcl2-like	NM_009743	-4.23	1.36E-14
Atp9a	ATPase, class II, type 9A	NM_015731	-4.21	0.00005
Dusp6	dual specificity phosphatase 6	NM_026268	-4.20	1.06E-35
Map4k5	H3060B09-3 NIA Mouse 15K cDNA Clone Set	BG067961	-4.16	7.78E-23
H2-T17	histocompatibility 2, T region locus 17	AW822416	-3.98	8.58E-15
Zdhhc14	ESTs	BB544336	-3.95	6.10E-07
Spo11	sporulation protein SPO11 homolog-S. cerevisiae	NM_012046	-3.83	6.15E-23
Fos	FBJ osteosarcoma oncogene	AV026617	-3.80	0.0006
Gtf2h4	general transcription factor IIH, polypeptide 4	BB168668	-3.75	7.80E-37
Cxxc5	CXXC finger 5	NM_133687	-3.73	2.08E-07
Pacsin1	protein kinase C and casein kinase substrate in neurons 1	BI731319	-3.65	0.00359
Egr1	early growth response 1	NM_007913	-3.55	2.32E-36
H1f0	H1 histone family, member 0	NM_008197	-3.54	2.10E-22
Sytl2	synaptotagmin-like 2	NM_031394	-3.51	8.82E-07
cd4	mutant T-cell surface glycoprotein CD4	U75219	-3.48	3.03E-34
Nr4a1	nuclear receptor subfamily 4, group A, member 1	NM_010444	-3.47	1.16E-25
XT-II	xylosyltransferase II (XT-II gene).	AJ291751	-3.47	0.00012
Bcl2l	Bcl2-like	U10100	-3.44	2.26E-10
Wdfy2	WD repeat and FYVE domain containing 2	BB794924	-3.38	9.20E-09
Mad1l1	mitotic arrest deficient 1-like 1	BC010702	-3.36	2.15E-13
Nab2	Ngfi-A binding protein 2	NM_008668	-3.35	1.60E-13
H6pd	hexose-6-phosphate dehydrogenase (glucose 1-dehydrogenase)	BC027358	-3.34	1.10E-06
Syngr1	synaptogyrin 1	NM_009303	-3.27	0.00113
Ccrk	cell cycle related kinase	NM_053180	-3.26	5.98E-08
Grca	gene rich cluster, A gene	NM_013533	-3.24	1.18E-10
Glcci1	ESTs, Highly similar to AC006042_1	AA152997	-3.22	3.84E-42
Bach2	BTB and CNC homology 2	AW553304	-3.20	1.41E-14

H1f0	H1 histone family, member 0	BC003830	-3.19	1.01E-34
Mox2	antigen identified by antibody MRC OX-2	AF004023	-3.18	3.96E-20
Pfn2	profilin 2	NM_019410	-3.18	1.96E-07
Skir	ski/sno related	U36203	-3.15	0.00002
Img	integral membrane glycoprotein	NM_008377	-3.12	1.75E-11
St6gal1	H3152A02-3 NIA Mouse 15K cDNA Clone	BG075800	-3.12	1.58E-13
Bcl6	B-cell leukemia/lymphoma 6	U41465	-3.12	1.11E-15
Rorc	RAR-related orphan receptor gamma	AJ132394	-3.07	1.57E-23
Nr1d2	nuclear receptor subfamily 1, group D, member 2	NM_011584	-3.04	1.75E-24
Acvrl1	activin A receptor, type II-like 1	BC014291	-2.99	0.00056
Emid1	EMI domain containing 1	NM_080595	-2.99	0.00062
Ephx1	epoxide hydrolase 1, microsomal	NM_010145	-2.98	5.63E-17
Prep	prolyl endopeptidase	NM_011156	-2.98	8.33E-31
Atp9a	ATPase, class II, type 9A	AF011336	-2.98	0.00203
Rgs10	regulator of G-protein signalling 10	NM_026418	-2.97	5.21E-38
Car2	carbonic anhydrase 2	NM_009801	-2.96	1.18E-12
Cd4	CD4 antigen	NM_013488	-2.96	1.31E-28
N30.7TCRA	Mouse mRNA for T-cell receptor insulin (A-chain) reactive alpha chain VJC	U95921	-2.94	9.24E-32
Slc37a2	solute carrier family 37 (glycerol-3-phosphate transporter), member 2	BC022752	-2.93	1.12E-07
Capn3	calpain 3	AF127766	-2.90	1.13E-30
Zfp36	zinc finger protein 36	X14678	-2.90	1.90E-28
Mef2a	myocyte enhancer factor 2A	BC019116	-2.88	0.00476
Neu3	neuraminidase 3	NM_016720	-2.85	1.21E-10
Idb2	inhibitor of DNA binding 2	NM_010496	-2.85	1.80E-14
Img	integral membrane glycoprotein	AV174595	-2.82	3.76E-09
Itm2a	integral membrane protein 2A	BI966443	-2.82	0
Tdag	T-cell death associated gene	NM_009344	-2.82	1.04E-14
Gsta4	glutathione S-transferase, alpha 4	NM_010357	-2.78	4.33E-07
Vamp1	Mus musculus adult male cerebellum cDNA	AK018783	-2.72	1.29E-11
Nphs2	nephrosis 2 homolog, podocin (human)	NM_130456	-2.71	0.0002
Chst10	ESTs	BB549997	-2.69	1.54E-06
Gem	GTP binding protein	U10551	-2.68	0.00002
Slco3a1	solute carrier organic anion transporter family, 3a1	NM_023908	-2.68	2.80E-08
Pkcz	protein kinase C, zeta	NM_008860	-2.66	0.00358
Tnfrsf4	tumor necrosis factor receptor superfamily 4	NM_011659	-2.65	1.91E-06
Tcra	T-cell receptor insulin -reactive alpha chain VJC	U07662	-2.64	6.64E-38
Hs6st1	heparan sulfate 6-O-sulfotransferase 1	NM_015818	-2.62	2.02E-07
Clk3	CDC-like kinase 3	AF033565	-2.61	1.58E-20
Il7r	interleukin 7 receptor	AI573431	-2.61	2.42E-28
putative	Mouse mRNA for T-cell receptor insulin (A-chain) reactive alpha chain VJC	X01134	-2.58	1.22E-36
Rhoip3-pending	Rho interacting protein 3	U73200	-2.58	3.51E-30
Hbb-bh1	hemoglobin Z, beta-like embryonic chain	AV024771	-2.57	1.60E-19
Ldh2	lactate dehydrogenase 2, B chain	NM_008492	-2.55	2.44E-31

Tnfaip3	tumor necrosis factor, alpha-induced protein 3	NM_009397	-2.54	1.55E-09
Mtss1	metastasis suppressor 1	BC024131	-2.53	4.47E-16
IL2 receptor	Mus musculus interleukin 2 receptor mRNA	AF054581	2.50	2.52E-08
Pfc	RIKEN cDNA 1500032P08 gene	BB800282	2.61	0.00308
Hsp105	heat shock protein 105	BI499717	2.61	8.01E-25
Sdh1	sorbitol dehydrogenase 1	AV253518	2.64	0.00002
Depdc6	DEP domain containing 6	BC004774	2.71	0.00045
Sas	sarcoma amplified sequence	NM_025982	2.74	2.21E-20
Papss2	ESTs	BF786072	2.80	0.00008
Cxcr6	chemokine (C-X-C motif) receptor 6	NM_030712	2.81	1.09E-06
Tagln2	transgelin 2	AV212626	2.94	5.88E-08
Pdgfrb	platelet derived growth factor receptor, beta	AA499047	2.94	0.0015
Gja1	ESTs	BB039269	3.04	8.53E-06
Ly6c	lymphocyte antigen 6 complex, locus C	NM_010741	3.09	6.56E-18
Comtd1	Mus 10 day old male pancreas cDNA	AK007659	3.10	0.00218
Dtx1	deltex 1 homolog (Drosophila)	AB015422	3.30	4.92E-14
Hspa8	Mus musculus adult male lung cDNA	AK004608	3.31	4.83E-34
Myo6	ESTs	BE133806	3.32	0.00005
Myo1f	myosin If	NM_008660	3.36	0.00053
Gm2a	GM2 ganglioside activator protein	BC004651	3.39	5.96E-14
Angptl2	602356479F1 NCI_CGAP_Mam1 cDNA clone	BG244279	3.52	3.15E-11
Wwox	Mus musculus adult male pituitary gland cDNA	AK019911	3.60	0.00072
Cdk6	cyclin-dependent kinase 6	NM_009873	3.73	0.00216
Evi5	ecotropic viral integration site 5	AI255184	3.76	0.0046
Hsp70-1	heat shock protein, 70 kDa 1	M12573	3.81	5.59E-08
Eef2k	eukaryotic elongation factor-2 kinase	BC003433	4.12	0.00011
Ephb2	ESTs	AV221401	4.13	2.51E-06
Il1rrp	interleukin 1 receptor related protein	NM_008365	4.16	1.17E-15
Fcna	ficolin A	NM_007995	4.21	2.51E-07
Trf	transferrin	AF440692	4.25	2.28E-07
Gig1	glucocorticoid-induced gene 1 mRNA	AW413620	4.26	5.14E-25
LOC58860	disintegrin metalloprotease (decysin)	NM_021475	4.30	0.00009
Ccl6	chemokine (C-C motif) ligand 6	BC002073	4.32	1.98E-06
Ifi202b	interferon activated gene 202B	NM_011940	4.33	4.46E-21
Myo6	myosin VI	NM_008662	4.42	0.00013
D130038B21Rik	RIKEN cDNA D130038B21 gene	BC025514	5.16	4.66E-10
Fcgr3	Fc receptor, IgG, low affinity III	NM_010188	5.26	0.0002
Scya9	small inducible cytokine A9	AF128196	5.37	0.00042
Gja1	ESTs	BB142324	5.39	0.00008
Scd1	stearoyl-Coenzyme A desaturase 1	NM_009127	5.40	0.00047
Pla2g7	Mus musculus adult male cerebellum cDNA	AK005158	5.43	1.96E-07
Api6	apoptosis inhibitory 6	NM_009690	5.45	0.00317
Alox15	arachidonate 15-lipoxygenase	L34570	5.46	7.89E-08
Baat	bile acid-Coenzyme A dehydrogenase: amino acid n-acyltransferase	NM_007519	5.57	0.00369
Cd38	ESTs	BB256012	5.63	0.00288
C4	complement component 4 (within H-2S)	NM_009780	5.64	1.88E-12

D10Ertd322e	H3047G06-3 NIA Mouse 15K cDNA Clone Set	BG066857	5.73	0.00325
C1nh	complement component 1 inhibitor	NM_009776	5.83	0.00004
Fn1	fibronectin 1	BC004724	5.96	2.53E-12
Gypa	glycophorin A	NM_010369	6.32	0.00303
Ctla2a	cytotoxic T lymphocyte-associated protein 2 α	NM_007796	6.75	7.45E-16
Eraf	erythroid associated factor	NM_133245	6.97	4.94E-09
Pbx3	pre B-cell leukemia transcription factor 3	NM_016768	7.61	0.00007
Pgcp	BB468025 RIKEN full-length enriched	BB468025	8.51	0.00021
Zac1	zinc finger protein regulator of apoptosis and cell cycle arrest	AF147785	8.63	1.08E-10
Rnf128	Mus musculus adult male liver cDNA	AK004847	8.73	0.00009
F5	coagulation factor V	NM_007976	8.74	0.00021
LOC58209	similar to megakaryocyte stim. factor precursor	NM_021400	8.76	1.79E-17
Wnt5b	wingless-related MMTV integration site 5B	NM_009525	8.93	0.00037
Fgfr1	fibroblast growth factor receptor 1	M33760	9.16	0.00068
Eomes	ESTs	BB128925	10.01	0.00009
Planh2	plasminogen activator inhibitor, type II	NM_011111	10.24	1.09E-07
Fizz1-pending	found in inflammatory zone 1	NM_020509	10.29	0
Dyrk3	dual-specificity tyrosine-(Y)-phosphorylation regulated kinase 3	BC006704	10.38	0.00252
Ptpn13	protein tyrosine phosphatase, non-receptor 13	BM236743	10.83	0.00003
Snrpn	small nuclear ribonucleoprotein N	AI836293	11.85	0.00068
M32486	Mouse 19.5 mRNA	NM_019631	11.96	7.47E-08
Slc4a1	solute carrier family 4-anion exchanger, member 1	BB448377	12.37	1.43E-07
Slc22a3	solute carrier family 22, member 3	NM_011395	15.00	2.88E-09
Saa3	serum amyloid A 3	NM_011315	15.05	0.00215
Ssb4	SPRY domain-containing SOCS box 4	BC023083	15.86	8.77E-15
Snurf	SNRPN upstream reading frame	NM_033174	16.53	4.92E-11
Ly84	lymphocyte antigen 84	D13695	18.45	2.31E-09
Chi3l3	chitinase 3-like 3	NM_009892	28.95	0
Chi3l4	chitinase 3-like 4	AY065557	33.05	0
Ril-pending	reversion induced LIM gene	NM_019417	41.95	7.79E-16

Supplemental Data 2: Genes activated or repressed by Notch in doxycycline-regulated T-ALL cell line

Primary Sequence Name	Sequence Description	Publid ID	Fold change	p-value
Soat1	sterol O-acyltransferase 1	BG064396	-18.93	4.76E-19
Ccrk	cell cycle related kinase	NM_053180	-15.67	0.00087
Slamf1	signaling lymphocytic activation molecule family member 1	BB132695	-14.32	1.41E-06
Mxd4	Max dimerization protein 4	BE291523	-13.91	0.00031
Ccr9	chemokine (C-C motif) receptor 9	NM_009913	-10.79	0
Ly6c	lymphocyte antigen 6 complex, locus C	NM_010741	-10.06	2.24E-44
Tcfcp2l3	transcription factor CP2-like 3	AF411213	-9.52	0.00445
Rora	RAR-related orphan receptor alpha	NM_013646	-9.37	0.00244
Gats	opposite strand transcription unit to Stag3	BC026208	-8.29	0.00046
Fprl1	formyl peptide receptor-like 1	NM_008042	-8.21	0.00177
Papss2	3'-phosphoadenosine 5'-phosphosulfate synthase 2	BF786072	-7.82	0.00064
Epsti1	epithelial stromal interaction 1 (breast)	AK017174	-7.82	0.00452
Rora	RAR-related orphan receptor alpha	BI660199	-7.32	1.95E-09
Kctd12	potassium channel tetramerisation domain containing 12	BM220945	-6.56	1.82E-37
Cd4	CD4 antigen	NM_013488	-6.24	2.50E-09
Itk	IL2-inducible T-cell kinase	L10628	-6.23	1.38E-06
Ly6a	lymphocyte antigen 6 complex, locus A	BC002070	-5.92	8.59E-12
Tnfrsf6	tumor necrosis factor receptor superfamily, member 6	NM_007987	-5.91	0.00405
Ccr9	chemokine (C-C motif) receptor 9	AJ131357	-5.91	0
Plec1	plectin 1	AW123286	-5.43	0.00301
Dlx1	distal-less homeobox 1 ect assay	NM_010053	-5.05	8.81E-11
Tktl1	transketolase-like 1	C79967	-4.72	0.00001
Ctsl	cathepsin L	J02583	-4.60	0
Tktl1	transketolase-like 1	NM_031379	-4.49	9.09E-09
Igsf4a	immunoglobulin superfamily, member 4A	NM_018770	-4.48	0.00003
Serpini1	serine (or cysteine) proteinase inhibitor, clade I, member 1	NM_009250	-4.40	1.25E-29
Ifngr1	interferon gamma receptor 1	NM_010511	-4.27	1.44E-39
Glcci1	glucocorticoid induced transcript 1	AA152997	-4.08	0
Grca	gene rich cluster, A gene	NM_013533	-4.05	1.01E-10
Trp53inp2	tumor protein p53 inducible nuclear protein 2	AK003956	-3.99	0.00442
Mtap7	microtubule-associated protein 7	NM_008635	-3.97	0.00154
Utrn	utrophin	X83506	-3.96	0.0015
Satb1	special AT-rich sequence binding protein 1	BG092481	-3.95	6.09E-41
Serpini1	Mus musculus serine (or cysteine) proteinase inhibitor, clade I, member 1	NM_009250	-3.89	1.01E-19
Cd200	Cd200 antigen	AF004023	-3.82	9.79E-21
Itgam	integrin alpha M	NM_008401	-3.64	7.26E-06

Rorc	RAR-related orphan receptor gamma	AJ132394	-3.63	4.46E-13
Ssbp2	single-stranded DNA binding protein 2	AY037837	-3.62	1.45E-07
Fbxo32	F-box only protein 32	AF441120	-3.57	0.00331
Hmgcs2	3-hydroxy-3-methylglutaryl-Coenzyme A synthase 2	BC014714	-3.53	8.10E-28
Ifngr2	interferon gamma receptor 2	BF537076	-3.51	0.00022
Rapgef4	Rap guanine nucleotide exchange factor (GEF) 4	AK004874	-3.46	1.22E-24
Fbxl12	F-box and leucine-rich repeat protein 12	NM_013911	-3.45	0
Lztfl1	leucine zipper transcription factor-like 1	NM_033322	-3.39	6.55E-27
Socs1	suppressor of cytokine signaling 1	AB000710	-3.28	0.00021
Ltb	lymphotoxin B	NM_008518	-3.24	7.11E-16
Tcra	T-cell receptor alpha chain	U95921	-3.22	1.66E-32
Prkd2	protein kinase D2	AW557946	-3.20	1.03E-14
Cpt1a	carnitine palmitoyltransferase 1a, liver	BB021753	-3.18	0.00181
Satb1	special AT-rich sequence binding protein 1	AV172776	-3.13	0
Ms4a6b	membrane-spanning 4-domains, subfamily A, member 6B	NM_027209	-3.12	2.56E-38
Lrrfip1	leucine rich repeat (in FLII) interacting protein 1	NM_008515	-3.11	0.0028
Lgals1	lectin, galactose binding, soluble 1	AI642438	-3.10	0
Ypel1	yippee-like 1 (Drosophila)	NM_023249	-3.09	6.23E-06
Prkd2	protein kinase D2	BB204677	-3.05	8.29E-11
Lgals1	lectin, galactose binding, soluble 1	NM_008495	-3.03	9.20E-35
Zdhhc2	zinc finger, DHHC domain containing 2	BB224658	-2.99	0.00045
Hfe	hemochromatosis	AJ306425	-2.91	5.26E-06
Emp1	epithelial membrane protein 1	U25633	-2.91	1.58E-17
Sdccag8	serologically defined colon cancer antigen 8	AA690806	-2.85	0.00272
Ypel3	yippee-like 3 (Drosophila)	BI660196	-2.85	2.90E-07
Pycard	PYD and CARD domain containing	BG084230	-2.79	0.00424
Hist1h1c	histone 1, H1c	BB533903	-2.78	2.85E-13
Tec	cytoplasmic tyrosine kinase, Dscr28C related (Drosophila)	NM_013689	-2.74	2.85E-06
Tcra	T-cell receptor alpha chain	X01134	-2.74	1.17E-31
Tcra	T-cell receptor alpha chain	U07662	-2.72	1.61E-35
Cd52	CD52 antigen	NM_013706	-2.66	6.89E-18
Rnasel	ribonuclease L (2', 5'-oligoisoadenylate synthetase-dependent)	BF714880	-2.66	7.17E-06
Foxb1	forkhead box B1	U90538	-2.61	3.74E-08
Plxdc1	plexin domain containing 1	AF378760	-2.60	6.75E-15
Mr1	major histocompatibility complex, class I-related	BB210729	-2.60	7.60E-07
Rab3d	RAB3D, member RAS oncogene family	BB349707	-2.54	0.0005
Itga4	integrin alpha 4	NM_010576	-2.53	6.98E-08
Cd47	CD47 antigen	NM_010581	-2.53	5.10E-20
Gpr65	G-protein coupled receptor 65	NM_008152	2.50	4.95E-11
Ipo4	importin 4	NM_024267	2.51	8.07E-11
Myc	myelocytomatosis oncogene	BC006728	2.52	1.43E-28

Slc19a1	solute carrier family 19 (sodium/hydrogen exchanger), member 1	NM_031196	2.53	0.00228
Slc12a2	solute carrier family 12, member 2	BG069505	2.57	0.00022
Pla2g12a	phospholipase A2, group XIIA	AY007382	2.57	2.91E-12
Rpo1-4	RNA polymerase 1-4	BB729239	2.57	2.38E-11
Nedd4	Neural precursor cell expressed, developmentally down-regulted gene 4	BG073415	2.58	5.04E-08
Smyd2	SET and MYND domain containing 2	BC023119	2.60	7.19E-27
Ptpn13	protein tyrosine phosphatase, non-receptor type 13	BM236743	2.61	4.44E-08
Wdr4	WD repeat domain 4	BE854862	2.62	0.00029
Shmt1	serine hydroxymethyl transferase 1 (soluble)	AF237702	2.63	1.63E-22
Chchd4	coiled-coil-helix-coiled-coil-helix domain containing 4	NM_133928	2.63	8.73E-17
Rpo1-2	RNA polymerase 1-2	NM_009086	2.64	1.19E-09
Nrarp	Notch-regulated ankyrin repeat protein	BI696369	2.64	1.15E-08
Grwd1	glutamate-rich WD repeat containing 1	BB251524	2.65	6.66E-09
Siat7d	sialyltransferase 7 ((alpha-N-acetylneuraminyl 2,3-betagalactosyl-1,3)-N-acetyl galactosaminide alpha-2,6-sialyltransferase) D"	AK007601	2.65	5.11E-06
Nr4a1	nuclear receptor subfamily 4, group A, member 1	NM_010444	2.66	4.25E-10
Thbs2	thrombospondin 2	NM_011581	2.67	3.05E-06
Gja1	gap junction membrane channel protein alpha 1	BB039269	2.67	3.12E-07
Nfkbiz	nuclear factor of kappa light polypeptide gene enhancer in B-cells inhibitor, zeta	AB026551	2.69	0.00065
Fbxo31	F-box only protein 31	NM_133765	2.73	0.00001
Tpbg	trophoblast glycoprotein	BQ177165	2.75	0.00036
Grwd1	glutamate-rich WD repeat containing 1	BB251524	2.75	1.99E-22
Gsto1	glutathione S-transferase omega 1	NM_010362	2.76	9.96E-08
Slc11a2	solute carrier family 11 (proton-coupled divalent metal ion transporters), member 2	BG065264	2.84	2.81E-15
Ssb4	SPRY domain-containing SOCS box 4	BC023083	2.84	2.54E-08
Cyb561	cytochrome b-561	BC006732	2.87	0.00001
Gadd45b	growth arrest and DNA-damage-inducible 45 beta	AI323528	2.88	0.00232
Stc1	stanniocalcin 1	BQ032752	2.88	1.89E-11
Gas5	growth arrest specific 5	BI650268	2.94	8.76E-32
Ifrd2	interferon-related developmental regulator 2	BB540964	2.98	7.91E-07
Mdn1	midasin homolog (yeast)	NM_133874	2.99	5.48E-13
Rgs3	regulator of G-protein signaling 3	AF350047	3.02	0.00007
Sgtb	small glutamine-rich tetratricopeptide repeat (TPR)-containing, beta	BC017611	3.06	0.0001
Rnu3ip2	RNA, U3 small nucleolar interacting protein 2	BC014703	3.10	9.70E-09

Endog	endonuclease G	AV104666	3.14	0.00084
Stc2	stanniocalcin 2	AF031035	3.20	1.42E-08
Notch1	Notch gene homolog 1 (Drosophila)	NM_008714	3.22	5.88E-35
Zbtb16	Zinc finger and BTB domain containing 16	AA419994	3.23	0.00025
Hrb	HIV-1 Rev binding protein	BB130716	3.23	3.66E-38
Notch3	Notch gene homolog 3 (Drosophila)	NM_008716	3.26	1.13E-20
Ppan	peter pan homolog (Drosophila)	BC014688	3.33	9.75E-19
Mettl1	methyltransferase-like 1	NM_010792	3.33	4.44E-10
Lef1	lymphoid enhancer binding factor 1	NM_010703	3.66	0
Shmt1	serine hydroxymethyl transferase 1 (soluble)	NM_009171	3.70	2.25E-17
Rsu1	Mus musculus Ras suppressor protein 1	NM_009105	3.83	2.12E-22
Dsp	Desmoplakin	BC026631	3.83	5.51E-23
Nefh	neurofilament, heavy polypeptide	M35131	3.84	0.00172
Srm	spermidine synthase	NM_009272	3.88	3.76E-41
Frmd4b	FERM domain containing 4B	BG067753	3.97	0.00005
Il31ra	interleukin 31 receptor A	AB083111	4.01	3.89E-07
Hrb	HIV-1 Rev binding protein	BQ174030	4.12	0
Smyd5	SET and MYND domain containing 5	BF160651	4.15	0.00014
Hk2	hexokinase 2	NM_013820	4.39	5.21E-31
Comtd1	catechol-O-methyltransferase domain containing 1	AK007659	4.41	0.00008
Itgb5	integrin beta 5	BB543646	4.41	0.00005
Kai1	kangai 1 (suppression of tumorigenicity 6, prostate)	NM_007656	4.46	0
Heyl	hairy/enhancer-of-split related with YRPW motif-like	BB310549	4.55	0.00035
Irf4	interferon regulatory factor 4	U34307	4.61	3.39E-25
Heyl	hairy/enhancer-of-split related with YRPW motif-like	BG695100	4.63	3.99E-24
Iltifb	interleukin 10-related T cell-derived inducible factor beta /// interleukin 22	AJ249492	4.89	0
Hrb	HIV-1 Rev binding protein	BB130716	4.94	0
Cited1	Cbp/p300-interacting transactivator with Glu/Asp-rich carboxy-terminal domain 1	U65091	4.98	8.36E-07
Myl4	myosin, light polypeptide 4	NM_010858	5.08	2.26E-15
Frmd4b	FERM domain containing 4B	BB009122	5.12	1.68E-15
Gadd45g	growth arrest and DNA-damage-inducible 45 gamma	AK007410	5.16	1.19E-10
Egr1	early growth response 1	NM_007913	5.34	0
Chst2	carbohydrate sulfotransferase 2	NM_018763	5.48	0.00013
Plce1	phospholipase C, epsilon 1	AV306884	5.99	0.00374
Cd2	CD2 antigen	NM_013486	6.07	1.03E-08
Mef2b	myocyte enhancer factor 2B	D87833	6.31	0.00007
Nab2	Mus musculus Ngfi-A binding protein 2	NM_008668	7.13	8.97E-25
Lamb1-1	laminin B1 subunit 1	BG970109	7.33	0.00311
Ptcra	pre T-cell antigen receptor alpha	NM_011195	7.90	0
Ifi202b	interferon activated gene 202B	NM_011940	8.37	0

Gfra1	glial cell line derived neurotrophic factor family receptor alpha 1	BE534815	8.97	0.00183
Mafb	v-maf musculoaponeurotic fibrosarcoma oncogene family, protein B (avian)	AW412521	8.98	0.00074
Il2ra	interleukin 2 receptor, alpha chain	AF054581	9.54	0
Adam19	Mus musculus a disintegrin and metalloproteinase domain 19 (meltrin beta)	NM_009616	10.63	0
Mina	myc induced nuclear antigen	AK013451	10.97	0.00139
Nr2f2	nuclear receptor subfamily 2, group F, member 2	AI463873	11.05	1.74E-07
Dtx1	deltex 1 homolog (Drosophila)	AB015422	11.50	0
Cntnap2	contactin associated protein-like 2	AU079588	11.62	8.42E-25
Cdh1	cadherin 1	NM_009864	13.86	1.69E-15
Esm1	endothelial cell-specific molecule 1	BC020038	17.27	2.46E-10
Hes1	hairy and enhancer of split 1 (Drosophila)	BC018375	19.52	1.28E-35
Il10	interleukin 10	NM_010548	19.57	6.49E-26